Fluvial and marine sedimentation at a passive continental margin

Vis, G.J.

2009

CHAPTER 4

Sedimentary changes during the last ~2500 years have been reconstructed from cored sedimentary records from the deltaic floodplain of the Lower Tagus Valley and the Tagus mudbelt on the continental shelf offshore Lisbon. We used a multi-proxy approach consisting of sedimentology, grainsize, pollen data and magnetic susceptibility. In the floodplain grainsize coarsened and sedimentation rate and magnetic susceptibility increased during the late Holocene due to an increased flooding frequency and/or intensity. On the Tagus shelf the mudbelt grainsize fined, together with a higher sedimentation rate and increased magnetic susceptibility. The fining grainsize is explained by an increased suspended sediment flux towards the shelf and subdued winnowing. Floodplain and shelf records were correlated by radiocarbon dating and changes in sediment characteristics. We identified four depositional phases (~2300/~1600/~1100/~670 cal BP) on the floodplain and the shelf. These are tentatively explained by land-use changes in the Tagus catchment.

Late Holocene sedimentary changes in floodplain and shelf environments of the Tagus River (Portugal)

4.1 INTRODUCTION

Mankind has a profound impact on system earth and is able to reshape natural environmental systems, thereby affecting their stability. Past changes in land-use and forest cover have caused significant changes in river discharge, soil erosion and deposition in delta's and offshore environments (e.g. Bosch and Hewlett, 1982; Hornbeck *et al.*, 1993; Sahin and Hall, 1996; Lang *et al.*, 2003; Andréassian, 2004; Jordan *et al.*, 2005; Ward *et al.*, 2008).

On the Iberian Peninsula the effect of soil erosion on fluvial sediment loads and deposition has been felt during the last ~2000 years. The sediment
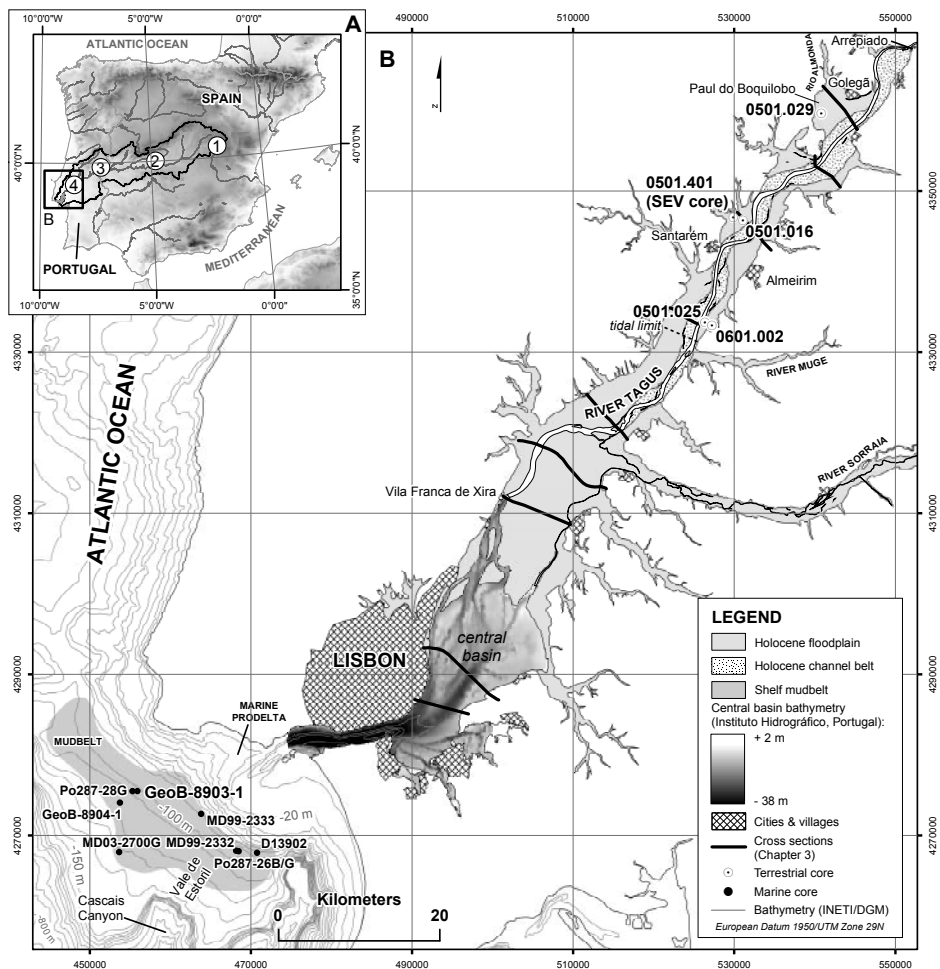
Figure 4.1 | Location map of the Lower Tagus Valley. The inset map (A) shows the Tagus catchment and study area on the Iberian Peninsula, Digital Elevation Data from Jarvis *et al.* (2006). 1: Mesozoic Spanish Cordillera; 2: Spanish Tertiary Sedimentary Tagus Basin; 3: Palaeozoic Hesperian Massif; 4: Lower Tagus Basin (LTB). The main map (B) shows the location of the terrestrial and marine cores.

load of the Ebro River in northeast Spain increased fourfold since ~700 cal BP due to catchment deforestation, which caused increased delta shoreline progradation (Guillén and Palanques, 1997). Chester and James (1991) argued that the temporal correlations between phases of intensive agriculture, deforestation and valley alluviation during the last two millennia in south Portugal were most likely the result of anthropogenic forcing. According to Thorndycraft and Benito (2006a) slackwater deposits from the last 1300 years in Spain, reflect increased human impact on the landscape. For the Muge River, a Lower Tagus tributary, evidence of increased overbank sedimentation since ~2150 cal BP, has been attributed to progressive human impact on catchment vegetation (Van der Schriek *et al.*, 2007a, b).

Studies conducted on seafloor sedimentary sequences along continental margins, mainly focus on palaeoceanography, while a minority addresses the forcing factors controlling terrestrial material transport to the ocean. Human impact was identified on the Eel and California shelves, where accumulation rates increased dramatically during the past centuries due to land use changes (Leithold *et al.*, 2005; Sommerfield and Wheatcroft, 2007). On the Adriatic Sea floor accelerated sedimentation and increased input of terrigenous material were caused by widespread deforestation and cultivation (Oldfield *et al.*, 2003). Recent (<2000 years) deposition of fine-grained sediments on the Gironde shelf has been linked to increased sediment supply resulting from soil erosion in the catchment (Lesueur *et al.*, 1996).

The studies mentioned above have in common that they view the sedimentary system either from a "land-based" perspective or from an "ocean-based" perspective. Thus it is timely to improve our understanding of sedimentation of the complete fluvial-estuarine-shelf depositional system. Therefore this chapter aims to: 1) correlate fluvial and marine sedimentary records, 2) identify depositional phases in both environments, and 3) explore the external forcing mechanisms (climate, man) in both records. Because the sedimentary records are located at the downstream end of the Tagus depositional system, they contain a "smoothed" signal of complex processes like sediment erosion, flux, storage and winnowing.

Fluvial setting

The Tagus River has a length of ~1000 km and a catchment area of 80,630 km^2 (Bettencourt and Ramos, 2003; Le Pera and Arribas, 2004). The Tagus originates at an elevation of about 1600 m in eastern Spain and flows westwards (Fig. 4.1) finally entering the NNE-SSW oriented Lower Tagus Basin. Presently, the main soil types—in FAO UNESCO terminology—in the catchment are Cambisols, Regosols, Podzols and Luvisols with typical depths-to-rock of <80 cm. Land use is dominated by arable land, forest, extensive pastoral forest

parks ("dehesa") and olive orchards (European Soil Portal, 2008). The average discharge of the regulated Tagus River near its mouth is 400 m³/s. The river is characterised by extreme seasonal and annual variability with peak discharges more than 30 times the average discharge (Benito *et al.*, 2003a; Bettencourt and Ramos, 2003). The present-day Lower Tagus floodplain (Fig. 4.1) is 5-10 km wide and ~85 km long, has an elevation of ~22 m near Golegã in the north and ~2 m near Vila Franca de Xira in the south, with an average gradient of ~24 cm/km. South of Vila Franca de Xira the river enters a large central basin.

Estuarine setting

The central basin south of Vila Franca de Xira is characterised by a semi-diurnal mesotidal regime with floods typically lasting an hour longer than ebbs, making it an ebb-dominated tide. The mean tidal amplitude in the central basin is 1.5 m at neap tide and 4 m at spring tide (Portela and Neves, 1994; Bettencourt and Ramos, 2003). The average water depth in the central basin is 5 m (Fig. 4.1) and the basin floor is dominated by silt and clay; sand is only present in the narrow tidal inlet channel south of Lisbon (Portela and Neves, 1994). This up to 40 m deep channel connects the basin to the Atlantic Ocean and ebb flow speeds of 2-3 m/s are reached (Bettencourt and Ramos, 2003). Due to its sheltered position, waves play a very minor role within the central basin, where only a small fraction of the tidal energy reaches the fluvial domain (Fortunato *et al.*, 1999).

Marine setting

The Atlantic Ocean west of Lisbon consists of a passive continental margin with a narrow continental shelf (<30 km). The Atlantic coast off Portugal is affected by a high-energy wave regime with winter wave heights of up to 10 m (Instituto-Hidrográfico-Portugal, 2008). The Atlantic surface waters (< ~100 m) are dominated by the Portugal Current System (PCS), consisting of a slow southward current in the open ocean and a fast, seasonally reversing coastal current (Fiúza, 1983; Arhan *et al.*, 1994; Peliz and Fiúza, 1999). During late spring and summer, the Azores high-pressure system is located over the central North Atlantic and the Greenland low-pressure system is weak, causing prevalent northerly and north-westerly winds, leading to a southward coastal PCS and generating coastal upwelling (Fiúza, 1983; Haynes and Barton, 1990; Peliz and Fiúza, 1999). Autumn and winter are characterised by a northward flowing coastal PCS, because the Açores high-pressure system is located over the southern North Atlantic and the deep Greenland low-pressure system causes strong winds from the southwest, triggering coastal downwelling (Frouin *et al.*, 1990; Haynes and Barton, 1990).

4.2 METHODS

Terrestrial and marine cores

We selected three cores (0501.016, .025 and .029) from a dataset of 126 cores
and 9 cross sections from the Lower Tagus Valley (Fig. 4.1, Table 4.1) which
best recorded depositional phases based on the distribution of facies units and
palaeogeography (Chapters 2 and 3). These cores were used for a multi-proxy
approach by analysing grainsize, loss-on-ignition (LOI), radiocarbon age,
pollen content and magnetic susceptibility (MS). Two nearby cores (0501.401
and 0601.002) were used for additional radiocarbon dates, which were pro-
jected to cores 0501.016 and 0501.025 respectively. Coring locations (Table
4.1) were measured using a Garmin GPS-12 receiver (horizontal resolution
~5 m). The cores were manually recovered using Edelman augers for sediment
above the groundwater table and the gauge for sediment below the groundwa-
ter table. The sediments were described in the field at 10 cm intervals following
the method explained in Berendsen and Stouthamer (2001) and lithology was
converted to USDA terminology. The elevation of corings 0501.016, .025 and
.401 (Fig. 4.1) relative to ordnance datum was measured using Trimble DGPS
equipment (vertical resolution ~5 mm) and the elevation of corings 0501.029
and 0601.002 was taken from topographic maps (IgeoE, Portugal).

The terrestrial cores are located in distal overbank settings where fine-
grained sediment is deposited from suspended load of overbank flood water.
A period with such events is registered in the sedimentary record as a fine-
grained sediment layer, reflecting multiple overbank floods. In low-lying areas
which aggrade rapidly, like the Lower Tagus Valley, it is generally assumed that
important hiatuses are absent at lithological boundaries (Törnqvist and Van
Dijk, 1993). The cross sections indicate that the depositional phases identified
in the cores have a large aerial extent in the Lower Tagus Valley and therefore
most likely reflect deposition due to external forcing.

Nine marine cores from the Tagus mudbelt on the continental shelf
offshore Lisbon were used (Fig. 4.1, Table 4.1). Of these cores, one piston core
(GeoB-8903-1) was used for a multi-proxy approach using grainsize, radiocar-
bon age and MS. The other cores were used to reconstruct the spatial sediment
distribution using MS signals. Although local accumulation rates may be dif-
ferent, we assume a more or less even sediment accumulation on the mudbelt
as a result of deposition from suspension from the Tagus outflow.

Sample treatment

Grainsize was measured using a Fritsch A22 Laser Particle Sizer following the
methods described by Konert and Vandenberghe (1997), including removal
of organic matter and carbonates. The marine core contained very little opal as

was confirmed by visual inspection using a microscope, so no additional measures to remove this were taken. Grainsize of the terrestrial cores was measured at 5-10 cm intervals, marine core GeoB-8903-1 was measured at a 1 cm interval. Grainsize statistics (mean and D90 = grainsize at which 90 % is finer) were calculated using the program GRADISTAT (Blott and Pye, 2001). Matlab 7.4.1 software was used to calculate equal-depth intervals for the contour plots which were visualised using Surfer 8 software.

A LECO TGA-601 was used to determine loss-on-ignition of 110 dried and grounded samples of approximately 2 g of core 0501.029 (Fig. 4.2) resulting in "classic"LOI_{550}. Due to heating, structural water and -OH bounds in the (clay) minerals were lost as well, causing a slight overestimation of the LOI.

Pollen samples were prepared according to Faegri and Iversen (1975); clastic material was removed using a sodium polytungstate heavy liquid separation. Samples were counted at the Friedrich-Schiller University in Jena (Germany). The percentage of anthropogenic indicator pollen was calculated based on the regional pollen sum.

Radiocarbon dating

A set of 26 radiocarbon dates was used to construct the chronological framework (Table 4.2). The 9 terrestrial radiocarbon samples consisted of terrestrial botanical macrofossils or bulk samples. Botanical macrofossil samples (from generally 1 cm thick sediment slices) were boiled with sodium pyrophosphate and washed through a 125 μm sieve. Macrofossils were picked from the residue and determined at VU University Amsterdam. The terrestrial radiocarbon ages were calibrated using the program OxCal v3.10 (Bronk Ramsey, 2005) using the IntCal04 terrestrial age calibration data from Reimer *et al.* (2004).

The 17 marine radiocarbon dates were based on planktonic foraminifera and marine shells and molluscs. The marine radiocarbon ages were calibrated using the program CALIB v5.0 (Stuiver and Reimer, 1993; Stuiver *et al.*, 2005) and the Marine04 age calibration data from Hughen *et al.* (2004). The marine calibration incorporates a time-dependent global ocean reservoir correction of about 400 years. Abrantes *et al.* (2005) proved that this is a good estimate for marine material off Portugal for the last ~110 years, however, older dated material may have been affected by different conditions. Therefore and to correct for local variations, the difference in reservoir age of the study area and the global ocean was determined ($\Delta R = 262 \pm 164$ y) using the marine reservoir correction database by Stuiver and Braziunas (1993). All mentioned radiocarbon dates are expressed as calibrated calendar ages (cal BP) with age spans at the 2σ range.

Magnetic Susceptibility

Magnetic susceptibility measurements were volume-based low field (κ) and measured using Multi Sensor Core Logging 7.6 (MSCL) equipment (Geotek Ltd.), mounted with an MS2C Bartington magnetic susceptibility meter with loop sensor. Cores were measured every centimetre (every 0.5 cm for 0501.029) during 10 s. The upper 4 m of cores 0501.016 and .025 and the upper 2 m of core 0501.029 were recovered using an Edelman auger; in that case, each data point represents the average MS of a ten centimetre interval.

Marine core D13902 was measured at the Southampton Oceanography Centre (Abrantes *et al.*, 2008). All other marine cores were measured at the Research Centre Ocean Margins (RCOM) in Bremen, Germany (Monteiro *et al.*, 2002; Segl *et al.*, 2004; Labeyrie and Turon, 2005a, b; Segl and Alt-Epping, 2005a, b).

4.3 RESULTS

Terrestrial cores

Core 0501.029 (Fig. 4.2)

This core was recovered in nature reserve Paul do Boquilobo (Fig. 4.1). The total core covers the last ~7000 years and measures 12 m, of which the upper 6 m are used here. The Holocene Tagus channel was always located ~4 km northwest from this site, implying continuous low-energy backswamp conditions (Chapter 3); clay units reflect periods of more frequent Tagus flooding.

The lithological column (Fig. 4.2a) shows at the base calcareous gyttja (6-4.7 m below surface) deposited between 3390-3210 cal BP (UtC-14747) and ~2200 cal BP at a rate of ~1.2 mm/y. The overlying peat interval (4.7-3.1 m) with LOI values up to 60 % (Fig. 4.2e) accumulated at a rate of ~1.3 mm/y until 1180-960 cal BP (UtC-14749) and 1060-790 cal BP (UtC-14750), when peat growth abruptly ended due to the onset of clay deposition at 3.1 m depth. This upper clay layer was deposited at a higher sedimentation rate of ~3.1 mm/y, contains plant roots and has low LOI values (~8 %). The onset of sedimentation coincides with a MS peak of 230x10-5 SI at 3.1 m depth (Fig. 4.2b), just above a charcoal-rich layer—burnt soil is known to give high MS values (Thompson *et al.*, 1980; Weston, 2002). Generally, MS increased strongly from ~3.4 m upwards, coinciding with decreasing LOI values, marking the transition from peat-dominated to clay-dominated deposition. Above the MS peak at 3.1 m depth, MS values remain relatively high, fluctuating around an average of ~7 · 10^{-5} SI. The interval below 3.4 m depth holds virtually no MS signal.
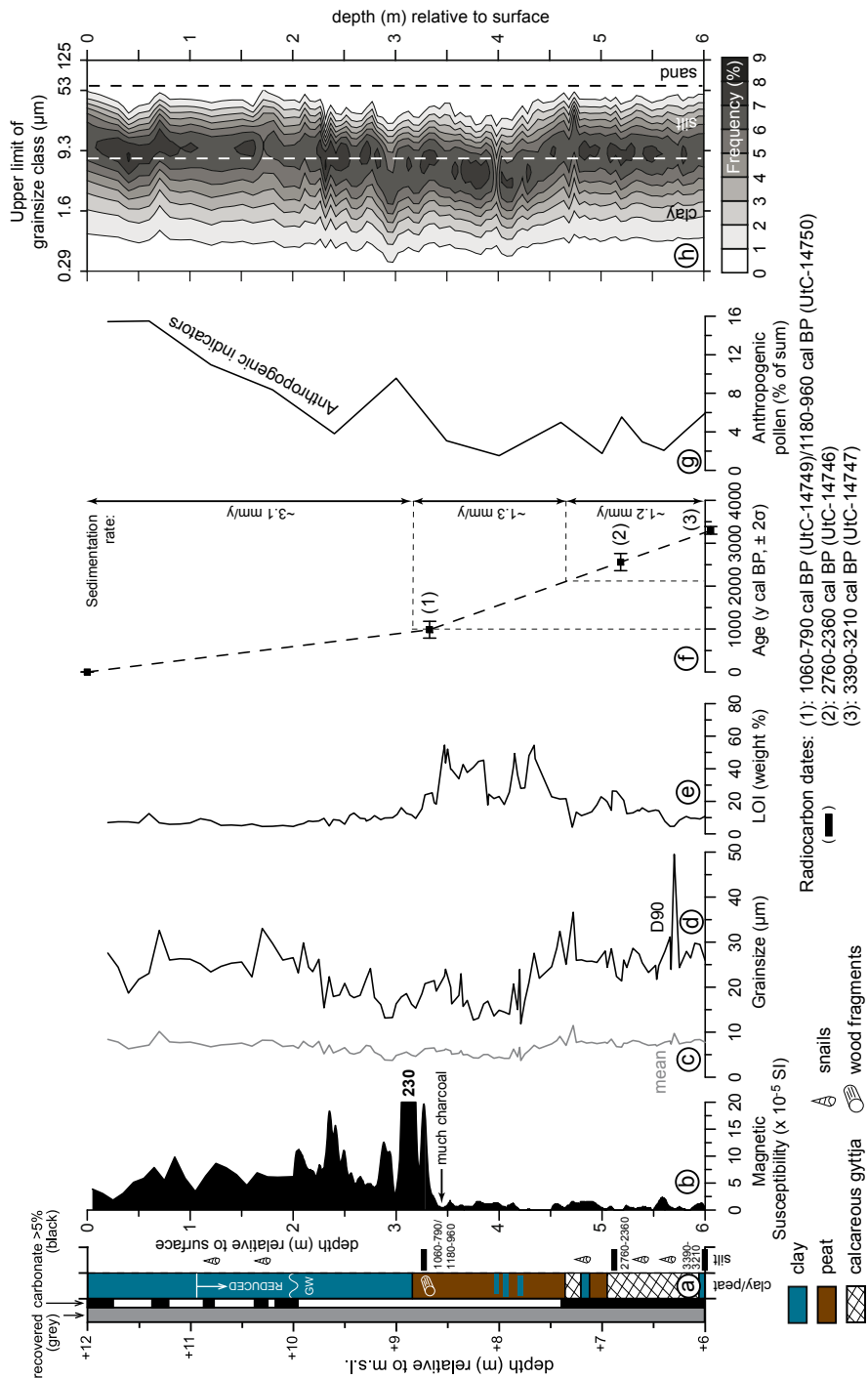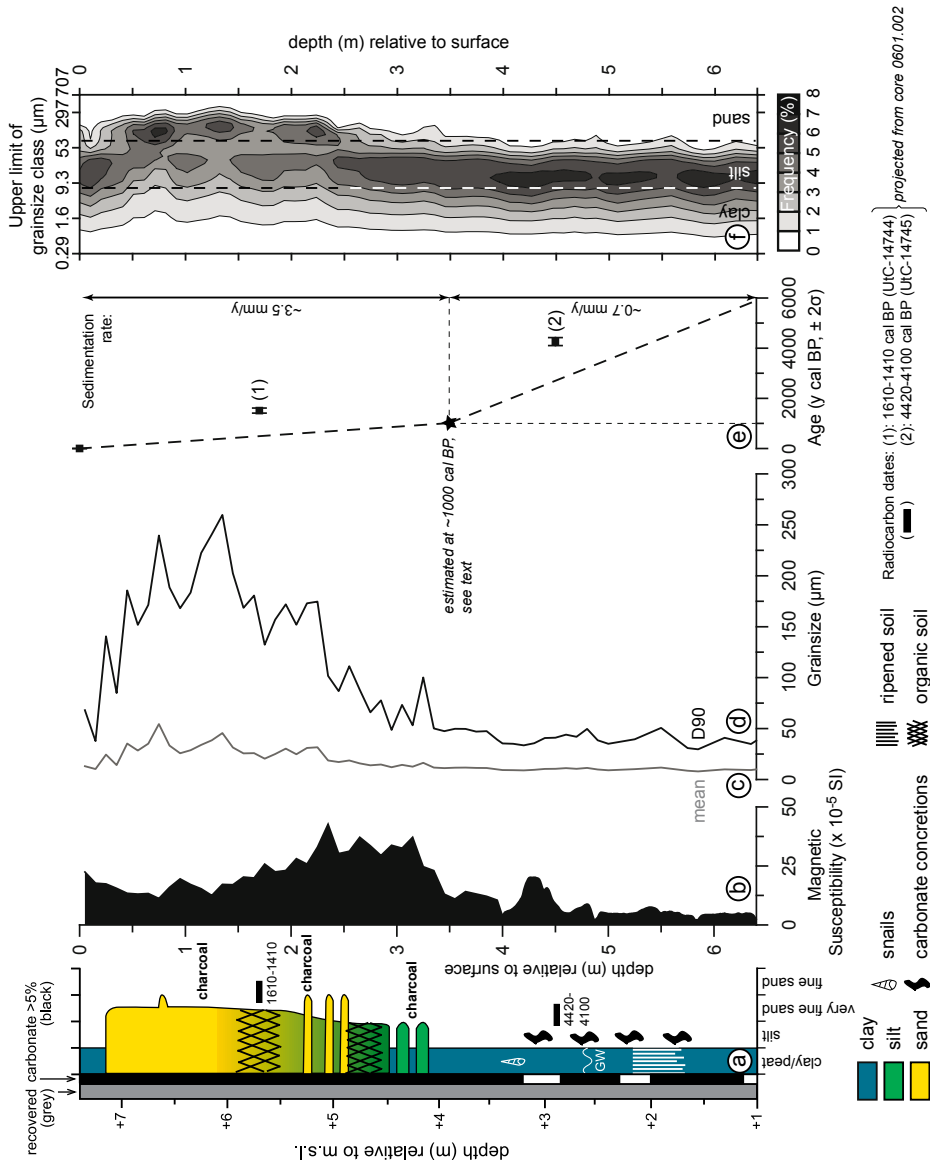
Figure 4.2 | Terrestrial core 0501.029 from Paul do Boquilobo; a) lithological column; b) magnetic susceptibility; c) mean grainsize; d) D90 grainsize; e) loss-on-ignition (LOI); f) radiocarbon age and sedimentation rate; g) pollen percentage indicating anthropogenic impact; h) grainsize distribution.
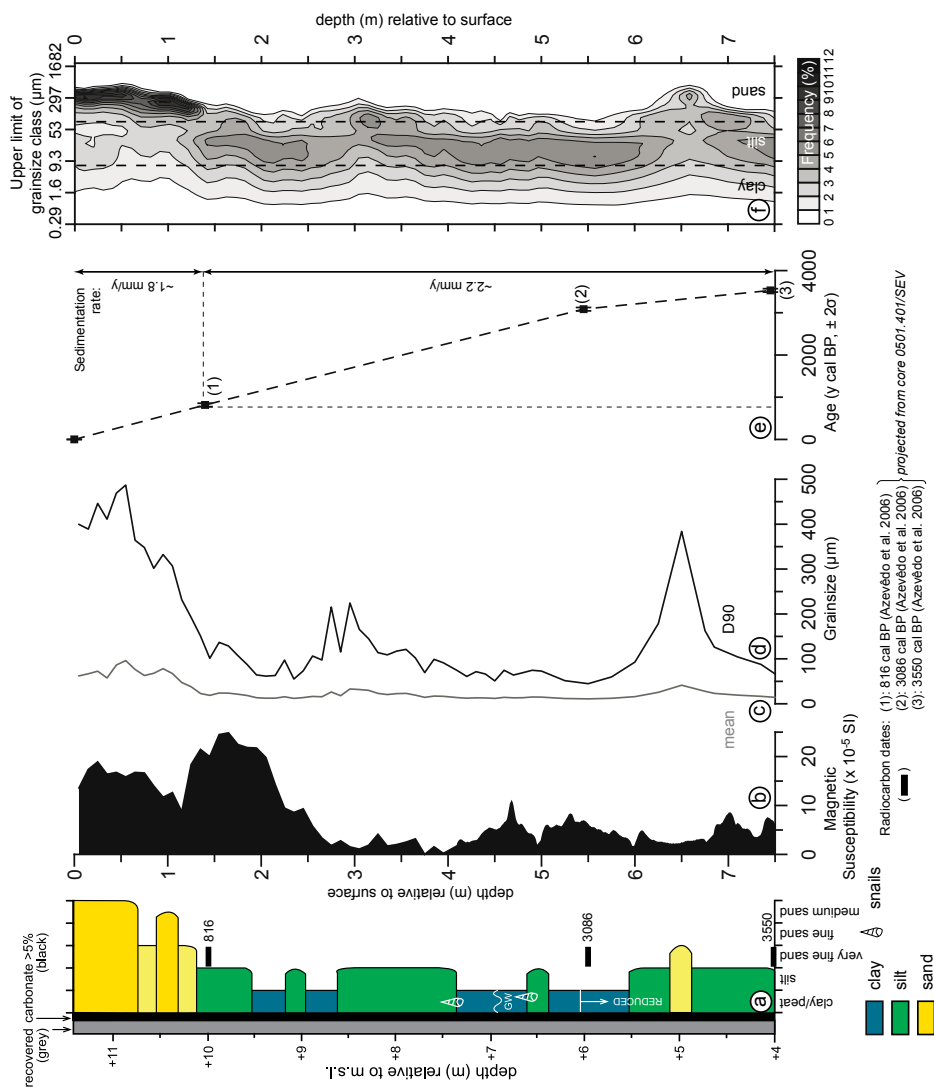
Figure 4.3 | Terrestrial core 0501.016 from Almeirim; a) lithological column; b) magnetic susceptibility; c) mean grainsize; d) D90 grainsize; e) radiocarbon age and sedimentation rate; f) grainsize distribution.

Figure 4.4 | Terrestrial core 0501.025 from Benfica do Ribatejo; a) lithological column; b) magnetic susceptibility; c) mean grainsize; d) D90 grainsize; e) radiocarbon age and sedimentation rate; f) grainsize distribution.

Core name	Cruise	Core type	Lat (°N)	Long (°W)	X (m)	Y (m)	Elevation (m)	Length (m)	Source
0501.016	Terrestrial core	Edelman auger + gauge	39° 15'57"	8° 38'27"	531.088	4346.563	11.38	23	This study
0501.025	Terrestrial core	Edelman auger + gauge	39° 08'51"	8° 42'00"	526.038	4333.421	7.42	13	This study
0501.029	Terrestrial core	Edelman auger + gauge	39° 23'06"	8° 31'55"	540.407	4359.849	12.00	12	This study
0501.401	Terrestrial core	Edelman auger + gauge	39° 16'16"	8° 38'48"	530.589	4347.131	11.15	19.4	Azevêdo et al. (2006a)
0601.002	Terrestrial core	Edelman auger + gauge	39° 08'44"	8° 41'44"	526.420	4333.197	5.00	6.5	This study
D13902	Discovery D249	Piston core	38° 33'24"	9° 20'13"	470.762	4267.846	-90.00	6	Abrantes et al. (2008)
GeoB-8903-1	Poseidon PO304	Gravity core	38° 37'30"	9° 30'29"	455.895	4275.498	-102.00	5.4	Segl & Alt-Epping (2005a)
GeoB-8904-1	Poseidon PO304	Gravity core	38° 36'43"	9° 31'58"	453.734	4274.061	-112.00	5.6	Segl & Alt-Epping (2005b)
MD99-2332	Marion Dufresne MD114	Giant Piston core	38° 33'32"	9° 22'01"	468.149	4268.103	-97.00	3.2	Labeyrie & Turon (2005a)
MD99-2333	Marion Dufresne MD114	Piston core	38° 36'00"	9° 25'01"	463.813	4272.684	-91.00	3.47	Labeyrie & Turon (2005b)
MD03-2700G	Marion Dufresne MD134	Giant Piston core	38° 33'24"	9° 32'01"	453.626	4267.928	-106.00	3.97	SEDPORT project
Po287-26B	Poseidon PO287	Box core	38° 33'30"	9° 21'48"	468.464	4268.040	-96.00	0.52	Monteiro et al. (2002)
Po287-26G	Poseidon PO287	Gravity core	38° 33'30"	9° 21'48"	468.464	4268.040	-96.00	3.05	Monteiro et al. (2002)
Po287-28G	Poseidon PO287	Gravity core	38° 37'30"	9° 30'54"	455.290	4275.501	-105.00	~6.2	Monteiro et al. (2002)

Table 4.1 | Location and collection details of terrestrial and marine cores. Longitude-lattitude in UTM/WGS84, coordinates (X-Y) in European Datum 1950/UTM Zone 29N.

Core	Lab. Nr.	14C age yrs. BP ± 1σ	dR ± SD (y)	Age cal BP 2σ	Mean cal BP	Calibration curve	Coordinates (x-y/z) (m)	Sample depth (cm)	Material	14C type	Source
0501.029	UtC-14747	3089 ± 38	--	3390-3210	3300	intcal04.14c	540.407-4359.849/+12	604-607	terrestrial macrofossils	AMS	This study
0501.029	UtC-14746	2530 ± 60	--	2760-2360	2560	intcal04.14c	540.407-4359.849/+12	516-520	terrestrial macrofossils	AMS	This study
0501.029	UtC-14749	1022 ± 37	--	1060-790	925	intcal04.14c	540.407-4359.849/+12	331-334	organic fraction < 125 μm	AMS	This study
0501.401	unknown	unknown	--	816	816	intcal04.14c	530.589-4347.131/+11.15	103-104	peat/wood	unknown	Azevêdo et al. (2006a)
0501.401	unknown	unknown	--	3086	3086	intcal04.14c	530.589-4347.131/+11.15	454-455	peat/wood	unknown	Azevêdo et al. (2006a)
0501.401	unknown	unknown	--	3550	3550	intcal04.14c	530.589-4347.131/+11.15	649-650	peat/wood	unknown	Azevêdo et al. (2006a)
0601.002	UtC-14744	1630 ± 35	--	1610-1410	1510	intcal04.14c	526.420-4333.197/+5	140-150	bulk clay	AMS	This study
0601.002	UtC-14745	3849 ± 47	--	4420-4100	4260	intcal04.14c	526.420-4333.197/+5	280-290	bulk clay	AMS	This study
GeoB-8903-1	KIA 30888	< 0	262 ± 164	0	0	marine04.14c	455.895-4275.498/-102	8-12	plankt. forams (G. bulloides)	AMS	Abrantes et al. (2008)
GeoB-8903-1	KIA 28966	610 ± 35	262 ± 164	0	0	marine04.14c	455.895-4275.498/-102	51-53	plankt. forams (G. bulloides)	AMS	Abrantes et al. (2008)
GeoB-8903-1	KIA 30890	735 ± 55	262 ± 164	418-0	209	marine04.14c	455.895-4275.498/-102	65-70	plankt. forams (G. bulloides)	AMS	Abrantes et al. (2008)
GeoB-8903-1	KIA 28967	760 ± 25	262 ± 164	423-0	212	marine04.14c	455.895-4275.498/-102	139-141	plankt. forams (G. bulloides)	AMS	Abrantes et al. (2008)
GeoB-8903-1	KIA 28968	685 ± 30	262 ± 164	0	0	marine04.14c	455.895-4275.498/-102	171-173	plankt. forams (G. bulloides)	AMS	Abrantes et al. (2008)
GeoB-8903-1	KIA27064	760 ± 45	262 ± 164	428-0	214	marine04.14c	455.895-4275.498/-102	198	plankt. forams (G. bulloides)	AMS	Abrantes et al. (2008)
GeoB-8903-1	KIA 27065	1035 ± 30	262 ± 164	650-0	325	marine04.14c	455.895-4275.498/-102	248	plankt. forams (G. bulloides)	AMS	Abrantes et al. (2008)
GeoB-8903-1	KIA 27066	1660 ± 35	262 ± 164	1272-649	961	marine04.14c	455.895-4275.498/-102	333	plankt. forams (G. bulloides)	AMS	Abrantes et al. (2008)
GeoB-8903-1	KIA 27067	2000 ± 40	262 ± 164	1661-935	1298	marine04.14c	455.895-4275.498/-102	413	plankt. forams (G. bulloides)	AMS	Abrantes et al. (2008)
GeoB-8903-1	KIA 27320	2885 ± 40	262 ± 164	2724-1913	2319	marine04.14c	455.895-4275.498/-102	493	plankt. forams (G. bulloides)	AMS	Abrantes et al. (2008)
PO287-26G	OS-42381	545 ± 25	263 ± 164	232-169	201	marine04.14c	468.464-4268.040/-96	86-87	mollusc	AMS	Abrantes et al. (2008)
PO287-26G	KIA 23661	1310 ± 25	264 ± 164	915-764	840	marine04.14c	468.464-4268.040/-96	86-88	turritella	AMS	Abrantes et al. (2008)
PO287-26B	AAR-8368.2-K	440 ± 25	265 ± 164	73-33	53	marine04.14c	468.464-4268.040/-96	51-52	mollusc	AMS	Abrantes et al. (2008)
D13902	AAR-7825	492 ± 39	266 ± 164	148-12	80	marine04.14c	470.762-4267.846/-102	75.4-76.4	mollusc	AMS	Abrantes et al. (2008)
D13902	AAR-7207	1160 ± 45	267 ± 164	772-653	713	marine04.14c	470.762-4267.846/-102	110.4-111.4	mollusc	AMS	Abrantes et al. (2008)
D13902	AAR-7828	2007 ± 37	268 ± 164	1568-1403	1486	marine04.14c	470.762-4267.846/-102	151-152	mollusc	AMS	Abrantes et al. (2008)
D13902	AAR-7210	2340 ± 55	269 ± 164	1999-1733	1866	marine04.14c	470.762-4267.846/-102	199-200	mollusc	AMS	Abrantes et al. (2008)

Table 4.2 | Radiocarbon dates from the Lower Tagus Valley and the Tagus mudbelt. Coordinates (X-Y) in European Datum 1950/UTM Zone 29N.

Synchronous with the change from peat to clay-dominated deposition and the increase of MS, the input of pollen indicating anthropogenic impact increased (Chenopodiaceae, *Artemisia*, Campanulaceae, *Echium*-type, *Urtica*, *Xanthium*-type, *Cannabis/Humulus*, *Olea europaea*, *Cerealia*, *Juglans*, *Polygonum aviculare* and Brassicaceae) (Fig. 4.2g), coeval with a decline of tree vegetation. The mean grainsize shows minor coarsening from 3.1 m upwards, especially expressed in the D90 and grainsize distribution (Fig. 4.2c, d, h).

Core 0501.016 (Fig. 4.3)
Core 0501.016 was recovered ~1.5 km northwest of the present Tagus channel in a floodplain/distal levee setting (Chapter 3), thus recording changes in Tagus proximal overbank sedimentation (Fig. 4.1). The sediments of the 23 m long core accumulated since ~9000 cal BP; for this study the upper 7.5 m were used (Fig. 4.3). Chronology is based on three projected radiocarbon dates from coring SEV (Azevêdo *et al.*, 2006a), located 900 m to the northwest (0501.401, Fig. 4.1).

The basal part of the lithological column (7.5-1.4 m) shows an alternation of silt and clay layers with minor mean grainsize changes (Fig. 4.3c). This lower part was deposited at a rate of ~2.2 mm/y between ~3550 cal BP and ~816 cal BP. The sandy interval around 6.5 m depth is attributed to a large flood (Fig. 4.3d, f). The upper 1.4 m, deposited after ~816 cal BP at a rate of ~1.8 mm/y, consist of very fine to medium sand in a coarsening-upward unit. The coarsening is well expressed in the D90, which reaches values up to ~450 μm and the grainsize distribution is strongly skewed and somewhat bimodal with a large medium sand and a minor silt peak, implying levee-type sedimentation (Fig. 4.3f).

In the basal 4.5 m of the core, clay intervals contain higher MS values than silt intervals, suggesting a relationship between finer grainsize and magnetic-particle content (Fig. 4.3a, b) (cf. Oldfield *et al.*, 1985). Around 4.7 m depth a MS peak occurs *within* the clay interval (Fig. 4.3b) and between 3 and 2 m depth MS rises *within* clay layers, suggesting increased magnetic-particle concentration. From ~2 m depth upwards, the MS signal reaches unprecedented values around $15 \cdot 10^{-5}$ SI and both the silt and sand intervals show high MS values.

Core 0501.025 (Fig. 4.4)
This southernmost core was recovered ~300 m east of the Tagus channel (Fig. 4.1) and holds a record of overbank and levee sedimentation (Chapter 3). The core measures ~13 m deposited since ~8000 cal BP, of which the upper 6.4 m were used for this study. Using three radiocarbon dates, a chronology was constructed. The upper two dates were projected to this core from core 0601.002

which is located ~350 m to the east (Chapter 3, Fig. 3.5), based on the stratigraphic position just above a ripened soil (UtC-14745) and on a distinctive organic soil level which was found in both cores (UtC-14744).

The lithological column shows a basal silty clay interval (6.4-3.5 m) deposited at a rate of 0.7 mm/y. A level of soil ripening around 5.5 m depth (Fig. 4.4a) marks the top of tidal marsh deposits, which were deposited here between ~7000 and ~5000 cal BP (Chapter 3). The overlying silty clay (3.5-0 m) resulted from Tagus overbank sedimentation at a rate of 3.5 mm/y (Fig. 4.4d). In this interval charcoal fragments and two organic soil levels were found. The upper soil level was best-developed and dated at 1610-1410 cal BP (UtC-14744). The coarsening-upward unit and the sand layers around 2.5 m depth match a levee-type environment, which is supported by a bimodal grainsize distribution with a silt and a fine sand population between 2.5 and 0.5 m depth (Fig. 4.4f). Both the mean and D90 grainsize (Fig. 4.4 c, d) show a fining-upward trend from ~0.5 m upwards.

The MS signal is low (noise) in the basal clayey 2 m of the core and subsequently rises to a peak of $\sim 20 \cdot 10^{-5}$ SI around 4.2 m depth within the clay interval (Fig. 4.4b). Around 3.5 m depth, MS rises to $\sim 33 \cdot 10^{-5}$ SI, simultaneously with coarsening lithology as visible in the D90 curve (Fig. 4.4d). From 2.5 m depth upwards, MS slowly decreases to $\sim 15 \cdot 10^{-5}$ SI while lithology coarsens further; possibly because of less fine-grained magnetic particles in the sandy sediment.

Interpretation of terrestrial cores

In the upper 2-3 m of all cores the grainsize coarsens upwards, implying an increased flooding frequency and/or intensity. Sedimentation rates increase up to threefold in this interval. Although compaction of the organic-rich deposits in the lower part of core 0501.029 created syn-sedimentary accommodation space, the sudden change from peat accumulation to clay deposition at 3.1 m depth must have been controlled by a sudden increase of Tagus overbank sedimentation. Increased overbank sedimentation is corroborated by a tripled sedimentation rate, low values of LOI, the coarsening-upward grainsize and by 2-3 m of overbank deposits covering a ~850 years old floodplain soil in the Golegã cross section north of core 0501.029 (Chapter 3, Fig. 3.2). Furthermore, the regional anthropogenic pollen content increases strongly in the upper 3 m of this core and simultaneously there is a strong increase of the MS signal in the upper part of the other cores.

The sedimentary and ecological changes mentioned above strongly suggest increased human impact on floodplain sedimentation. The strong increase of MS can be explained by the increased supply of magnetic particles from eroded soils and sediments (cf. Thompson *et al.*, 1980; Dearing *et al.*, 1986;

Faleh *et al.*, 2005). Burning possibly enhanced in-situ soil MS in the catchment (Thompson *et al.*, 1980; Weston, 2002), as supported by the increased amount of charcoal in the younger (<500 yr) levee and fluvial channel deposits.

The lower 6 m in core 0501.016 (Fig. 4.3) and the lower 3 m in core 0501.025 (Fig. 4.4) have a relatively stable grainsize distribution, apart from some sand intervals in core 0501.016. Although the MS signals are equally stable in both cores, around 4.5 m depth a MS peak is present within a uniform clay layer. This suggests a larger supply of magnetic particles to both sites (cf. Oldfield *et al.*, 1985). Fine-grained (< 0.03 μm) magnetic particles in palaeosols are responsible for increased in-situ MS values (Oldfield *et al.*, 1985; Maher and Thompson, 1991; Zheng *et al.*, 1991; Maher and Thompson, 1992). Furthermore, widely occurring Cambic Bw horizons in Cambisols in the Tagus catchment (European Soil Portal, 2008) show relatively high MS values in the upper 20-50 cm because of weathering and pedogenic Fe_2O_3 formation (FitzPatrick, 1983; Hanesch and Scholger, 2005). Therefore, the MS peaks in both cores may indicate that fine grained soil material was eroded from the catchment (cf. Faleh *et al.*, 2005) and at least partly deposited in the Lower Tagus Valley floodplain.

Marine core

Core GeoB-8903-1 (Figs. 4.5 and 4.6)

Recovered from the Tagus mudbelt at 102 m water depth, core GeoB-8903-1 (Figs. 4.1 and 4.5) measures 5.4 m and is dominated by silt and clay. Using 10 AMS radiocarbon dates based on planktonic foraminifera, a chronology was established. The upper 2 m are constrained by six dates, which all lie within the last ~400 years cal BP (2σ) (Table 4.2). Four C-14 ages between 0.65 and 1.98 m depth (735 ± 55 BP (KIA 30890), 760 ± 25 BP (KIA 28967), 685 ± 30 BP (KIA 28968) and 760 ± 45 BP (KIA 27064)) have overlapping 1σ standard deviations, making them virtually coeval. The similar ages of the upper six radiocarbon dates may be the result of the tsunami of 1755 AD. However, in core GeoB-8903-1 sedimentary characteristics pointing to erosion/deposition caused by a tsunami were not identified (Alt-Epping *et al.*, 2009).

The lithological column (Fig. 4.5a) shows a silt-dominated basal interval (5.4-3.1 m depth), which was deposited at a rate of ~1.2 mm/y since about 2724-1913 cal BP (KIA 27320). Shortly after that date, between 5 and 4.5 m depth, the MS signal shows the first peak of ~6 · 10^{-5} SI, and a temporal grainsize fining (Fig. 4.5b-d). Between 4.5 and 3.1 m depth, grainsize mean and D90 fluctuate without showing a trend (Fig. 4.5f). The upper 3.1 m accumulated at a rate of ~3.9 mm/y since ~1100-470 cal BP (based on linear interpolation from KIA 27066 to KIA 27065). Between 3.1 and 2 m depth the mean and D90 grainsize fine upwards until 428-0 cal BP (KIA 27064)
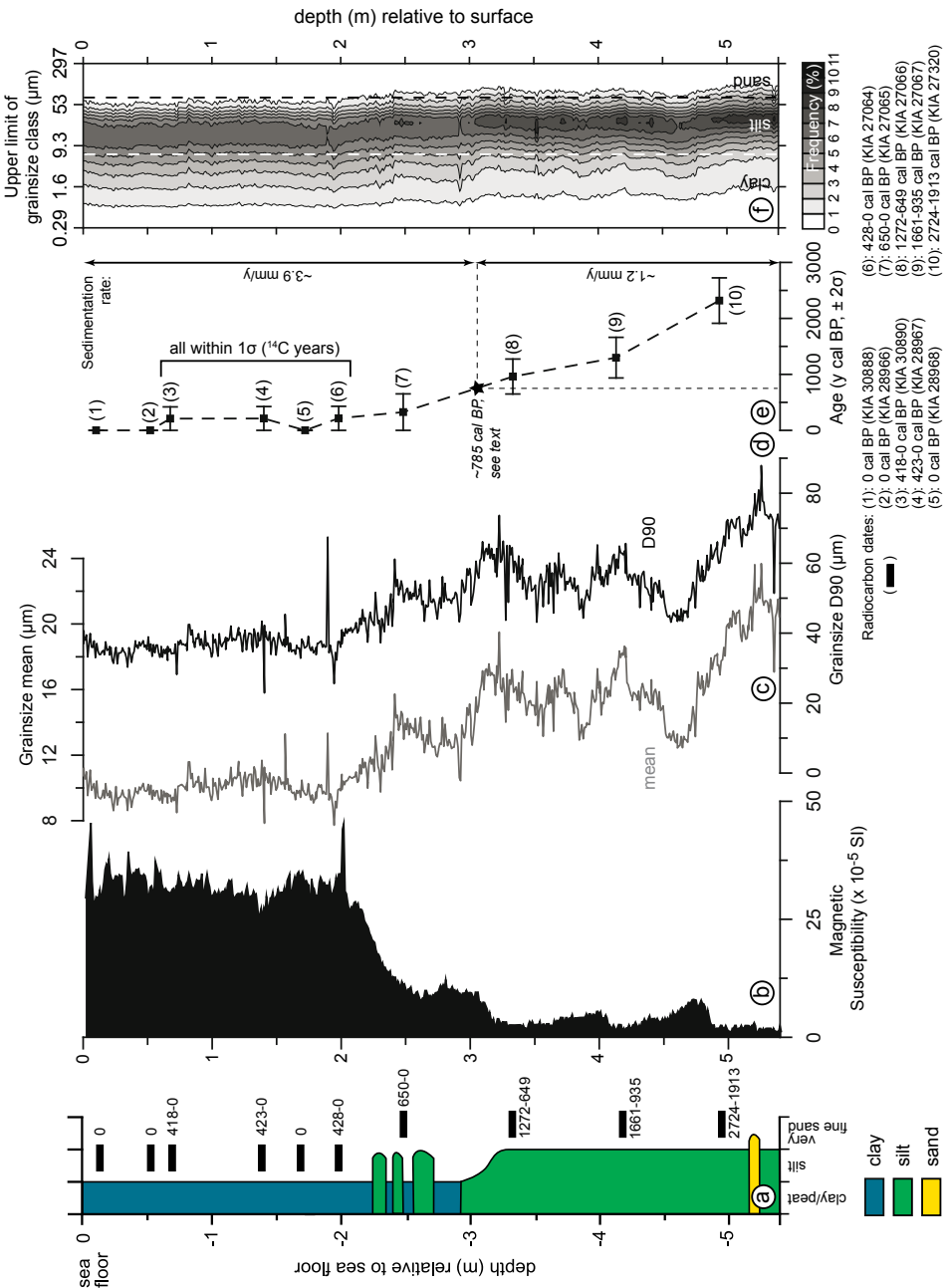
Figure 4.5 | Marine core GeoB-8903-1 from the Tagus mudbelt; a) lithological column; b) magnetic susceptibility; c) mean grainsize; d) D90 grainsize; e) radiocarbon age and sedimentation rate; f) grainsize distribution.
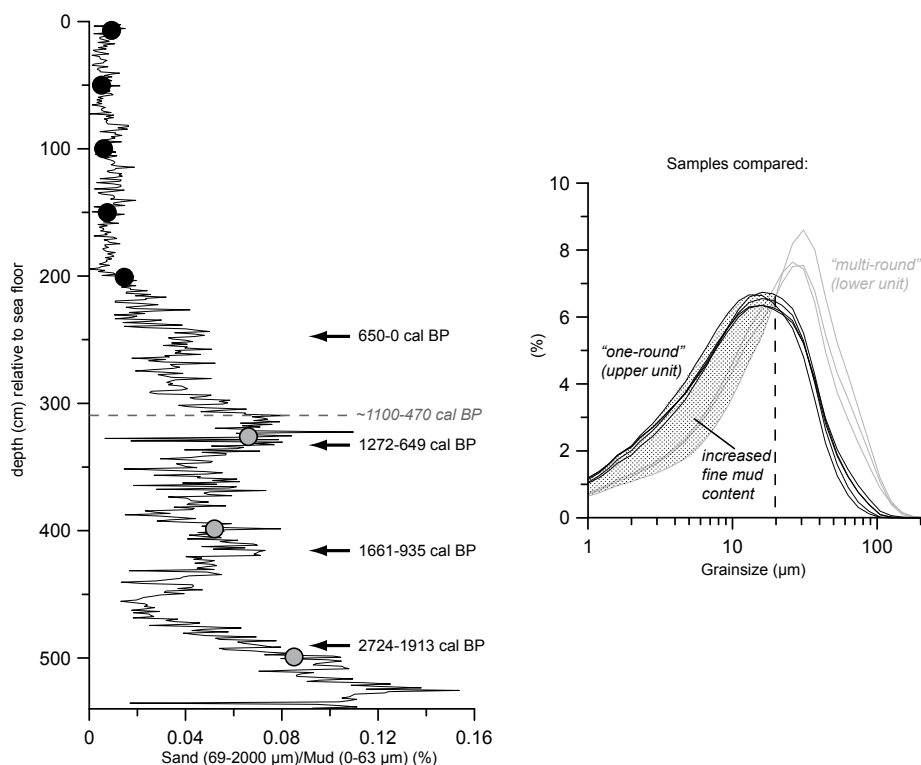
Figure 4.6 | Sand/mud ratio for marine core GeoB-8903-1 (left) and selected grainsize frequency diagrams from circled intervals (right). An upcore increase of fine mud content is visible in both the sand/mud ratio and the grainsize frequency diagrams, with the transition around 1100-470 cal BP.

and between 3.1 and 2.7 m depth the MS shows a peak with values around $10 \cdot 10^{-5}$ SI in a finer grained layer. Above that peak, MS rises rapidly to values around $33 \cdot 10^{-5}$ SI at ~2 m depth simultaneously with further grainsize fining. The upper 2 m are finest grained and very uniform and homogeneous with continuously high MS values (Fig. 4.5b, c). The observed correspondence between the major MS patterns and the grainsize changes suggests that the clay-dominated intervals contain most magnetic particles. This is corroborated by XRF-Fe measurements by Abrantes *et al.* (2008) and by an excellent correlation (R^2=0.9) between MS and the finest grainsize end-member in the core (EM1, average grainsize 6 μm, Alt-Epping *et al.*, 2009).

The MS changes of this marine core resemble the MS signal of the floodplain cores. However, the coeval grainsize changes are the opposite from the changes on land. Grainsize shows a fining-upward trend offshore, with overall decreasing sand (from 10 to 0.5 %) and silt (from 70 to 55 %) concentrations in favour of clay (from 20 to 40 %) concentrations (Fig. 4.5f). This offshore grainsize fining can be explained by mixing processes occurring in the Tagus estuary and sedimentary processes taking place on the Tagus shelf.

119

Suspended sediments in the Tagus estuary were thoroughly mixed due to tidal currents and the turbidity maximum (Vale and Sundby, 1987; Barros, 1996). Subsequent transport to the shelf occurred as surficial and bottom nepheloid layers (Jouanneau *et al.*, 1998), where further mixing took place (McCave *et al.*, 1995). The strong mixing of suspended sediment during offshore transport, limits reasons to assume that the grainsize change in core GeoB-8903-1 reflects an altered composition of the source of suspended sediment.

To examine sedimentary processes on the shelf, we compared individual grainsize distributions from eight levels in core GeoB-8903-1 (Fig. 4.6). A distinct change was observed between 3.2 and 2.0 m depth. The grainsize distributions of the three deepest samples have a higher concentration in the fraction 20-200 μm, whereas the upper five samples have a higher concentration in the fraction 0-20 μm. This implies an upward increase in the <20 μm fraction (cf. Alt-Epping *et al.*, 2009). The grainsize distributions of the three deepest samples closely resemble "multi-round" distributions (Kranck *et al.*, 1996b). These are sediments which have been resuspended and settled causing further sorting after initial deposition. Each resuspension event ("round") removed the fine-grained particles and changed the grainsize distribution, thereby steepening the fine-grained limb of the grainsize distribution. The five upper grainsize distributions closely resemble "one-round" distributions (Kranck *et al.*, 1996a), which result from settling from suspension without subsequent reworking. This means that the grainsize distribution of the upper five samples resembles the distribution of the parent suspension. Therefore, these samples have experienced considerably less postdepositional sorting (winnowing) than the lower three samples.

The decreased effect of winnowing in the upper ~3.1 m resulted in preservation of the fine mud fraction (Fig. 4.6). Winnowing apparently was less effective in the upper interval, suggesting changed boundary conditions. Either winnowing occurred less than before, or the relative effect of winnowing decreased due to rapid sedimentation resulting from an increased suspended sediment flux. The latter explanation is supported by a threefold increase in sedimentation rate for the upper ~3.1 m. The increased suspended sediment flux also has a hydrodynamic meaning, since silt in the 10-63 μm fraction is deposited as sortable single grains, whereas silt and clay in the 0-10 μm fraction demonstrate cohesive behaviour of flocculated aggregates (McCave *et al.*, 1995). An increased suspended sediment concentration also led to more flocculation and a larger depositional flux of sediment in the 0-10 μm fraction. When silt and clay in the 0-10 μm fraction reach the ocean floor, the cohesive sediment behaviour also hampers resuspension and sorting, making winnowing less effective as well.
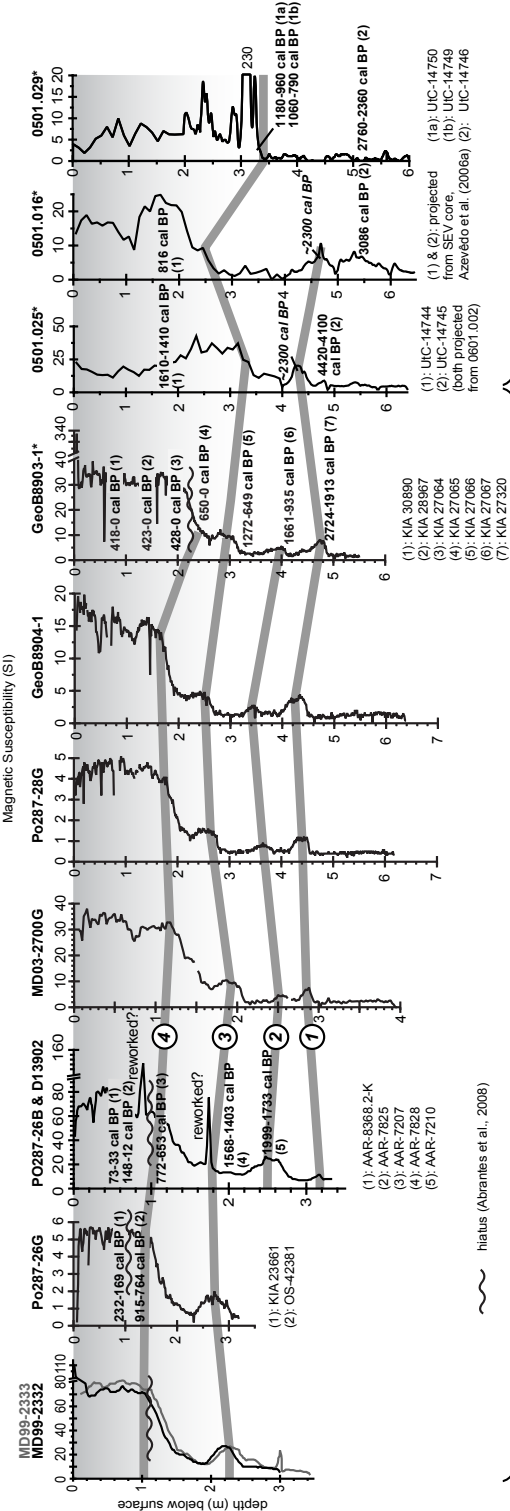
Land-sea correlation

To explain the large-scale depositional changes in the Tagus terrestrial and marine system we correlated the three floodplain records and the marine record presented above together with records from eight previously studied mudbelt cores (Fig. 4.7, Table 4.1). The latter cores were used to extrapolate the results from core GeoB-8903-1 to the entire Tagus mudbelt using radiocarbon dates and MS signals. Striking similarities in timing are visible between the floodplain and mudbelt cores, suggesting that deposition was controlled by external forcing.

The two oldest depositional phases correspond with modest grainsize fining in core GeoB-8903-1. They coincide with relatively small MS peaks in five cores across the mudbelt (Fig. 4.7, Nos. 1 and 2). Phase 1 has an age of 2724-1913 cal BP (KIA 27320, core GeoB-8903-1). Phase 2 has an average age of ~1600 cal BP, based on a date in core D13902 (1999-1733 cal BP, AAR-7210) and in core GeoB-8903-1 (1661-935 cal BP, KIA 27067).

Depositional phase 1 was identified in two terrestrial cores (0501.025 & .016) (Fig. 4.7, No. 1). In core 0501.025 a level just below this peak was dated at 4420-4100 cal BP (UtC-14745). This date is based on a bulk clay sample which may be contaminated with old carbon. Other studies have also found too old ages for bulk samples (up to 1500 years) due to old carbon in the depositional system (Colman *et al.*, 2002; Van der Schriek *et al.*, 2007b). The date of ~3086 cal BP in core 0501.016 is in agreement with the estimated age of ~2300 cal BP for depositional phase 1. Depositional phase 2 could not be identified in the terrestrial cores.

Clearly recognisable in all cores is depositional phase 3 (Fig. 4.7), which preludes the upper interval with high MS values (No. 4). The average age of depositional phase 3 is ~1100 cal BP, based on dates in marine cores D13902 (1568-1403 cal BP, AAR-7828) and GeoB-8903-1 (1272-649 cal BP, KIA 27066) and dates in terrestrial core 0501.029 (1060-790 cal BP, UtC-14749 and 1180-960 cal BP, UtC-14750). Grainsize changes are modest, showing some grainsize decrease offshore and a modest increase on land.

During depositional phase 4 grainsize strongly decreases offshore and increases onshore and sedimentation rates increase up to threefold. All cores show high MS values (Fig. 4.7, No. 4). Deposition of this upper interval starts ~670 cal BP, based on dates of 915-764 cal BP (KIA 23661), 772-653 cal BP (AAR-7207), 650-0 cal BP (KIA 27065) and 816 cal BP. Hiatuses and instantaneously deposited layers associated with the 1755 tsunami may be present in the upper 2-3 m of some marine cores (Abrantes *et al.*, 2008, Fig. 7). Because the grainsize decrease and MS increase at level No. 4 predates these hiatuses, a strong external forcing is assumed for this depositional phase. In the terrestrial cores, the relatively small fluctuations of MS in the upper interval (above No.

depth (m) below surface

Magnetic Susceptibility (SI)

TERRESTRIAL CORES

MARINE CORES

0501.029*
230
1180-960 cal BP (1a)
1060-790 cal BP (1b)
2760-2360 cal BP (2)
(1a): UtC-14750
(1b): UtC-14749
(2): UtC-14746

0501.016*
816 cal BP (1)
~2300 cal BP
3086 cal BP (2)
(1) & (2): projected from SEV core,
Azevêdo et al. (2006a)

0501.025*
1610-1410 cal BP (1)
~2300 cal BP
4420-4100 cal BP (2)
(1): UtC-14744
(2): UtC-14745
(both projected from 0601.002)

GeoB8903-1*
418-0 cal BP (1)
423-0 cal BP (2)
428-0 cal BP (3)
650-0 cal BP (4)
1272-649 cal BP (5)
1661-935 cal BP (6)
2724-1913 cal BP (7)
(1): KIA 30890
(2): KIA 28967
(3): KIA 27064
(4): KIA 27065
(5): KIA 27066
(6): KIA 27067
(7): KIA 27320

GeoB8904-1

Po287-28G

MD03-2700G

PO287-26B & D13902
73-33 cal BP (1)
148-12 cal BP (2)
772-853 cal BP (3)
reworked?
1568-1403 cal BP (4)
1999-1733 cal BP (5)
(1): AAR-8368.2-K
(2): AAR-7825
(3): AAR-7207
(4): AAR-7828
(5): AAR-7210

Po287-26G
232-169 cal BP (1)
915-764 cal BP (2)
(1): KIA 23661
(2): OS-42381

MD99-2333
MD99-2332

hiatus (Abrantes et al., 2008)

3) can be related to grainsize changes, caused by levee progradation in the floodbasin environment.

4.4 DISCUSSION

Value of magnetic susceptibility

Local formation or dissolution of magnetic particles may however hamper the interpretation of MS records. Under poorly drained or prolonged water-logged reducing conditions, ferric iron (Fe(III)) changes to the more soluble ferrous iron (Fe(II)), which is accompanied by loss of reddish and brownish soil colours in favour of a grey colour (Weston, 2002; Grimley and Arruda, 2007). Despite the grey colour of the sediment and reducing conditions below 1 m depth in the waterlogged core 0501.029, the MS values are high (Fig. 4.2b), implying that the magnetic particles were not dissolved and removed or formed in-situ and therefore they were transported to the site and deposited with the sediment. The other two terrestrial cores were taken from dry floodplain sites with reducing conditions at 6-7 m below the surface (Figs. 4.3 and 4.4) and therefore they were not affected much by dissolution of magnetic particles. Although the floodplain soils are young and immature and situated in a dynamic environment, formation of in-situ magnetic particles through pedogenesis may have occurred. However, the major MS changes in these two terrestrial cores occur in homogeneous, fully oxidized floodplain sediments far above the groundwater level.

In the marine environment formation of autochthonous biogenic magnetite and the magnetic sulphide greigite may have complicated the MS signal. Greigite can form at or near the sediment/water interface in a decade or less in the marine realm (Oldfield *et al.*, 2003). However, in the marine cores the striking similarity of the MS signals despite varying sediment layer thicknesses, indicates that biogenic magnetite and greigite formation was of minor importance.

Bulk density changes may have occurred due to post-depositional compaction. However, no correction was made for dry bulk density because the well oxygenated clastic fluvial sediments have not experienced much compaction. Offshore, the sediments are much softer and experienced more compaction than on land. The upper metres of the marine cores consist of very soft sediment. In case of a constant supply of magnetic particles, an increasing

Figure 4.7 | Land-sea correlation of 9 marine cores and 3 terrestrial cores. The cores indicated with (*) originate from this study. Four phases were distinguished: 1) ~2300 cal BP; 2) ~1600 cal BP; 3) 1100 cal BP and 4) since ~670 cal BP. Italic ages are interpreted values; see text for explanation. Merging of records of cores PO287-26B and D13902, and hiatuses are based on Abrantes *et al.* (2008).

MS signal is expected with depth, because the upper lower-density sediment contains fewer particles. Nonetheless, the soft upper sediments contain the highest MS values, which confirms a higher supply of magnetic particles to the shelf.

Although volume-based magnetic susceptibility is the most basic magnetic susceptibility measurement, the results of this study suggest its applicability for correlation of deposits in conjunction with other sedimentological data (grainsize, LOI, pollen, radiocarbon ages). The similarity of magnetic susceptibility patterns and their timing in the studied cores shows that volume-based magnetic susceptibility can be used as a tool to correlate terrestrial and marine records.

Climate change

The last 2500 years have experienced climatic changes like the Medieval Warm Period (900-1200 AD/1050-750 cal BP) and the Little Ice Age (1550-1900 AD/400-50 cal BP). In addition, during the 20th century Tagus winter discharge was largely controlled by the North Atlantic Oscillation, a relationship which probably also existed during previous periods of the Holocene (Trigo *et al.*, 2004). Although these climate changes have occurred, their impact on the sedimentary records is unclear. Furthermore, the major climate change from a humid to a drier climate around 5000 cal BP was not recognised in the fluvial records of the Lower Tagus Valley (Chapter 3). On the other hand, the limited chronological resolution of our cores hampers identification of short-term climatic changes. Recently it has been shown for the temperate-climate Meuse River that increased mean annual discharge and frequency of high-flow events can be ascribed to land use changes (mainly deforestation), while the effects of climatic change are insignificant (Ward *et al.*, 2008).

Since land-use changes during the last few thousand years in the Tagus catchment may have caused increased runoff, offshore proxy records should be interpreted with caution. For instance, indicators of increased freshwater discharge in the marine realm do not necessarily reflect increased *precipitation* on the continent but may reflect increased runoff and discharge due to the absence of the buffering effect of natural vegetation.

Abrantes *et al.* (2005) and Lebreiro *et al.* (2006) interpreted a larger mean grainsize and low MS values during the Medieval Warm Period in mud-belt cores PO287-26B and D13902 as climate-related decreased runoff. Increased fine-grained deposition, high MS values and the presence of freshwater diatoms in marine sediments during the Little Ice Age, have been interpreted as increased rainfall and a larger Tagus discharge. The MS pattern of these cores closely matches the MS patterns of other cores on the Tagus shelf (Fig. 4.7). Our results from nearby core GeoB-8903-1 (Figs. 4.5 and 4.6) suggest

Archaeological period	yrs. BC/AD	cal BP
Middle Ages	400-1500 AD	1550-450
Islamic period	*711-1492 AD*	*1239-458*
Roman Era	250 BC-400 AD	2200-1550
Iron Age	650-250 BC	2600-2200
Bronze Age	1750-650 BC	3700-2600

Table 4.3 | Archaeological chronology for the Iberian Peninsula (Schattner, 1998; Figueiral and Carcaillet, 2005).

that increased MS values and decreased grainsize were caused by reduced winnowing due to an increased influx of suspended sediment caused by increased Tagus water and sediment discharge. This is corroborated by Thorndycraft and Benito (2006b) who attribute increased fluvial activity since 1300 cal BP in the Spanish part of the Tagus catchment to increased human impact.

Anthropogenic impact on sedimentation

The Tagus catchment is large and the data presented in this study are obtained from the downstream end of the catchment. Therefore, the records in the Lower Tagus Valley and on the shelf provide a smoothed, time-integrated signal of deposition. Upstream of the Lower Tagus Valley (Fig. 4.1) the Tagus is situated in an about 300 km long incised V-shaped valley. Therefore, water and suspended sediment is rapidly transported downstream, thus enabling a link between catchment erosion and sediment deposition in the Lower Tagus Valley. In addition, the intense precipitation in the Tagus catchment during winter storms leads to strong erosion on bare soils and high peak floods. The four depositional phases that have been distinguished above (Fig. 4.7) will be compared with records of human activity in the Tagus catchment. The first human cultivation on the Iberian Peninsula occurred between 6000 and 5000 cal BP (the Neolithic) (Savory, 1968; Múgica *et al.*, 1998; Jorge, 1999).

Depositional phases 1 and 2 | around ~2300 and ~1600 cal BP
Depositional phase 1 occurred around ~2300 cal BP, which coincides with the late Iron Age-early Roman Era and phase 2 occurred around ~1600 cal BP, which is at the end of the Roman Era (Table 4.3). On land, only the oldest phase was registered in the sediments close to the river, without showing a grainsize change (0501.016 and .025; Figs. 4.3 and 4.4). On the shelf, the mudbelt cores registered both phases (Fig. 4.7, Nos. 1 and 2) and in GeoB-8903-1 this coincides with a temporally finer grainsize. On the shelf sediments deposited before ~2300 cal BP were coarse due to relatively strong winnowing.

An increased influx of fine-grained sediment caused subdued winnowing and accumulation of fine-grained sediment.

The modest grainsize changes, sedimentation-rate changes and small MS peaks, imply that sediment supply remained relatively stable during these phases and the increase of Tagus runoff and flooding were probably limited. In the lower Muge valley (Fig. 4.1), a tributary of the Lower Tagus River, increased sedimentation was registered since ~2150 cal BP, which has been attributed to human impact on catchment vegetation (Van der Schriek *et al.*, 2007a).

In the Tagus catchment small-scale vegetation changes were registered between ~2300 and ~1600 cal BP. Around 2500 cal BP a period of local deforestation and over-grazing was registered in the Portuguese Serra da Estrêla (Van den Brink and Janssen, 1985; Van der Knaap and Van Leeuwen, 1995). During the Iron Age, landscapes became more open in central Spain, settlement patterns changed and forest cover progressively degraded, indicating increasing human impact (Atienza *et al.*, 1990; Atienza *et al.*, 1991; Gil-Romera *et al.*, 2008). From ~2000 cal BP onwards vegetation reconstructions indicate that the extent of montane forest in the central Spanish Tagus catchment decreased gradually and signs of human disturbance were detected (Andrade *et al.*, 1990; Andrade *et al.*, 1996; Franco *et al.*, 1997; Múgica *et al.*, 1998). Archaeological evidence suggests that agricultural practices virtually did not change from Roman through Islamic times (711 AD/1239 cal BP), which may be a reason for the limited changes in the sedimentary record until depositional phase 3 (Gerli, 2003).

Depositional phases 3 and 4 | around ~1100 and ~670 cal BP
From ~1100 cal BP onwards, deposition in the Tagus system changed drastically. On land, grainsize and sedimentation rate of the overbank deposits increased together with strongly increasing MS values (Fig. 4.7, No. 3). At the distal swamp site of core 0501.029 (Fig. 4.2), peat growth abruptly ended to be followed by clay deposition. At that site, the regional pollen composition reveals an increased human impact and sedimentation rate (Fig. 4.2). Around 1100 cal BP, the mudbelt cores registered increased MS values (Fig.7, No. 3) and simultaneously, marine core GeoB-8903-1 registered a fining grainsize due to an increased suspended sediment flux (Figs. 4.5 and 4.6). The depositional changes reflect an increased supply of sediment and magnetic particles from the Tagus catchment.

The change in deposition reached its maximum around ~670 cal BP (depositional phase 4). The terrestrial sediments show upward coarsening trends, high sedimentation rates and high MS values (Figs. 4.2-4.4). Pollen types associated with human activity and agriculture reach maximum values
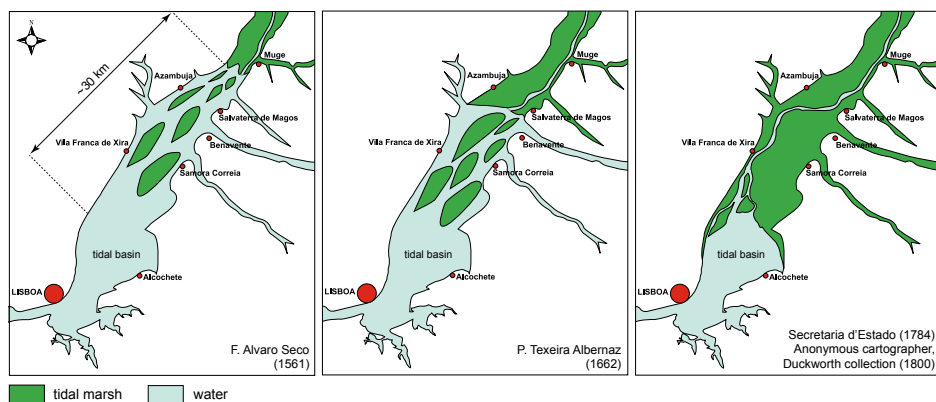
Figure 4.8 | Three maps from the downstream part of the Lower Tagus Valley showing rapid silting of ~30 km of the valley between 1561 and 1800 AD. Maps (A) and (B) are based on maps in Freire (1985) and map (C) is based on two maps (Secretario d'Estado, 1784; Anonymous, 1800).

(Fig. 4.2). Furthermore, the Tagus channel belt was considerably reworked during the last ~600 years, implying strong fluvial activity (Chapter 3). In all marine cores, MS signals increased (Fig. 4.7, No 4) while grainsize in core GeoB-8903-1 became finer (Figs. 4.5 and 4.6).

In the Lower Tagus Valley, already in the 1100s AD (850 cal BP) rapid growth of sand islands in the river (*mouchões*) occurred (Azevêdo, 2001), probably as a result of increased sediment supply related to catchment deforestation and erosion. The generally young age of the Tagus channel deposits agrees with an increased flooding frequency and/or intensity which also transported coarser sediment further onto the floodplain during floods (Chapter 3). In the Tagus catchment in central Spain major phases of increased flood magnitude were reconstructed for the periods 1000-800 cal BP and 520-250 cal BP and attributed to human impact (Thorndycraft and Benito, 2006a). Furthermore, most radiocarbon dates in their study are from the last ~1300 years, suggesting a large Medieval sediment flux. Historic maps clearly show rapid infilling of the Lower Tagus Valley central basin during the last ~500 years as the result of the increased sediment flux (Fig. 4.8).

Palaeo-environmental and historical data demonstrate the increasing human pressure on the landscape during and after the Middle Ages (1550-450 cal BP). Grazing, burning, agriculture and deforestation increased dramatically, leading to the disappearance of natural vegetation and strong erosion of organic top soils (Van den Brink and Janssen, 1985; Janssen, 1994; Van der Knaap and Van Leeuwen, 1995; Múgica *et al.*, 1998). Since 1273 AD (677 cal BP) millions of sheep destroyed the vegetation along their migration routes, causing slope erosion (Gerli, 2003). It was only at the end of the 1600s AD

127

(350 cal BP) that landscape degradation was halted with the establishment of new laws (Klein, 1920; Slicher van Bath, 1960). Mining of ores was of minor importance in terms of sediment supply, since large ore occurrences are rare within the Tagus catchment. However, metal production required much wood, which may have originated partly from the Tagus catchment, adding to the deforestation (Smith, 1979). Regeneration of Mediterranean evergreen forest was difficult due to the marked seasonality of the Mediterranean climate, combined with fire and overgrazing. This resulted in development of a secondary forest—garrigue or maquis—which easily degraded to pasture susceptible to erosion (Tomaselli, 1977; Williams, 2000).

The identified increased sediment flux during especially the last ~1100 years, is most comfortably explained by increased sediment supply from the Tagus catchment due to land-use changes within the catchment in general. The increased sediment delivery to the river and the higher discharges probably occurred due to a reduced vegetation cover, evapotranspiration and water holding capacity of the soil as found all over the globe (e.g. Bosch and Hewlett, 1982; Knox, 2000; 2001; 2006; Andréassian, 2004; De Moor *et al.*, 2008).

4.5 CONCLUSIONS

During the last 2300 years in the Lower Tagus Valley floodplain, grainsize coarsened, sedimentation rate increased up to threefold, LOI values decreased and magnetic susceptibility increased. Contrary to the floodplain, on the Tagus mudbelt on the shelf grainsize fined, together with an up to three times higher sedimentation rate and increased magnetic susceptibility values. These sedimentary changes in the floodplain can be related to an increased flooding frequency and/or intensity, supplying coarser sediment onto the floodplain. Increased magnetic susceptibility values have been interpreted by increased deposition of eroded soil material from the upstream catchment.

The fining grainsize on the offshore mudbelt is explained by an increased suspended sediment flux towards the shelf. The higher concentration of fine mud resulted in subdued winnowing and therefore a better preservation of fine-grained sediment. Furthermore, the higher concentration of suspended sediment probably led to a larger depositional flux.

The radiocarbon age framework and sedimentary characteristics provide a tool to correlate terrestrial and marine sediments and to distinguish synchronous depositional phases. Depositional phases 1 (around ~2300 cal BP) and 2 (around ~1600 cal BP) show minor changes in grainsize, sedimentation rate and magnetic susceptibility. Depositional phases 3 (around ~1100 cal BP) and 4 (since ~670 cal BP) show large changes in grainsize, sedimentation

rate and magnetic susceptibility. Climate impact on the sedimentary records could not be established and most of the sedimentary changes can be related to increased human impact in the Tagus catchment.

CHAPTER 5

The present paper aims to reconstruct Tagus flooding history for the last ~6500 years, and to explain fluvial activity changes in terms of allogenic (climate, human impact) and autogenic (system intrinsic) processes. The flooding history has been determined by cored sedimentary records located ~18 km apart in distal, low-energy backswamps on both sides of the Tagus channel. In these low-energy backswamps, fine-grained sediment layers deposited from suspended load of overbank flood water, reflect periods with multiple overbank floods. By means of a multi-proxy approach (sedimentology,

Holocene flooding history of the Lower Tagus Valley (Portugal)

magnetic susceptibility, grainsize, loss-on-ignition, carbonate content and pollen) sedimentary and environmental changes were identified. At both sites, synchronous lithological intervals accumulated, implying a regional origin for the changes in fluvial activity since ~6500 cal BP. Based on lithological changes, three phases of high fluvial activity (6500-5500, 4900-3500 and 1000-0 cal BP) and two phases of low fluvial activity (5500-4900 and 3500-1000 cal BP) were identified. The progressive decline of regional forest since the end of the African Humid Period (~6000 cal BP) is not reflected in the Tagus flooding history by increased (peak) flood discharges. The dominant allogenic controls of fluvial activity in the Lower Tagus Valley were relative sea level (6500-5500 cal BP), climate (5500-1000 cal BP), and human impact (1000-0 cal BP).

Photo: flooded road due to Tagus flooding, November 2006 (between Valada and Azambuja).

5.1 INTRODUCTION

In northern Tunisia, phases of increased fluvial activity alternating with periods of soil formation have been matched with short-term North Atlantic cooling events (Zielhofer and Faust, 2008). In slackwater deposits of the Spanish Llobregat River periods reflecting increased flooding have been identified for the last 2700 years (Thorndycraft *et al.*, 2005). Further, a database of Spanish radiocarbon dated fluvial units has been used to investigate the relationship between environmental changes and Holocene flooding dynamics (Macklin *et al.*, 2006; Thorndycraft and Benito, 2006a, b; Benito *et al.*, 2008). Six clusters of increased fluvial activity since ~11,000 cal BP have been recognised in the middle Spanish reach of the Tagus River using slackwater deposits and palaeo-flood water-level indicators (Benito *et al.*, 2003c). Phases of increased flooding were associated with regional climatic or environmental changes (Benito *et al.*, 2003b). The Tagus sites mentioned above, are located in the middle bedrock-confined reach of the Tagus River with a lack of data between 7000 and 1000 cal BP (Benito *et al.*, 2003c). In addition, in the middle-reach sites the signal from large downstream Portuguese tributaries is missing.

On the Tagus continental shelf, marine records have been studied for palaeo-discharges and climatic changes, especially for the last 2000 years. Abrantes *et al.* (2005) established a correlation between Tagus discharge and climatic variability during the last two millennia. Discharge was low during the Medieval Warm Period (MWP; 1400-650 cal BP) and increased during the Little Ice Age (LIA; 650-50 cal BP). They attributed the lower discharge during the MWP to a more persistent positive North Atlantic Oscillation (NAO) state or more frequent extreme NAO maxima, while the LIA is coupled to a more persistent negative NAO state or more frequent extreme NAO minima, causing more precipitation and discharge (Abrantes *et al.*, 2005; Lebreiro *et al.*, 2006).

The studies cited above show that the Holocene Tagus flooding and discharge history are still fragmentary. The upstream bedrock-confined Tagus reach contains large hiatuses, while offshore marine studies only cover the last ~2000 years of Tagus palaeo-discharges. Records from the aggrading Holocene floodplain in the Lower Tagus Valley (LTV) have not been studied yet in terms of flooding history. The sediments contain a continuous record of overbank deposition and indications for climate change. Flooding history in the Lower Tagus Valley has only been studied for the period 1855-1998 AD (Azevêdo *et al.*, 2004). Therefore, this chapter aims to reconstruct Tagus flooding history for the last ~6500 years, which is the maximum age of Lower Tagus Valley fluvial deposits (Chapter 3) and to explain fluvial activity changes in terms of allogenic (climate, human impact) and autogenic (system intrinsic)
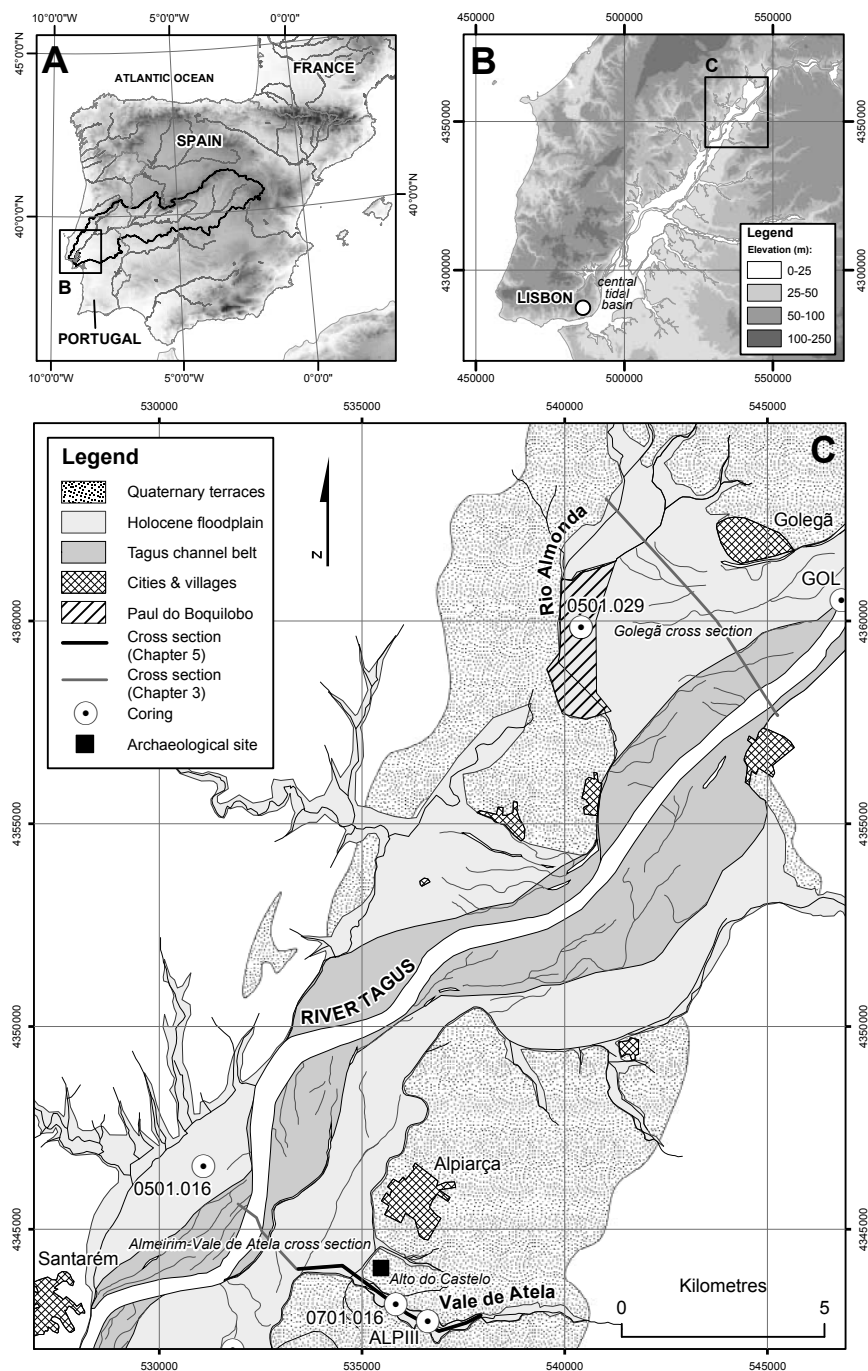
Figure 5.1 | Location map of the Lower Tagus Valley: (A) Tagus catchment and location of Lower Tagus Valley on the Iberian Peninsula, Digital Elevation Data from Jarvis *et al.* (2006); (B) the Lower Tagus Valley and location of study area; (C) study area and location of cross sections and corings. Coordinates (X-Y) in European Datum 1950/ UTM Zone 29N.

processes.

Two Lower Tagus Valley sites with low-energy backswamp conditions at opposite sides of the river channel were selected, in order to extract the regional fluvial activity signal (Paul do Boquilobo and Vale de Atela, Fig. 5.1). The sediments accumulated during the last ~6500 years and contain alternating fine-grained and organic layers (gyttja, peat and humic clay). To reconstruct floodplain geometry two cross sections from a previous study were used (Chapter 3), one of which was combined with new data (Figs. 5.2 and 5.3). A twofold approach was used for the analyses of cores: a sedimentological approach consisting of the determination of grainsize, magnetic susceptibility (MS), loss-on-ignition (LOI) and carbonate content and an ecological approach consisting of pollen-based vegetation reconstruction.

The Tagus River has a length of ~1000 km and a catchment area of 80,630 km^2 (Bettencourt and Ramos, 2003; Le Pera and Arribas, 2004). The Tagus originates at an elevation of about 1600 m in eastern Spain (Fig. 5.1) and flows westwards to the NNE-SSW oriented Lower Tagus Basin (LTB). The average discharge near its mouth is 400 m^3/s, but the river is characterised by extreme seasonal and annual discharge variability with peaks more than 30 times the average (Benito *et al.*, 2003a; Bettencourt and Ramos, 2003).

5.2 METHODS

The distribution of Lower Tagus Valley facies units and palaeogeography have been described previously (Chapter 3). Based on this large-scale framework, two sites have been selected with the most complete Holocene record. Cross sections at these sites have an average coring spacing of 300 m. Coring locations were measured using a Garmin GPS-12 receiver (horizontal resolution ~5 m) and the elevation relative to mean sea level (m.s.l.) was measured using Trimble DGPS equipment (vertical resolution ~5 mm). Elevations of the coring locations in Vale de Atela were deduced from detailed surface elevation measurements (INETI, 1994). The manual corings were done using Edelman augers for sediment above the groundwater table and the gauge and the Van der Staay suction-corer for sediment below the groundwater table (Van de Meene *et al.*, 1979). The sediments were described in the field following the method explained in Berendsen and Stouthamer (2001) and lithological classifications were converted to USDA terminology. Cores 0501.029 and 0701.016 were taken using a gauge and core ALPIII was taken using a Livingstone sampler.

In low-energy backswamps, fine-grained deposits accumulate when discharge exceeds the bankfull stage. In that situation fine-grained sediment is

deposited from suspended load of overbank flood water. A period with such events is registered in the sedimentary record as a fine-grained sediment layer, reflecting multiple overbank floods. In regions with sufficient rainfall and/or groundwater seepage, a decrease in the number of overbank floods, leads to accumulation of organic layers (Törnqvist and Van Dijk, 1993). A radiocarbon date from the top of such organic layers, underlying fine-grained overbank deposits, gives the age of the onset of river sedimentation. The end of river sedimentation can be dated with a sample from the base of an organic layer overlying the fine-grained deposits (e.g. Törnqvist and Van Dijk, 1993; Berendsen and Stouthamer, 2000). Because accumulation of organic layers occurs first in the low-lying centre of a floodbasin, that area is best suited to register changes in fluvial activity (Van Dijk *et al.*, 1991).

In low-lying areas which aggrade rapidly, like the Lower Tagus Valley, it is generally assumed that important hiatuses are absent at lithological boundaries (Törnqvist and Van Dijk, 1993). However, because organic material from layers either below or above the fine-grained layer is dated, a somewhat older respectively younger age is obtained, which does not directly reflect the onset or end of sedimentation (see also discussion in Van Dijk *et al.*, 1991; Törnqvist and Van Dijk, 1993). When sampling the cores for the present study, no recognisable erosional contacts were observed.

Sample treatment

Grainsize was measured on cores 0501.029 (207 samples) and 0701.016 (147 samples) at 5-10 cm intervals using a Fritsch A22 Laser Particle Sizer which resulted in grainsize distributions in the range of 0.15-2000 µm. Samples were prepared following the methods described by Konert and Vandenberghe (1997). This implies that sediment with a grainsize smaller than 8 µm corresponds with clay. Grainsize statistics (mean and D90 = grainsize at which 90 % is finer) were calculated using the program GRADISTAT (Blott and Pye, 2001).

Mean clastic sedimentation rates were derived by calculating the mean proportion (%) of clay, silt and sand for each phase. This value was divided by 100 (%) and subsequently multiplied by the total clastic sedimentation rate for each phase. The total clastic sedimentation rate is the mean proportion of clastic material for each phase, divided by 100 (%) and multiplied by the total sedimentation rate (including non-clastic material); thus it is the clastic fraction of the total sedimentation rate.

A LECO TGA-601 was used to determine the LOI of 229 (core 0501.029) and 147 (core 0701.016) dried and grounded samples of approximately 2 g. During the first step of the treatment, samples were heated to a maximum of 105°C. Moisture evaporated from the sample and when the

weight remained constant with a maximum deviation of 0.5 % during 9 minutes, the dry weight of the sample was measured (W_{dr} (g)). Subsequently, the temperature was raised to 335°C with a rate of 10°C/min. The atmosphere in the oven consisted of 100 % oxygen and all easily combustible organic carbon was burned during this time interval. In order to determine the "classic" LOI, the temperature in the oven was further raised to 550°C with a rate of 10°C/min in a flow of normal air. When the weight remained constant within 0.5 % during 9 minutes, the residue was weighed (W_{gl} (g)) and W_{550} (in %) was calculated using: $W_{550}=((W_{dr}-W_{gl})/W_{dr}) \cdot 100$ %. W_{550} is considered equivalent to the "classic" LOI_{550}. Due to the heating, structural water and -OH bounds in the (clay) minerals were lost as well, causing an overestimation of the LOI; mostly this overestimation is equal to 7 % of the clay-content. Core 0701.016 contained no carbonate. The temperature for the 229 samples of core 0501.029 was raised to 1000°C with the same rate as before to determine the carbonate content. The sample was weighed again at 615°C (W_{615}(g)).To decelerate the dissociation of carbonates, the atmosphere in the oven consisted of a medium flow of pure CO_2. When the weight remained constant within 0.5 % during 9 minutes at 1000°C, the residue was weighed (W_{1000}(g)). The weight loss between 615 and 1000 °C is the weight loss of carbonates $W_{car}=W_{615}$(g)-W_{1000}(g). Carbonate content was calculated using: (W_{car}/W_{dr}) $\cdot$ (100/44) $\cdot$ 100 %.

Pollen samples (112) were prepared following the description by Faegri and Iversen (1975); the material was sieved through a 7-8 µm nylon mesh and clastic material was removed using a sodium polytungstate heavy liquid separation. Samples were embedded in glycerine jelly and sealed with paraffin wax and determined at the Friedrich-Schiller University in Jena (core 0501.029) and Utrecht University (core ALPIII). Pollen counts are presented as regional diagrams and diagrams of selected taxa are presented together with local ecological summary diagrams.

The regional diagrams were constructed using tree pollen (*Acer*, *Betula*, *Corylus*, *Fagus*, *Juglans*, *Pinus*, *Quercus*-type, *Tilia*, *Olea europaea*, *Ulmus*-type, *Fraxinus*-type, *Viburnum*-type), shrub pollen (*Cistus*-type, *Erica*-type) and herb pollen (*Polygonum aviculare*, Apiaceae, Asteroideae, Brassicaceae, *Callystegia*-type, Caryophyllaceae, *Centaurea*-type, Cichorioideae, Fabaceae, *Galium*-type, *Hypericum perforatum*-type, *Plantago*-type, Poaceae, Ranunculaceae, *Rhinantus/Parentucellia*-type, *Rumex acetosella/bucephalophorus*-type, *Sanguisorba minor*, *Sanguisorba officinalis*, *Veronica*-type, *Artemisia*, Campanulaceae, *Echium*-type, *Urtica*, *Xanthium*-type, *Cannabis/Humulus*-type, Lamiaceae, Cerealia, *Polygonum amphibium*, *Polygonum persicaria*, *Helianthenum*, *Juniperus*-type, *Phillyrea*, *Pistacia*-type, *Ruta chalepensis*, *Tamarix*, *Alisma*, *Asplenium*, cf. *Trollius*). In the local ecological diagrams aquatics (*Iso-*

etes, *Myriophyllum*-type, *Nuphar*, *Nymphea*), wetland (Cyperaceae, *Lythrum*, *Typha*, *Sparganium erectum*-type, *Equisetum*) and carr (*Alnus*, *Salix*) pollen were plotted. For core 0501.029 vegetation indicating groundwater seepage (*Myriophyllum*-type and *Equisetum*) was plotted as well, calculated as percentage of the local pollen sum.

Core ALPIII was collected in 1985 by Van Leeuwaarden and colleagues from Utrecht University in Vale de Atela. The unpublished pollen record and radiocarbon dates were kindly provided by him for use in this study.

Thirteen radiocarbon dates were used to construct the chronological framework (Table 5.1). The radiocarbon samples consisted as much as possible of terrestrial botanical macrofossils (Törnqvist *et al.*, 1992; Törnqvist and Van Dijk, 1993) that were manually selected from generally 1 cm thick sediment slices, otherwise bulk samples were used. Radiocarbon ages were calibrated using the program OxCal v3.10 (Bronk Ramsey, 1995, 2001, 2005) using the atmospheric data from Reimer *et al.* (2004). Radiocarbon ages are expressed as calibrated calendar ages (cal BP) with age spans at the 2σ range. Transitions between fluvial activity phases were dated using linear interpolation between dated levels.

Cores were scanned for magnetic susceptibility (MS) using Multi Sensor Core Logging 7.6 (MSCL) equipment (Geotek Ltd.), mounted with a MS2C Bartington magnetic susceptibility meter with loop sensor. Core 0501.029 was measured every 0.5 cm and core 0701.016 every centimetre during 10 s. The upper metres of the cores were recovered using an Edelman auger; in that case, each data point represents the average MS of a ten centimetre interval.

5.3 RESULTS

Tagus floodplain lithostratigraphy

At the base of the Golegã cross section (Fig. 5.2), poorly sorted, mainly coarse-grained sand and gravel were found (Table 5.2), which are interpreted as buried fluvial terrace deposits (FU-1A), probably of Pleistocene age (Chapter 3). The depression in the surface of FU-1A in the northwest of the cross section is interpreted as the incised palaeovalley of Rio Almonda. The basal ~2 m of sediment within this palaeovalley consist of structureless clay and silty clay belonging to brackish water marshes and tidal flats (FU-3A). Deposition of this unit ended shortly after 6860-6630 cal BP (GrA-31004).

In the southeast of the cross section, clay and (silty) clay loam with sand laminae (Table 5.2) are interpreted as deposited by intertidal and subtidal
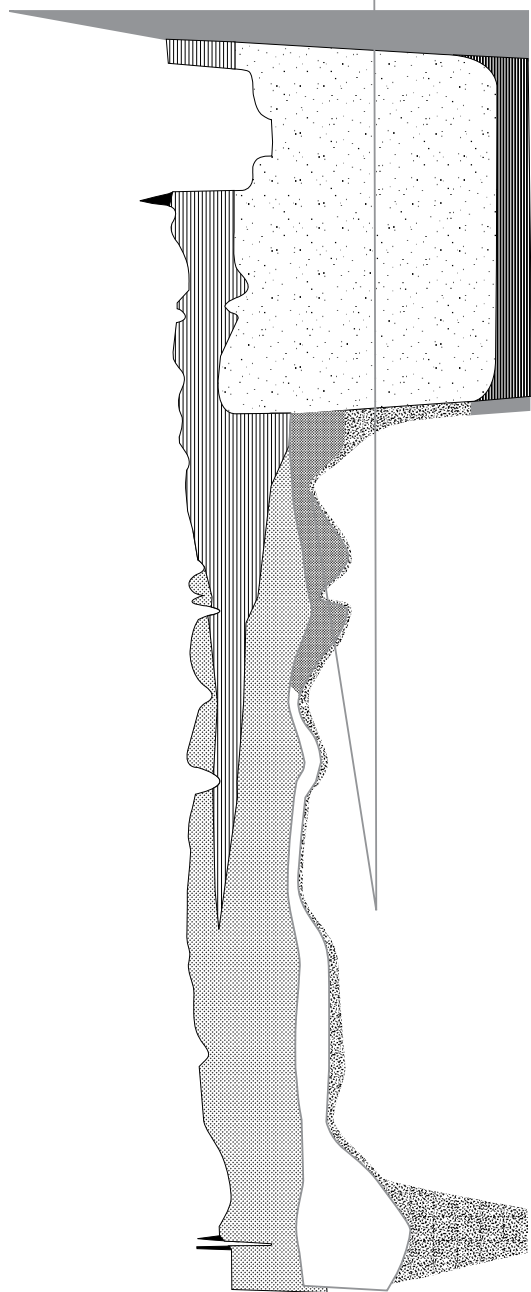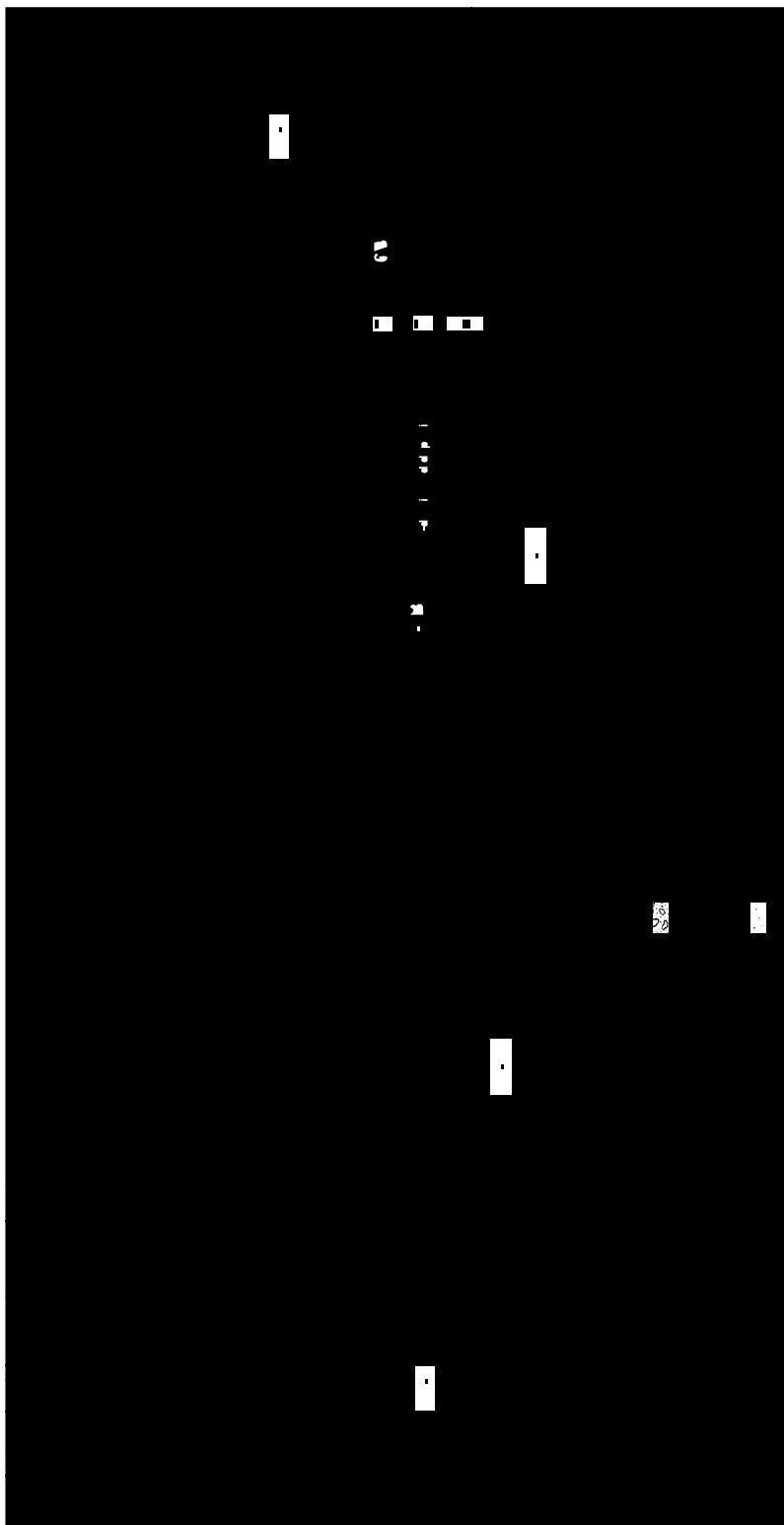
flats (FU-3B), deposited in the incised early Holocene Tagus valley (Chapter 3). Deposition of these tidal deposits ended shortly after 7270-7020 cal BP (GrA-32655). The overlying Tagus channel sediments consist of gravel-rich, medium to coarse-grained sand in a fining-upward sequence (FU-8).

The terrace deposits (FU-1A) in the central part of the cross section are overlain by clay-dominated condensed floodbasin deposits (FU-6A) with traces of soil formation and local peaty intervals (Table 5.2). Sedimentation rate was low, as testified by the pedogenesis in these relatively consolidated floodbasin deposits and deposition started 6680-6480 cal BP (GrA-30615). On top of this unit, silt and clay-dominated floodbasin deposits were found, containing some palaeosols (FU-6B), of which the upper one was dated at ~850 cal BP (Chapter 3). This unit forms a southward thinning wedge of floodbasin deposits in the Lower Tagus Valley (Chapter 3). Deposition of FU-6B started around 3390-3210 cal BP (UtC-14747) and simultaneously natural levees (FU-7) were deposited, consisting of laminated loam, silt loam and well-sorted, fine sand.

The low elevation (lowest point at ~12 m m.s.l.) of the Paul do Boquilobo backswamp surface (Fig. 5.1) results from the buried palaeovalley of Rio Almonda and the large distance from the Tagus channel (Fig. 5.2), implying that only during floods sediment was supplied to this site. Some local, coarser-grained deposits originate from the local stream Rio Almonda. During the Holocene, the Tagus channel was always located ~4 km from this site. Therefore low-energy conditions prevailed and a complete Holocene record accumulated slowly, in which alternating fine-grained and organic layers reflect fluvial activity, rather than lateral Tagus channel migration.

At the base of the Almeirim-Vale de Atela cross section (Fig. 5.3), poorly sorted, coarse-grained gravely sand was found (FU-1B, Table 5.2). In the Tagus valley, this unit has a steep downstream gradient (~60 cm/km) and is interpreted as a braided river deposit resulting from Late Pleistocene relative sea-level lowstand (Chapter 3). These deposits do not seem to have a steep gradient in the downstream part of Vale de Atela because the cross section does not exactly follow the valley axis (Fig. 5.3). The basal unit was deposited before 9030-8750 cal BP (GrA-32584).

The basal unit is overlain by structureless soft clay and silty clay deposited in brackish water marshes and tidal flats (FU-3A, Table 5.2). This unit was deposited between 9030-8750 cal BP (GrA-32584) and 7010-6740 cal BP

Lab. Nr.	Figure	14C age yrs BP ± 1σ	Age cal. BP 2σ	δ¹³C (‰)	Coordinates (x-y/z) (m) depth (cm)	Sample	Borehole nr.	Material	Significance	14C type	Remarks
GrA-30615	2	5790 ± 40	6680-6480	-27.18	540.407-4359.849/+12	1024-1029	0501.029	terrestrial botanical macrofossils	start sed.	AMS	Sieved at 200 μm
GrA-31004	2	5900 ± 45	6860-6630	-25.49	540.407-4359.849/+12	1046-1050	0501.029	terrestrial botanical macrofossils	end sed.	AMS	Sieved at 200 μm
GrA-32584	3	8030 ± 40	9030-8750	-29.18	531.088-4346.563/+11.38	2230-2240	0501.016	*Iris pseudacorus* seed	drowning	AMS	Sieved at 63 μm
GrA-32655	2	6265 ± 35	7270-7020	-27.43	544.750-4358.375/+17.40	1967-1974	0401.304	undifferentiated plant remains	clay layer	AMS	Sieved at 63 μm
UtC-1983	3	6040 ± 50	7010-6740	-28.10	536.620-4342.720/+7.5	760-761	ALP III	peat	end saltmarsh	bulk	unpublished
UtC-1984	3	5670 ± 40	6560-6320	-28.30	536.620-4342.720/+7.5	751-752	ALP III	peat	*Pinus* decline	bulk	unpublished
UtC-1985	3	3600 ± 40	4080-3770	-29.20	536.620-4342.720/+7.5	501-502	ALP III	peat	many herbs	bulk	unpublished
UtC-1986	3	2200 ± 40	2340-2120	-29.50	536.620-4342.720/+7.5	299-301	ALP III	peat	start *Olea*	bulk	unpublished
UtC-14746	2	2530 ± 60	2760-2360	-26.00	540.407-4359.849/+12	516-520	0501.029	terrestrial botanical macrofossils	max. wetness	AMS	Sieved at 125 μm
UtC-14747	2	3089 ± 38	3390-3210	-25.20	540.407-4359.849/+12	604-607	0501.029	terrestrial botanical macrofossils	active sed.	AMS	Sieved at 125 μm
UtC-14748	2	4129 ± 42	4830-4520	-23.23	540.407-4359.849/+12	711-712	0501.029	terrestrial botanical macrofossils	active sed.	AMS	Sieved at 125 μm
UtC-14749	2	1022 ± 37	1060-790	-28.40	540.407-4359.849/+12	331-334	0501.029	total organic fraction < 125 μm	start sed.	AMS	Sieved at 125 μm
UtC-14750	2	1136 ± 38	1180-960	-27.00	540.407-4359.849/+12	331-334	0501.029	roots of fraction > 125 μm	start sed.	AMS	Sieved at 125 μm

Table 5.1 | Radiocarbon dates from the Lower Tagus Valley. Coordinates (X-Y) in European Datum 1950/UTM Zone 29N.

Facies Unit	Interpretation	Lithology	Details
1A	fluvial terrace deposits	very fine to coarse-grained sand, usually poorly sorted and with gravel	compact sediment, unit has flat top and slopes seaward, incised into Miocene-Pliocene deposits plant roots in top
1B	high-gradient fluvial channels	fine to coarse-grained, angular sand, poorly sorted, with increasing gravel to base	fining-upwards, unit has rather flat top morphology and slopes seaward, incised into Miocene-Pliocene deposits
3A	brackish water marshes and tidal flats	generally structureless clay and silty clay with locally very fine sand lamination.	pyrite crystals and pyrite in diatoms, foraminifera and plant remains, bioturbation. Top 1.5-2 m + m.s.l.: very firm consistency, angular blocky structure, carbonized plant material, many carbonate concretions = pedogenesis. Underneath: soft, shell-like breaking, no ripening
3B	intertidal and subtidal flats	plastic, soft clay and (silty) clay loam with laminae and lenses of very fine to coarse-grained sand with some gravel. Clay-sand contacts sharp	Some sand layers disturbed and preserved as sand nests or spots = bioturbation
6A	condensed fluvial floodbasins	sandy loam, loam, silt loam and (silty) clay loam and humic clay, peaty clay and peat intervals	located on top of FU-1, rough consistency, small carbonate concretions, root traces, white & green spots, animal bioturbation, admixture of sand grains. Locally greenish, bluish colours. Alternating wet and dry conditions
6B	fluvial floodbasins	silt loam, (silty) clay loam and clay, very locally poorly sorted (loamy) coarse-grained sand with gravel deposited by small brook channels. Distal areas: gyttja, peat, peaty clay and humic clay layers	unit forms southwards thinning wedge. Ongoing sedimentation on active floodplain with shallow (ephemeral) flood-channels at surface. Contains iron-oxides, iron-concretions, manganese spots, carbonate concretions and is well oxygenated. More charcoal to top. A-horizons: ≤ 50 cm, dark brown-grey to dark brown, sometimes hard, dry and crumbly with white lines (no carbonate)
7	natural levees and crevasses	sandy loam, loam, silt loam and usually well sorted very fine to fine-grained sand in laminae	present on both sides along Tagus channel (FU-8). Shallow (ephemeral) flood-channels at surface. Often much charcoal present. Locally medium to coarse-grained sands, some in channels or splays
8	fluvial channels	medium to coarse-grained sand, with some gravel channel lags.	fining-upwards, pebbles & cobbles dominated by quartz & quartzite (≥ 93%), up to 5% granite, sand has colourful, "clean" appearance, charcoal present. In coring GOL: several stacked fining-upwards sequences

Table 5.2 | Summary of facies unit (FU) characteristics in the Golegã and Almeirim-Vale de Atela cross sections.

(UtC-1983). In the Tagus valley, pedogenesis and soil ripening took place in the marsh deposits, which accumulated ~2 m above m.s.l., equivalent with the spring tidal level (Portela and Neves, 1994; Bettencourt and Ramos, 2003). In Vale de Atela however, the top of this unit is found around ~0 m m.s.l. and no pedogenesis has taken place (Fig. 5.3).

In the Tagus valley FU-3A is overlain by silt, clay and organic deposits of fluvial floodbasin origin (FU-6B). In the tributary Vale de Atela, FU-6B consists of organic-rich freshwater deposits (Table 5.2), which possibly resulted from local groundwater-table rise due to damming of the tributary valley entrance by more rapid aggradation in the main Tagus valley (Fig. 5.3). The wet situation in Vale de Atela persisted by continuous Tagus valley aggradation, causing a continuous rise of the groundwater table and accumulation of organic deposits. In Vale de Atela, FU-6B can be subdivided into two subunits. The basal subunit, deposited since 7010-6740 cal BP (UtC-1983), is peat-dominated (Fig. 5.3) with remains of *Alnus* and *Salix* wood and reed. The upper subunit, deposited since ~1000 cal BP as supported by charcoal, brick and pottery fragments, is silt and clay-dominated, with little organic material. Coeval with FU-6B, natural levee deposits consisting of laminated loam, silt loam and well-sorted fine sand (FU-7) accumulated. The Tagus and Vale de Atela channels (Fig. 5.3) consist of medium to coarse-grained sand in fining-upward sequences (FU-8).

The low elevation of the present-day Vale de Atela valley floor is the result of limited clastic sediment deposition and compaction of the organic valley-fill deposits. This is supported by the mean clastic sedimentation rate (~0.9 mm/y, Fig. 5.5i), which is about half that of the Tagus valley (core 0501.016, Chapter 4). Although the local stream Vale de Atela also supplied sediment, its small catchment (~80 km²) and limited representation in the sedimentary record, suggest relatively minor importance compared to the Tagus River. Furthermore, core data clearly show fine-grained sediment layers originating from the Tagus valley (FU-6B, Fig. 5.3). During the last ~6500 years, backswamp conditions persisted in the sheltered tributary valley behind the Tagus levees and especially Tagus floods supplied suspended sediment, enabling the reconstruction of the Tagus flooding history.

Core sedimentology

Core 0501.029 is dominated by clay layers and clay content is generally above 50 % (Fig. 5.4a, b). Core 0701.016 is dominated by peat layers (Fig. 5.5a, b), implying very low-energy backswamp conditions. Furthermore, mean clastic sedimentation rate is lower in core 0701.016 (~0.9 mm/y, Fig. 5.5i) than in core 0501.029 (~1.2 mm/y, Fig. 5.4j). However, the grainsize of core 0701.016 is generally coarser than that of core 0501.029. Especially the most organic in-
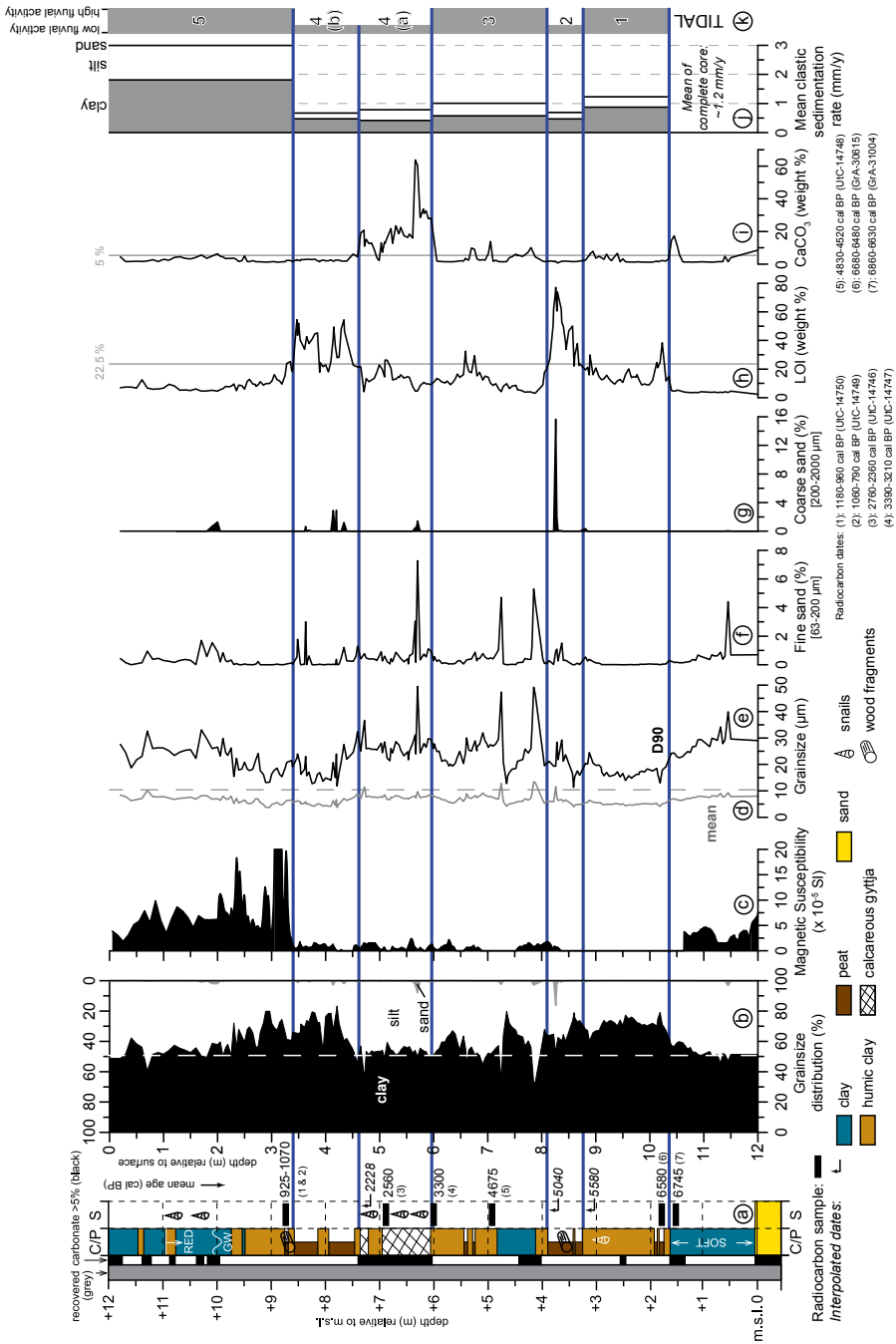
Figure 5.4 | Core 0501.029 from Paul do Boquilobo (location, see Fig. 5.1); a) lithology (C = clay, P = peat, S = sand); b) grainsize distribution; c) magnetic susceptibility; d) mean grainsize; e) D90 grainsize; f) fine sand fraction; g) coarse sand fraction; h) loss-on-ignition (LOI); i) carbonate content; j) mean clastic sedimentation rate (see Methods); k) reconstructed flooding phases (see text for explanation). Note that the lowest clay interval is of tidal origin.
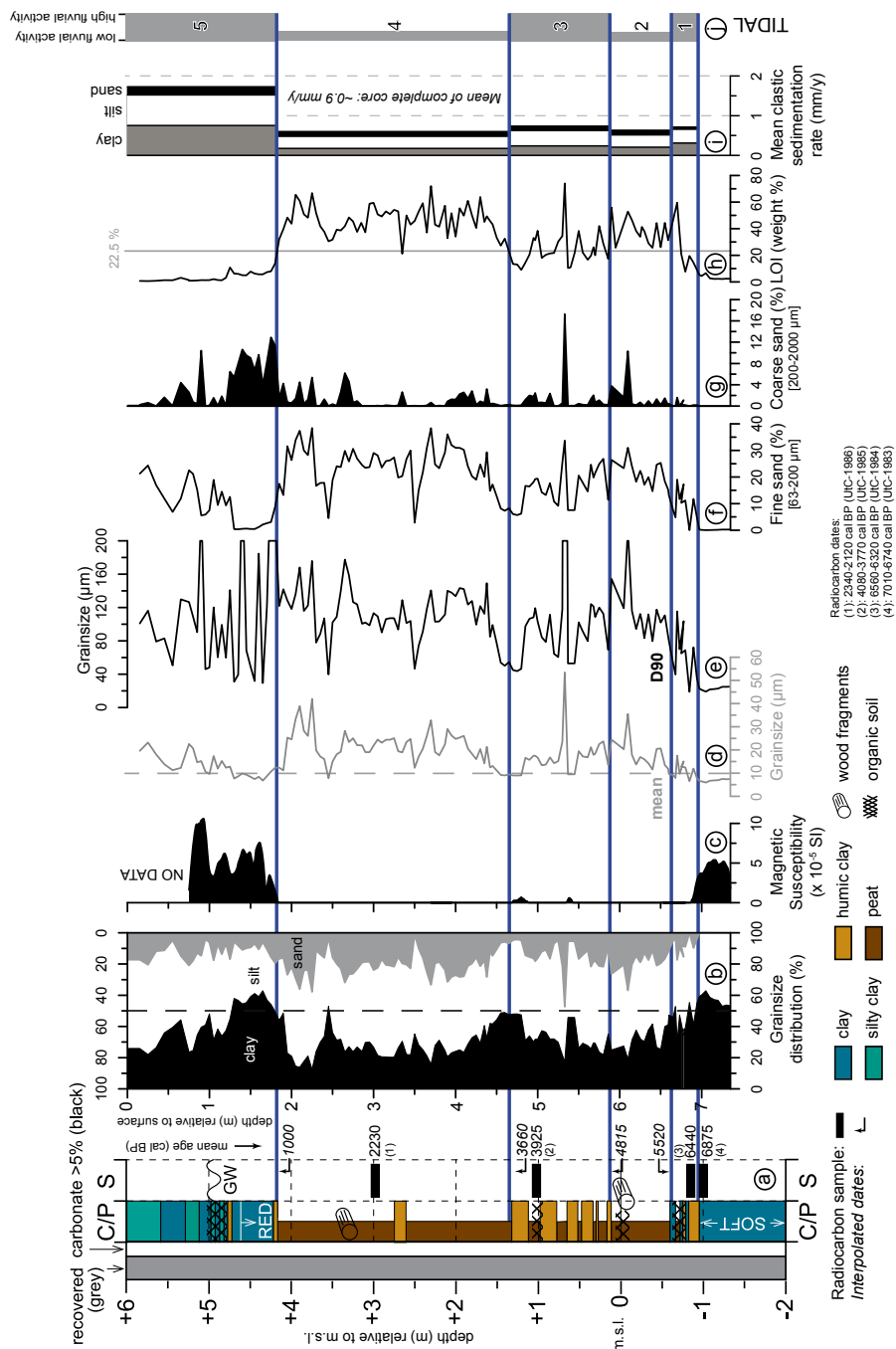
Figure 5.5 | Core 0701.016 from Vale de Atela (location, see Fig. 5.1); a) lithology (C = clay, P = peat, S = sand); b) grainsize distribution; c) magnetic susceptibility; d) mean grainsize; e) D90 grainsize; f) fine sand fraction; g) coarse sand fraction; h) loss-on-ignition (LOI); i) mean clastic sedimentation rate (see Methods); j) reconstructed flooding phases (see text for explanation). Note that the lowest clay interval is of tidal origin.

tervals show low clay content and relatively high silt and sand contents. When considering that fine-grained sediment is deposited from suspended load of overbank flood water, the relatively high content of fine and coarse-grained sand in the organic intervals implies that the sediment in the cores probably originated from different sources. Besides deposition by Tagus floods, local sources have also delivered sediment to the sites. Both sites are located far away from the Tagus channel and close to the sandy deposits along the valley sides. In such a situation it is likely that local, relatively coarse-grained sediment sources (local streams, colluvium, aeolian) dominate over regional, fine-grained sediment sources (Tagus) during periods of low fluvial activity (peat formation). Therefore, the grainsize patterns can not be used as a one-to-one proxy for Tagus fluvial activity as it is derived from different sources.

Basal interval

The basal coarse sand interval (12.5-12 m depth) in core 0501.029 (Fig. 5.4a) is part of the fluvial terrace deposits of FU-1A. The overlying soft, silty clay interval (12-10.4 m) with high MS values (Fig. 5.4c) was deposited by a brackish water marsh (FU-3A) until 6860-6630 cal BP (GrA-31004). At the base of core 0701.016 (Fig. 5.5a) a similar soft, silty clay interval (8-7 m) with high MS was found (Fig. 5.5c), which was deposited by a brackish water marsh until 7010-6740 cal BP (UtC-1983), when tidal conditions abruptly ended due to cessation of relative sea-level rise (Chapter 3). The high MS values in these intervals result from pyrite (visually identified using a microscope) and associated iron sulphide minerals (Kattenberg and Aalbersberg, 2004).

Phase 1

In core 0501.029, the tidal deposits are overlain by a (humic) clay-dominated interval (10.4-8.8 m) with low MS, LOI and carbonate values (Fig. 5.4c, h, i). Deposition started around 6680-6480 cal BP (GrA-30615) and ended ~5580 cal BP (Fig. 5.4a). In core 0701.016, the tidal interval is overlain by a thin interval (6.9-6.6 m) with (humic) clay layers and an organic soil horizon. In both cores this interval with generally low LOI and carbonate content (Figs. 5.4h, i and 5.5h), is interpreted to represent a phase with relatively high fluvial activity (i.e. increased overbank sedimentation due to increased (peak) flood discharge), prohibiting peat accumulation. This is corroborated by relatively high mean clastic sedimentation rates (Figs. 5.4j and 5.5i). Generally, this oldest fluvial phase occurred between ~6500 and 5500 cal BP (Figs. 5.4 and 5.5, Phase 1). This interval is thicker in core 0501.029 than in core 0701.016, because fluvial aggradation and deposition started earlier in the north (Chapter 3).

Phase 2

The interval between 8.8-8.1 m in core 0501.029 is peat-dominated, with LOI values up to 78 % (Fig. 5.4h). The clastic fraction in the peat is clay-dominated (Fig. 5.4b). A peak of coarse sand (~15 %, Fig. 5.4g) within the interval with the highest LOI values (~78 %, Fig. 5.4g), is interpreted to reflect a local sediment source. Accumulation of this interval ended ~5,040 cal BP. Core 0701.016 contains a similar peat interval (6.6-5.9 m) with LOI values up to 56 % (Fig. 5.5h). Silt and sand dominate the clastic fraction (Fig. 5.5b) and some coarse sand is present (Fig. 5.5g). A coarse sand peak (~10 %, Fig. 5.5g) coinciding with a high LOI value (~51 %, Fig. 5.5h), is interpreted as an organic layer which accumulated during low fluvial overbank sedimentation, leading to a relatively increased importance of coarse-grained local sediment sources. The coarsening-upward grainsize in this peat interval possibly reflects build-up of the fluvial wedge in the main Tagus valley. Peat accumulation ended ~4815 cal BP. At both sites the peat accumulated between ~5500 and 4900 cal BP (Figs. 5.4 and 5.5, Phase 2). The synchronicity indicates that this phase was characterised by relatively low Tagus fluvial activity, resulting in undisturbed peat growth. Low fluvial activity results in less sediment supply, as supported by lower mean clastic sedimentation rates (Figs. 5.4j and 5.5i).

Phase 3

In the humic, silty clay interval in core 0501.029 (8.1-6 m), the relatively large grainsize fluctuations (Fig. 5.4b, e) are possibly due to silt and fine sand fluxes caused by individual Tagus floods. Around 3390-3210 cal BP (UtC-14747) sedimentation of this interval ended. Core 0701.016 contains a similar interval with humic, silty clay-dominated layers separated by thin peat layers (5.9-4.7 m). A coarse sand peak (~18 %, Fig. 5.5g) coincides with a high LOI value (~72 %, Fig. 5.5h) is interpreted as coming from a local sediment source. Deposition of this interval ended ~3660 cal BP. The low LOI content in these intervals (Figs. 5.4h and 5.5h, Phase 3), and the presence of only a few peat layers, implies accumulation during a phase with relatively high fluvial activity with relatively high mean clastic sedimentation rates (Figs. 5.4j and 5.5i), as in Phase 1. At both sites, this interval was deposited between ~4900 and 3500 cal BP.

Phase 4(a/b)

The calcareous gyttja-dominated interval (6-4.7 m) in core 0501.029 contains carbonate values reaching up to 64 % (Fig. 5.4i). The silt content in this calcareous gyttja interval is relatively high (Fig. 5.4b), and some fine and coarse sand peaks occur (Fig. 5.4f, g), suggesting a larger contribution of local sediment sources. The presence of calcareous gyttja implies lacustrine circumstances at

the site. Based on the *Nuphar* lutea, Nymphaea alba and *Myriophyllum* pecti-natum pollen, water depth probably fluctuated seasonally between 0.5 and 3 m (Hannon and Gaillard, 1997). Carbonate content slowly decreases upwards, probably due to shallowing and peat growth. Calcareous gyttja accumulation ended ~2228 cal BP and was followed by peat accumulation (4.7-3.4 m) with LOI values up to 54 % (Fig. 5.4h). The clastic fraction in the peat is clay-dom-inated (Fig. 5.4b, j) and some intervals with high LOI values contain peaks of fine and coarse sand (Fig. 5.4f, g), which reflect local sediment sources. Peat ac-cumulated until ~1000 cal BP (UtC-14749 & UtC-14750) when peat growth abruptly ended.

In core 0701.016 (4.7-1.8 m), the equivalent of the calcareous gyttja and peat interval is formed by a peat-dominated interval with LOI values up to 67 % (Fig. 5.5h). The clastic fraction (Fig 5b) is silt and sand-dominated and the mean and D90 grainsize (Fig. 5.5d, e) fluctuate, probably reflecting Tagus floods and sediment input from local sources (e.g. Vale de Atela). At ~3.4 m depth, LOI values clearly decrease as a result of clastic sedimentation due to a large flood. Accumulation ended around ~1000 cal BP. The interval with wetter circumstances (Fig. 5.4, Phase 4a) and the overlying peat-dominated interval (Phase 4b) in core 0501.029 and the peat-dominated interval in core 0701.016 (Fig. 5.5, Phase 4) reflect a period with generally low Tagus fluvial activity. This is supported by low mean clastic accumulation rates (Figs. 5.4j and 5.5i). Phase 4 with very wet local conditions occurred between ~3500 and 1000 cal BP.

Phase 5
In both cores the upper interval is clay and silt-dominated (3.4-0 m, Fig. 5.4;1.8-0 m, Fig. 5.5) with a coarsening-upward tendency (Figs. 5.4b and 5.5b), strongly increased MS values (Figs. 5.4c and 5.5c) and decreasing LOI values (Figs. 5.4h and 5.5h). The changes in this interval (Phase 5) resulted from increased fluvial activity and increased supply of coarser sediment, which reflect strong human impact in the Tagus catchment (Chapter 4). The in-creased fluvial activity is corroborated by unprecedented tripling of the mean clastic sedimentation rates (Figs. 5.4j and 5.5i).

Palynology
The regional pollen diagrams show a general decrease of tree pollen and an increase of shrub and herb pollen (Fig. 5.6). Nine Local Pollen Assemblage Zones (LPAZ were identified in core 0501.029 (Fig. 5.7) and core ALPIII (Fig. 5.8), based on local vegetation development. The environmental interpre-tation for each LPAZ mainly reflects local hydrology in terms of permanently wet (groundwater level at or above the ground surface), regularly inundated
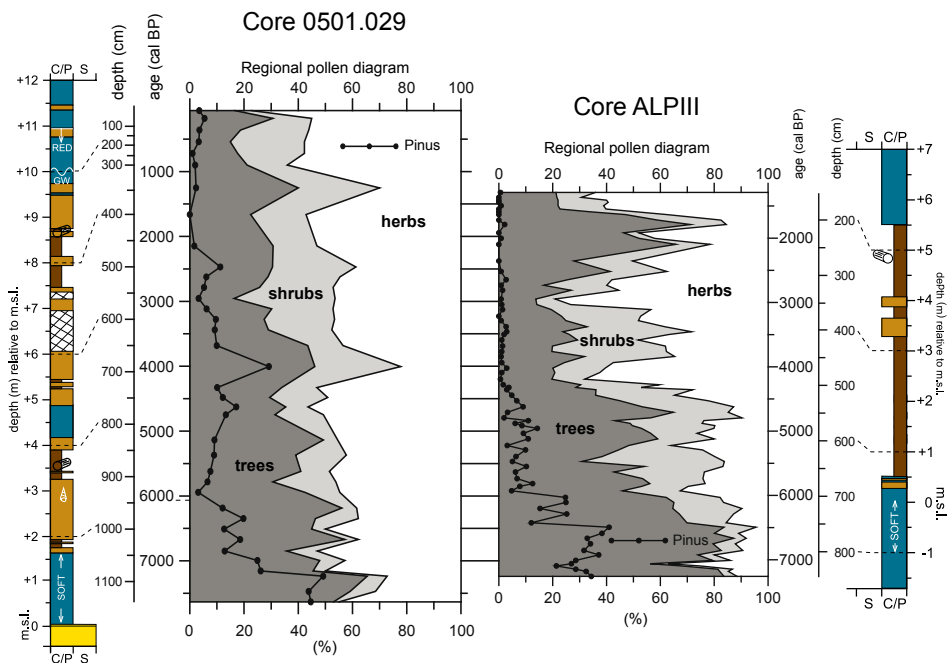
Figure 5.6 | Comparison of regional pollen diagrams for cores 0501.029 (Paul do Boquilobo) and ALPIII (Vale de Atela).

(wet conditions alternated with dry conditions; annually fluctuating local groundwater level), and dry (groundwater level below the ground surface). Human impact can be unrelated to any of these conditions, but it is likely that dryer environmental conditions are preferred for anthropogenic use of these low lying areas.

Paul do Boquilobo (core 0501.029, Fig. 5.7)

LPAZ PdB-1 (7600-7200 cal BP) | clay

This pollen zone is characterised by relatively high values of *Spiniferites*-type dinoflagellates and *Pinus* pollen. *Pinus* pollen are known to be overrepresented in fine-grained marine sediments, making their high values indicative for a marine environment, while Chenopodiaceae and Cichorioidae pollen are indicative for the presence of salt marsh vegetation. The high values of *Isoetes* in this zone (aquatics curve) are the result of freshwater influence. During high discharge the river flushes the high water channels and carries *Isoetes* spores downstream. Sediments and *Isoetes* spores settle where the river meets the brackish environment, causing a freshwater imprint in a brackish environment. Towards the top of this zone freshwater indicators gradually take over.
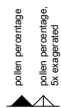
Paul do Boquilobo
Lower Tagus Valley
Portugal
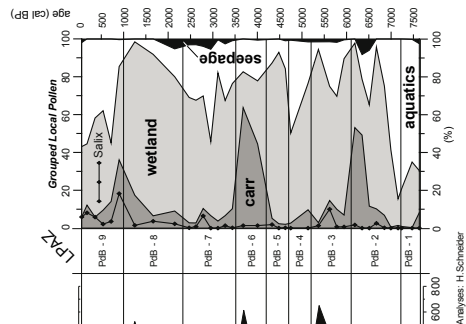
Analyses: H.Schneider

LPAZ PdB-2 (7200-6100 cal BP) | humic clay with some peat layers

Indicators for marine influence (*Spiniferites*-type and *Pinus*) rapidly decline and fresh water aquatic taxa (*Nymphaeae*, *Nuphar*, *Myriophyllum*, *Potamogeton*) appear in the record. Simultaneously, wetland communities (Cyperaceae, *Sparganium*, *Lythrum*, *Mentha*) and reed marsh taxa (Poaceae, and ferns like *Thelypteris* and *Dryopteris*) expand. This hydroseral succession leads to a hampering of the drainage and local wet conditions. In the absence of periodical flooding, seepage indicators (*Equisetum*, *Myriophyllum*) become more prominent in the record. Following this phase, floodplain forest (*Alnus* and *Salix*) increases, which indicates periodical flooding of the site and a progressive growing in with vegetation. This culminates in a completely *Alnus* dominated floodplain forest intermingled with *Vitis*.

LPAZ PdB-3 (6100-5200 cal BP) | humic clay with peat layer

The *Alnus*-dominated phase is succeeded by a more *Salix* dominated phase with *Dryopteris*. At the same depth, aquatic taxa (*Isoetes*, *Nuphar*, *Myriophyllum*, *Potamogeton*) are more prominent in the pollen assemblage. This change is indicative for an increase in water depth at the site and more permanently wet conditions the whole year through. Apparently, periodic inundation resulting in *Alnus* floodplain forest, declined. Hence the influence of groundwater seepage takes over (Fig. 5.7).

LPAZ PdB-4 (5200-4700 cal BP) | humic clay

In this zone floodplain forest species (*Alnus* and *Salix*) occur in low frequencies and aquatics show minimum values. Instead, Poaceae, *Typha latifolia*, Cyperaceae and *Dryopteris* become more frequent. This indicates a gradual hydroseral succession from *Salix* shrubs and open water towards wetland vegetation, dominated by reed marsh communities.

LPAZ PdB-5 (4700-4200 cal BP) | humic clay

The reed marsh changes its composition and becomes dominated by Asteraceae (Asteroideae and Cichorioidae), Brassicaceae and *Centaurea*. Groundwater seepage indicators in this interval are extremely low. The pollen assemblage might indicate an invasion of the reed marsh by ruderal perennials at the expense of the reed marsh taxa. At the same level spores of the liverwort *Phaeoceros* become frequent. This possibly indicates a dying back of the reed marsh due to drought. Later, this dry phase comes to an end, and floodplain forest

Figure 5.7 | Pollen percentage diagram of selected taxa from Paul do Boquilobo (core 0501.029) with Local Pollen Assemblage Zones (LPAZ). The Grouped Local Pollen diagram contains the pollen types which are indicated **bold italic**. Pollen counted by H. Schneider. See Fig. 5.4 for a legend of core lithology.

(*Alnus* and *Salix*) starts to increase again.

LPAZ PdB-6 (4200-3500 cal BP) | humic clay with some peat layers
At the base of this zone *Alnus*, *Dryopteris* and *Sparganium* return to the pollen assemblage, interpreted as a return to regular flooding. In the ecological diagram (Fig. 5.7) this is reflected by declining wetland vegetation, followed by the spread of floodplain forest (*Alnus* and *Salix*).

LPAZ PdB-7 (3500-2300 cal BP) | humic clay, calcareous gyttja
The sudden decline of floodplain forest coincides with the sudden spread of aquatics in the ecological diagram. Furthermore, Poaceae and Cyperaceae increase in the pollen record. It appears that the floodplain forest drowns and is replaced by open water with *Ranunculus aquatilis*, *Nymphaea*, *Nuphar* and *Myriophyllum* species. Bordering on open water, reed marsh communities are present and in some instances *Salix* shrubs. Groundwater seepage indicators are continuously present, suggesting a fairly stable environment. Regular indicators for human impact (*Plantago*, *Rumex acetosella*-type, *Artemisia*, *Urtica*, Brassicaceae, Asteraceae and Cerealia-type) point to anthropogenic use of the uplands in the surrounding area.

LPAZ PdB-8 (2300-1000 cal BP) | peat with humic clay layers
The base of this zone represents a very gradual transition whereby aquatics are gradually replaced by reed marsh communities mainly represented by Poaceae, Cyperaceae with some Apiaceae and *Sparganium*. On the dry parts of the floodplain and surrounding area, indicators for animal husbandry (grassland and ruderal communities), arable land and *Olea* cultivation are prominent, reflecting the Roman era. *Salix* is relatively abundant, indicating a permanently wet local environment. The interval where carr suddenly increases possibly reflects decreasing human impact at the end of the Roman era and the following Peoples Migration Period (Visigoths). At this level, river inundations increase and lithology changes from peat to humic clay.

LPAZ PdB-9 (1000-0) | humic clay changing upwards to
clay with some humic clay layers
Interpretations for the upper part of the diagram are less robust since anthropogenic influence in the pollen record is clearly present. The regional tree values show a strong decline due to deforestation (Figs. 5.6 and 5.7). Pastures and arable land (*Cerealia* pollen) are present in the uplands bordering the Tagus valley and in the drier parts of the floodplain, according to the high values in different grassland communities (Fig. 5.7). The *Olea* curve indicates the presence of olive groves. Locally the *Alnus* forest of the preceding zone (PdB-8)

was replaced by a *Salix* peak, followed by increasing aquatics. Drowning of the vegetation in combination with increasing anthropogenic indicators probably indicates that the clearances promoted the registered increase in fluvial activity.

## Vale de Alpiarça (core ALPIII, Fig. 5.8)

LPAZ Alp-1 (7300-6460 cal BP) | clay

Similar to the Paul do Boquilobo site, this sequence starts with relatively high values for *Pinus*, Chenopodiaceae and Asteraceae liguliflorae which are indicative for a marine or tidally influenced environment; possibly mud flats bordered by tidal marshes. Towards the top of this zone (since ~7000 cal BP) Poaceae starts to increase followed by a Cyperaceae increase. This environmental change may indicate silting up of the environment. Simultaneously, *Isoetes* spores gradually decline probably reflecting decreasing open water brackish environments where *Isoetes* spores concentrate. However, tidal influence remains as indicated by continuously high *Pinus* and Chenopodiaceae values. Possibly brackish and freshwater marshes start to spread in the valley whereby Chenopodiaceae pollen are produced by Atriplex species thriving on litter layers trapped in reed marshes. Consequently the aquatics decline, underlining the progressive spread of marshes at the expense of open water.

LPAZ Alp-2 (6460-5600 cal BP) | clay and humic clay with some peat layers

The *Pinus* pollen decline abruptly and simultaneously *Alnus* pollen increase suddenly. The reed dominated marshes from the preceding zone are replaced by *Alnus* floodplain forest. Since *Alnus* thrives under freshwater conditions and regular fluvial inundations, the registered change must be interpreted in terms of increased fluvial influence at the expense of tidal influence. At the same depth the heather species (*Calluna*, *Erica scoparia*) spread on the uplands bordering the valley, indicating gradual maquis establishment (Fig. 5.8). This may be an effect of dryer regional climatic conditions. Later, wetland vegetation dominated by Cyperaceae becomes more prominent in the local ecological diagram (Fig. 5.8), which can be explained by increased wet conditions in the valley. A risen water table is supported by increased *Salix* and *Isoetes* values towards the end of this zone.

LPAZ Alp-3 (5600-5250 cal BP) | peat

At the base of this zone, maquis suddenly shows peak values, which is a sign for drought or human impact on the uplands. *Alnus* forest is prominent and the sedge marsh becomes invaded by Poaceae and *Dryopteris*. The drought and concomitant changes in inundation frequency cause an even further sedge and fern decline. As a result, the lower water table in the valley causes the sedge vegetation to die back and short lasting ruderal vegetation with Asteraceae and

Alpiarça III
Vale de Atela
Portugal

Analyses: Wim van Leeuwaarden

154
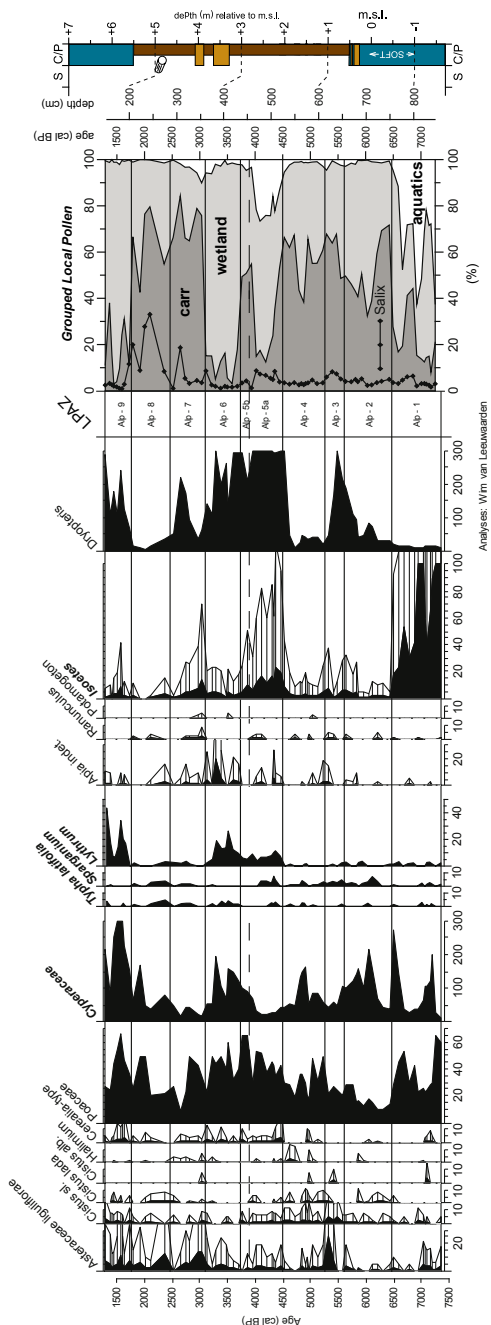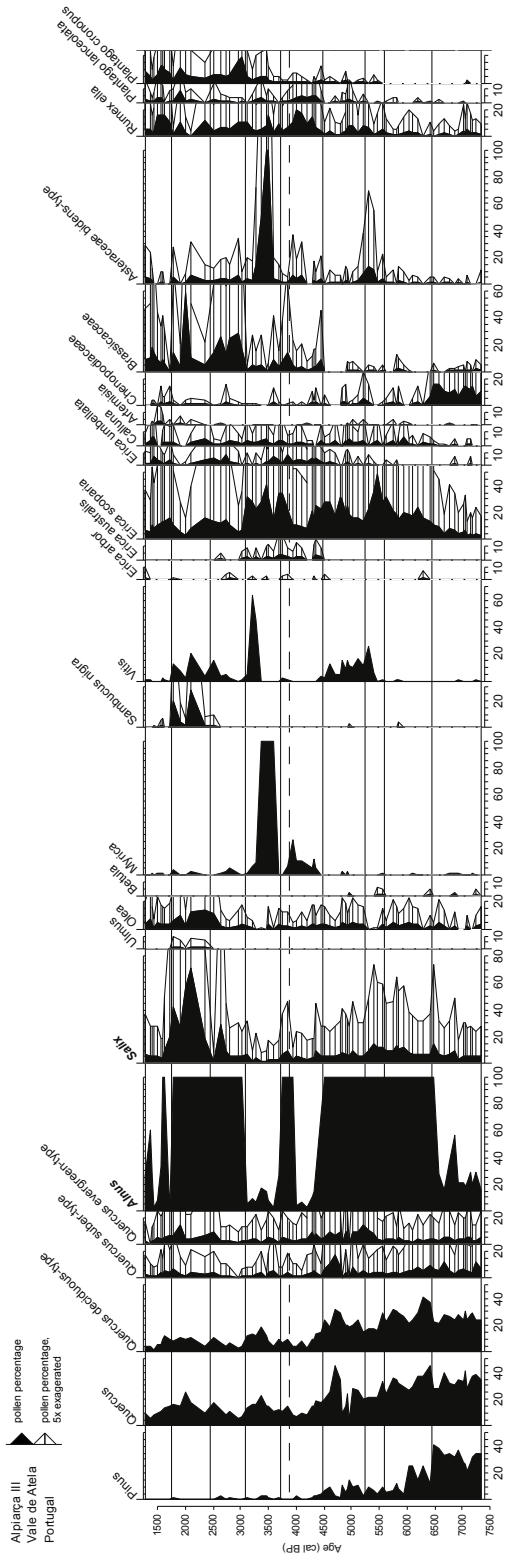
Chenopodiaceae to thrive.

LPAZ Alp-4 (5250-4470 cal BP) | peat

In this phase *Alnus* starts dominating the floodplain forest with *Vitis* as a major constituent. The local ruderal vegetation is replaced by a denser reed marsh in which sedges are important. This change is most likely caused by more seasonal peaked flood discharge. The low maquis in the uplands is partly replaced by oak shrubs of the high maquis. Hence the regional tree values increase (Fig. 5.6). The *Alnus* floodplain forest phase is interrupted around 4900 cal BP by a short phase with increased wetland vegetation, mainly sedges and willow. This phase coincides with a temporal decline in oak forest and an increase in high maquis (Ericaceae). The presence of *Plantago lanceolata* argues for the fact that these vegetation changes could be the effect of slash and burn phases. After this interruption, regional tree values increase again and the oak forest restores. Locally floodplain forest (carr) recovers. Around 4,600 cal BP, regional tree values (*Pinus* and Quercus) decline.

LPAZ Alp-5a (4470-3890 cal BP) | peat

Around 4450 cal BP *Alnus* floodplain forest declines and is replaced by wetland vegetation dominated by Poaceae, *Plantago lanceolata*, *Rumex acetosa/ acetosella*, Brassicaceae and Asteraceae. The combination of taxa makes an interpretation as pastureland likely and argues for a human destruction of the floodplain forest in order to create pastureland. The disappearance of *Alnus* floodplain forest allows for the increased penetration of light to the valley floor, favouring *Isoetes* growth on periodically inundated places and *Dryopteris* in the pastureland. The presence of *Cerealia* indicates the presence of arable land on the uplands bordering the valley. Due to reduction of *Alnus* floodplain forest, the fringe zone of the valley, where the valley sides meet the valley floor, is better registered. This zone is pre-eminently the place where upland seepage water surfaces and where *Myrica* shrubs thrive. This phase of human impact ends with a short restoration of *Alnus* forest.

LPAZ Alp-5b (3890-3725 cal BP) | peat

Human impact on valley floor vegetation temporary declines and the *Alnus* floodplain forest recovers massively. The alder woodland was no longer coppiced and the valley floor was less intensively used as pastureland. Coppiced

Figure 5.8 | Pollen percentage diagram of selected taxa from Vale de Atela (core ALPIII) with Local Pollen Assemblage Zones (LPAZ). Note that lithology and depth are from core ALPIII and therefore not equal to core 0701.016. The Grouped Local Pollen diagram contains the pollen types which are indicated **bold italic**. Pollen counted by W. van Leeuwaarden. See Fig. 5.5 for a legend of core lithology.

woodland can quickly produce prolific re-growth from the cut stump. In case this re-growth is not cut back or harvested, an *Alnus* floodplain forest quickly establishes.

LPAZ Alp-6 (3725-3075 cal BP) | peat with some humic clay layers
The *Alnus* floodplain forest rapidly disappears again and is replaced by sedge-dominated wetland or pastureland. The open vegetation allows for a better registration of the Myrica fringe zone of the valley. The peak values of Asteraceae *Bidens*-type refer to local occurrences of *Bidens* spp. on the valley floor, possibly close to the river on periodically exposed nutrient-rich sites. On the uplands, maquis vegetation spreads followed by an increase in oak forest (*Quercus suber*). Like in the preceding zone (ALP-5) the coppicing of *Alnus* forest apparently favoured *Frangula*, since the wood of this species was not of interest to prehistoric man.

LPAZ Alp-7 (3075-2450 cal BP) | peat with some humic clay layers
The *Alnus* floodplain forest including *Vitis*, re-establishes while wetland vegetation, mainly sedges, declines. Declining human impact on the vegetation probably allows for this restoration. At the same depth *Isoetes* increases and *Ranunculus*-type and *Potamogeton* reappear in the pollen record. This argues for a return to wet conditions on the valley floor, which is corroborated by a return of *Salix*, reflecting more permanently wet conditions. On the uplands the maquis vegetation declines together with the oak forest.

LPAZ Alp-8 (2450-1750 cal BP) | peat
Although locally on the valley floor almost permanently wet conditions prevail, as indicated by peak values of *Salix* in this zone, human impact seems to increase on the uplands, as documented by higher *Cerealia*-type, *Artemisia*, Chenopodiaceae, *Plantago* spec. and *Cistus*-type values (Fig. 5.8). The increase of *Olea* values argues for the establishment of olive grooves. *Myrica* appears to be replaced by *Sambucus* which could have been the result of eutrophication due to human pressure on the landscape.

LPAZ Alp-9 (1750-1300 cal BP) | peat
Floodplain forest (*Alnus* and *Salix*) is strongly reduced and replaced by herbaceous vegetation with Poaceae and Cyperaceae. The values of different tree species decrease rapidly and the *Cerealia* curve increases simultaneously with many herbs which are related to pasture and arable land.

Local ecological pollen diagrams reflect local, site-specific factors causing differences in vegetation in the two sites. In an effort to find coeval local

Age (cal BP)	Paul do Boquilobo (0501.029)	LPAZ	Vale de Atela (ALP III)	LPAZ	Synthesis of vegetation development	Flooding phase	
	human impact regular inundations	PdB-9	NO DATA		regular inundation, human impact increases upwards	5	high fluvial activity, strong human impact
–1000	permanently wet, more inundations towards top	PdB-8	human impact	Alp-9	~1500 cal BP	4 (b)	relatively low fluvial activity
–2000			permanently wet	Alp-8	permanently wet, gradually more inundations and human impact upwards		relatively low fluvial activity, wet circumstances
–3000	drowning, open water, groundwater seepage	PdB-7	more permanently wet conditions	Alp-7		4 (a)	
			wetland or pasture	Alp-6	~3250 cal BP		
–4000	regular inundation	PdB-6	human destruction of floodplain forest	Alp-5b Alp-5a	generally dry to regularly inundated some human impact	3	relatively high fluvial activity
	relatively dry	PdB-5	regular inundation, some human impact	Alp-4			
–5000	transition to dry	PdB-4					
	permanently wet	PdB-3	relatively dry	Alp-3	~5300 cal BP	2	relatively low fluvial activity
–6000			regular inundation, wetter towards top	Alp-2	regular inundation, wetter upwards	1	relatively high fluvial activity
	wet at base, regular inundation towards top	PdB-2	brackish environment	Alp-1			
–7000					~6750 cal BP		
	brackish environment	PdB-1			brackish environment, no fluvial deposits		Tagus fluvial activity
	NO DATA		NO DATA				

(Note: "Alto do Castelo" occupation spans the Alp-4 to Alp-6 interval; "low / high" Tagus fluvial activity scale at base.)

Figure 5.9 | Summary diagram of Local Pollen Assemblage Zones (LPAZ) from Paul do Boquilobo (core 0501.029) and Vale de Atela (core ALPIII) pollen diagrams. The third column provides a synthesis of vegetation development based on LPAZ's; intervals represent periods with largely similar local environmental circumstances. Right column (Flooding phase) shows summarised phases of fluvial activity from Fig. 5.10. Note the period of occupation of "Alto do Castelo" near the Vale de Atela site (see text and Fig. 5.1).

floodplain vegetation and environmental changes, a synthesis was developed (Fig. 5.9). Human impact is relatively prominent in Vale de Atela, because core ALPIII is located at ~2 km south east of the Late Copper Age to Bronze Age (~4950-2600 cal BP) settlement named Alto do Castelo (Van Leeuwaarden and Janssen, 1985; Schattner, 1998). Local hydrology and vegetation may change not only as a response to changed Tagus fluvial activity. Factors like discharge of the local streams Rio Almonda and Vale de Atela, hampered downstream drainage possibilities and changed seepage flux, may cause local vegetation change which is not related to Tagus fluvial activity. Nonetheless, it is likely that—similar to large-scale lithological changes—synchronous large-scale local vegetation changes recognised at both sites reflect regional fluvial activity and/or environmental changes.

The vegetation at both sites shows a brackish environment at the base (Fig. 5.9) which persisted longer in the south due to gradual downstream migration of the fluvial system since ~7000 cal BP (Chapter 3). Since ~6750 cal BP, a freshwater fluvial environment was present in the Lower Tagus Valley, characterised by regular inundation. This period, lasting until ~5300 cal BP, became wetter towards the end. The following period until ~3250 cal

BP, is typified by regular inundation, punctuated locally by short intervals of drought and human impact (Fig. 5.9). At both sites the wettest period was between ~3250 and ~1500 cal BP, when permanently wet and open water environments existed and groundwater seepage was relatively strong. Towards the end of this period, regular inundation was registered again. At the onset of the final period (~1500 cal BP to present) human impact and regular inundations increased.

5.4 DISCUSSION

The synchronicity of lithological intervals at the two sites located ~18 km apart on both sides of the Tagus channel, implies a regional origin for the changes in fluvial activity since ~6500 cal BP (Figs. 5.4 and 5.5). Changes in fluvial activity may also be reflected in the local vegetation development. The local floodplain vegetation basically reflects the hydrological situation due to fluctuations in inundation frequency and groundwater level. By combining the reconstructed fluvial activity phases (Figs. 5.4 and 5.5) and the local vegetation development (Figs. 5.7 and 5.8) the Tagus flooding history and the potential impact of the vegetation cover on flooding can be established (Fig. 5.9).

Fluvial activity and local vegetation

During Phase 1 (6500-5500 cal BP), fluvial activity was relatively high as deduced from relatively high mean clastic sedimentation rates (Figs. 5.4 and 5.5). This is reflected by the local vegetation, which indicates regular inundation and increasing wetness upwards (Fig. 5.9). The following Phase 2 (5500-4900 cal BP) with relatively low fluvial activity and increased organic deposition can not easily be correlated with local vegetation changes (Fig. 5.9). In Paul do Boquilobo the situation was permanently wet, while in Vale de Atela dry conditions prevailed. Possibly, decreased fluvial influence gives way to independent autogenic vegetation development at the two sites.

Phase 3 (4900-3500 cal BP), is characterised by relatively high fluvial activity and regular inundation in the Lower Tagus Valley (Figs. 5.4 and 5.5). However, local vegetation development shows relatively dry periods in Paul do Boquilobo. During this period Vale de Atela is dominated by anthropogenic activity with some periods with regular inundation (Fig. 5.9). The dominance of anthropogenic activity indicates relatively dry local circumstances, facilitating the agricultural use of the floodplain. This suggests that the local hydrological situation at the two sites was generally dry, despite increased Tagus (peak) flood discharges. This may be caused by a changed discharge regime with peak floods concentrated during the winter season when the floodplain was not

used for agriculture.

The gyttja and peat which accumulated during Phase 4a/b (3500-1000 cal BP) is interpreted as reflecting low fluvial activity with decreased Tagus (peak) flood discharges as confirmed by low mean clastic sedimentation rates (Figs. 5.4 and 5.5). However, during Phase 4a high groundwater levels prevailed at the studied sites as corroborated by the local vegetation development which reflects permanently wet conditions (Fig. 5.9). During Phase 4b permanently wet conditions persisted, although groundwater levels lowered in Paul do Boquilobo compared to Phase 4a. The low fluvial activity in the Lower Tagus Valley during Phase 4a/b is interpreted to reflect a discharge regime with less (peak) floods, possibly resulting from increased vegetation density due to the wetter circumstances. Increasing forest densities are known to lead to less peak floods and reduced sediment delivery (Keesstra, 2007).

During Phase 5 (1000-0 cal BP) highest mean clastic sedimentation rates at both sites were registered, reflecting high fluvial activity and higher (peak) flood discharges, probably resulting from deforestation (Chapter 4). This phase is reflected clearly in the vegetation development at both sites as a period with regular inundation and indications for human impact.

Fluvial activity and regional vegetation

Since ~6000 cal BP regional tree pollen decreased in favour of shrub and herb pollen (Fig. 5.6). This reflects regional aridification and related regional forest decline combined with some human influence as previously identified in south Portugal and Spain (Carrión *et al.*, 2007; Fletcher *et al.*, 2007). The same regional forest decline was also found in northwest Spain, but there human deforestation played an increasing role since ~4000 cal BP (Van den Brink and Janssen, 1985; Van der Knaap and Van Leeuwen, 1995; Santos *et al.*, 2000). In general, during dry periods vegetation cover decreases, leading to less rainfall interception, lower soil water-holding capacity and higher slope erosion rates and increased (peak) flood discharge (e.g. Bosch and Hewlett, 1982; Hornbeck *et al.*, 1993; Sahin and Hall, 1996; Van Rompaey *et al.*, 2002; Lang *et al.*, 2003; Andréassian, 2004; Jordan *et al.*, 2005; Ward *et al.*, 2008).

Coinciding with the onset of regional forest decline, the African Humid Period ended (since 6000-5500 cal BP) as a result of gradually decreased summer insolation, leading to weakening of the African summer monsoon in the Mediterranean regions and regional drying (Claussen *et al.*, 1999; DeMenocal *et al.*, 2000; Renssen *et al.*, 2006; Naughton *et al.*, 2007). The coincidence between regional aridification, the progressive decline of regional forest and the end of the African Humid Period suggests a relationship between these events, which may have affected fluvial activity. However, the Lower Tagus Valley fluvial sedimentation history does not reflect these changes, because

the mean clastic sedimentation rate does not show a systematic increase in the studied sites (Figs. 5.4j and 5.5i).

On the other hand, quantitative estimates of Tagus sediment budgets for the Late Glacial and Holocene periods, indicate an increased sediment flux supplied to the estuarine and marine parts of the depositional system since ~7000 cal BP compared to the early Holocene (Chater 6). An explanation for this apparent inconsistency may be that the sediment load of the river gradually increased, without a trend of increasing (peak) flood discharges registered in the distal floodbasin sites of Paul do Boquilobo and Vale de Atela. This situation was favoured by the conservatively maintained position of the Tagus channel, which was relatively deeply incised in its own floodplain (Chapter 3). Therefore, the increased sediment load was possibly directly transported to the downstream central tidal basin and offshore area, where it was deposited.

Controls on fluvial activity

During the last ~1000 years, flood generation, duration and magnitude in Atlantic river catchments of the Iberian Peninsula were closely related to changes in winter precipitation (Rodrigo *et al.*, 1999; Benito *et al.*, 2003b). To evaluate the controls on fluvial activity during a large part of the Holocene, a comparison has been made of the Lower Tagus Valley fluvial activity phases with periods of increased fluvial activity and flood clusters in Spain and Tunisia (Fig. 5.10). Floodplain deposition is the result of a combination of *allogenic* (climatic, tectonic, eustatic and anthropogenic) and *autogenic* (intrinsic behaviour and complex response) controls. Although a strict distinction between allogenic and autogenic influenced phenomena can not simply be made because complicated interactions among these controls exist (Ethridge *et al.*, 1998; Bridge, 2003; Holbrook *et al.*, 2003; Stouthamer and Berendsen, 2007), the dominant allogenic controls are identified below.

The first phase of relatively high fluvial activity in the Lower Tagus Valley (6500-5500 cal BP; Phase 1), does not coincide with increased fluvial activity and flood-cluster records from Spain, possibly because only one slack-water deposit (5700 cal BP) was found (Benito *et al.*, 2003c; Thorndycraft and Benito, 2006b; Benito *et al.*, 2008). However, Phase 1 coincides with a peak of increased fluvial activity in Tunisia (Zielhofer and Faust, 2008) (Fig. 5.10). The increased fluvial activity during Phase 1 also coincides with the build-up of the southward thinning wedge of Tagus floodbasin deposits (FU-6B) across the underlying tidal deposits (Chapter 3). The build-up of the southward thinning wedge is interpreted as a direct response to the end of relative sea-level rise. Therefore, the relatively high fluvial activity during Phase 1 is the result of dominant relative sea-level control on overbank sedimentation.

Between 5500 and 4900 cal BP an episode with relatively low fluvial
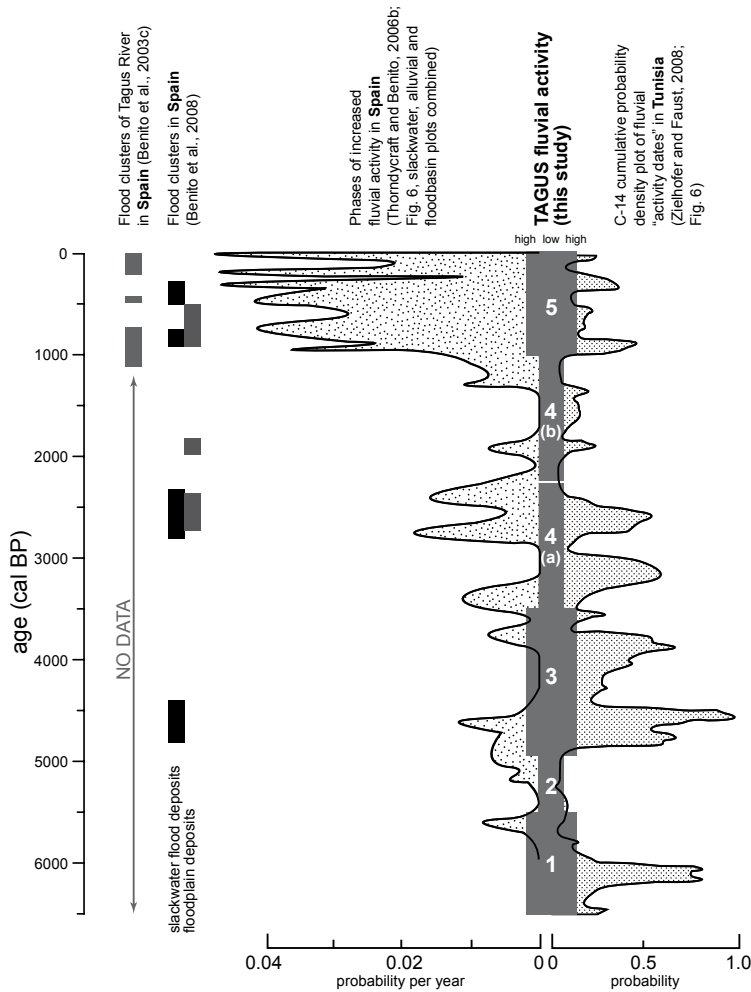
Figure 5.10 | Comparison of Lower Tagus Valley flood phases with fluvial activity from Tunisia and Spain.

activity occurred in the Lower Tagus Valley (Phase 2). This phase coincides with relatively low fluvial activity in Spain and Tunisia (Thorndycraft and Benito, 2006b; Zielhofer and Faust, 2008), suggesting a possible large-scale climatic control leading to less (peak) flood discharges (Fig. 5.10).

During Phase 3 (4900-3500 cal BP) increased fluvial activity was registered in the Lower Tagus Valley. The Lower Tagus Valley record and the Spanish and especially the Tunisian records show coinciding periods of increased fluvial activity (Fig. 5.10). Spanish records also show a cluster of slackwater flood deposits between 4820-4440 cal BP (Benito *et al.*, 2008). However, the Spanish and Tunisian records show temporally decreased fluvial activity between 4400 and 3800 cal BP, not coinciding with the Lower Tagus

Valley development (Thorndycraft and Benito, 2006b; Zielhofer and Faust, 2008). The coinciding periods of increased fluvial activity may be the result of a common large-scale climatic control. Nonetheless, the middle part of Phase 3 with high fluvial activity in the Lower Tagus Valley and low fluvial activity in Spain and Tunisia, implies that other controls or complex response processes (i.e. different rivers or river reaches respond differently or delayed to the same external control) are also active.

Phase 4a was characterised by accumulation of gyttja and peat with wet local circumstances and low Tagus fluvial activity (3500-2200 cal BP). During this wet phase, the 2800 cal BP event occurred in northwest Europe (Van Geel *et al.*, 1996). Simultaneously, wet conditions occurred in the Portuguese Serra da Estrêla (Van den Brink and Janssen, 1985; Van der Knaap and Van Leeuwen, 1995) and the northwest Spanish Lagoa Grande and Queixa Sierra (Santos *et al.*, 2000; Leira, 2005). The low fluvial activity in the Lower Tagus Valley during Phase 4a reflects a discharge regime with less (peak) floods, possibly resulting from increased vegetation density due to the wetter climatic circumstances. However, Spanish and Tunisian sites show high fluvial activity during this period and both slackwater and floodplain deposits registered flood clusters (Thorndycraft and Benito, 2006b; Benito *et al.*, 2008; Zielhofer and Faust, 2008) (Fig. 5.10). Because wet conditions were found in several Spanish and Portuguese sites, the wet conditions are probably the result of large-scale climatic control. However, high fluvial activity in Spain and Tunisia as opposed to low fluvial activity in the Lower Tagus Valley, suggests that other factors or complex response processes were controlling overbank sedimentation in the Lower Tagus Valley.

The wet conditions during Phase 4a were followed by less wet conditions (Phase 4b, 2200-1000 cal BP), with low fluvial activity in the Lower Tagus Valley (Fig. 5.10). This coincides partly with relatively low fluvial activity in Spain and Tunisia (Thorndycraft and Benito, 2006b; Zielhofer and Faust, 2008). Extensive soil formation occurred on the Lower Tagus Valley floodplain at the end of Phase 4b (Chapter 3), supporting relatively low fluvial activity. Because of similar low fluvial activity on the Iberian Peninsula and in Tunisia, Phase 4b is interpreted to reflect a period with common large-scale climatic control on fluvial activity.

Since ~1000 cal BP fluvial activity has been relatively high (Phase 5, Fig. 5.10), similar to the Spanish records (Benito *et al.*, 2003c; Thorndycraft and Benito, 2006b; Benito *et al.*, 2008). The increased fluvial activity during the last ~1300 years in Spain was mainly the result of human impact (Thorndycraft and Benito, 2006a, b). Similarly, the increased flooding in the Lower Tagus Valley is attributed to strong human impact on Tagus catchment vegetation (Chapter 4). According to Faust *et al.* (2004) the late Holocene fluvial

activity in northern Tunisia was chiefly driven by climate; human impact merely intensified or attenuated geomorphic processes. However, the strong effect of human impact (mainly deforestation) on fluvial activity in Spain and Portugal, suggests that increased human impact overruled climate as control on sedimentation in Iberian and Mediterranean regions.

Local floodplain-vegetation changes corroborate increased fluvial activity during Phases 1 and 5. Fluvial activity during these phases was primarily controlled by relative sea-level (Phase 1) and human impact (Phase 5). During Phases 2, 3 and 4b, local floodplain-vegetation changes and fluvial activity were negatively correlated, suggesting a disconnection between local vegetation development and fluvial activity. Because these phases coincide with periods of increased fluvial activity and flood clusters in Spain and Tunisia, they probably resulted from a large-scale control. It is therefore likely that fluvial activity during these phases was primarily controlled by climate. During Phase 4a local floodplain-vegetation and fluvial activity were also negatively correlated, however, local floodplain vegetation did reflect a wet regional climate, which was also found in other Portuguese and Spanish sites. Autogenic controls (e.g. floodplain vegetation filtering suspended sediment, levee height) and complex response processes may explain the discrepancy between the Lower Tagus Valley fluvial activity record and local floodplain-vegetation changes during Phases 2, 3 and 4a/b.

5.5 CONCLUSIONS

Due to continuous fluvial aggradation since ~6500 cal BP, the Lower Tagus Valley hosts a rare record of middle to late Holocene fluvial activity on the Iberian Peninsula. Two sites (Paul do Boquilobo and Vale de Atela) located ~18 km apart in distal, low-energy backswamps on both sides of the Tagus channel have registered the flooding history of the Tagus River. In these low-energy backswamps, fine-grained sediment layers which were deposited from suspended load of overbank flood water, reflect periods with multiple overbank floods. At both sites, synchronous lithological intervals accumulated, implying a regional origin for the changes in fluvial activity. Based on lithological changes, phases of high fluvial activity were identified between 6500-5500, 4900-3500 and 1000-0 cal BP and phases of low fluvial activity were identified between 5500-4900 and 3500-1000 cal BP.

Since ~6000 cal BP the regional forest declined progressively which is a sign of the regional drying trend which commenced after the end of the African Humid Period. However, this is not reflected by the Lower Tagus Valley flooding history which does not show systematic changes in sedimentation

rate and (peak) flood discharges.

Local floodplain vegetation registered alternating periods of wet, regularly inundated, dry and anthropogenically influenced conditions. Two out of five fluvial activity phases could clearly be linked with local floodplain-vegetation changes. During the other three phases autogenic controls and complex response processes probably caused the discrepancy between fluvial activity phases and local floodplain-vegetation changes.

A comparison between the Lower Tagus Valley flooding history and phases of fluvial activity in Spain and Tunisia shows that the dominant allogenic controls of fluvial activity in the Lower Tagus Valley were relative sea level (6500-5500 cal BP), climate (5500-1000 cal BP), and human impact (1000-0 cal BP). The results of the present study show that the fluvial archive as a record of environmental change is complex, as a result of the plethora of processes active in the fluvial realm.

6

Sediment volume estimates are fundamental for understanding sea level, tectonic and climatic controls of sedimentation patterns in source-to-sink fluvial systems at continental margins. Here we

Last glacial to recent sediment fluxes in the Tagus fluvial-marine system

present the first quantification of the migration of sediment depocenters of a major river on the Iberian Peninsula under conditions of rapid relative sea-level rise and climatic aridification since the end of the African Humid Period. The Tagus depositional system was studied using a dataset of terrestrial and marine cores covering the period since 18,000 cal BP. The quantitative estimates of sediment volume through time show that in different parts of the Tagus fluvial-marine depositional system: (1) during low relative sea level in the last glacial period, sediment bypassing favoured sedimentation on the Tagus Abyssal Plain; (2) during relative sea-level rise the main sediment depocenter shifted towards the shelf, where it arrived at 13,500 cal BP, and soon after the main depocenter migrated to the Lower Tagus Valley at about 12,000 cal BP; and (3) during high relative sea level, the main depocenter was located in the Lower Tagus Valley with a dramatic higher (up to 2.5 times) sediment flux and storage, favoured by more arid climate conditions, and land-use changes. Our study indicates that future erosion rates will intensify even further as a result of the predicted increase in arid conditions on the Iberian Peninsula, in line with modelling results.

Photo: the Atlantic Ocean: the final destination of Tagus sediments (west of Lisbon).

6.1 INTRODUCTION

Studies of sediment depocenter migration in late Quaternary fluvial-marine depositional systems provide thorough insights in sea level, tectonic and climatic controls, but often lack a quantitative approach (Blum and Törnqvist, 2000; Sommerfield and Lee, 2004). Here we present a new quantitative approach for assessing the migration of depocenters of a large fluvial-marine sediment dispersal system on the Iberian Peninsula for the period since 18,000 cal BP. The Iberian Peninsula has witnessed aridification since the mid Holocene (Magny *et al.*, 2002), and the large Tagus fluvial-marine system on the Iberian passive margin was strongly controlled by relative sea-level (RSL) change (Chapter 3).

We used an extensive dataset of sedimentological and palynological data derived from 385 terrestrial and 11 marine cores with a well calibrated chronology based on 127 radiocarbon dates (Fig. 6.1). Valley-fill history and
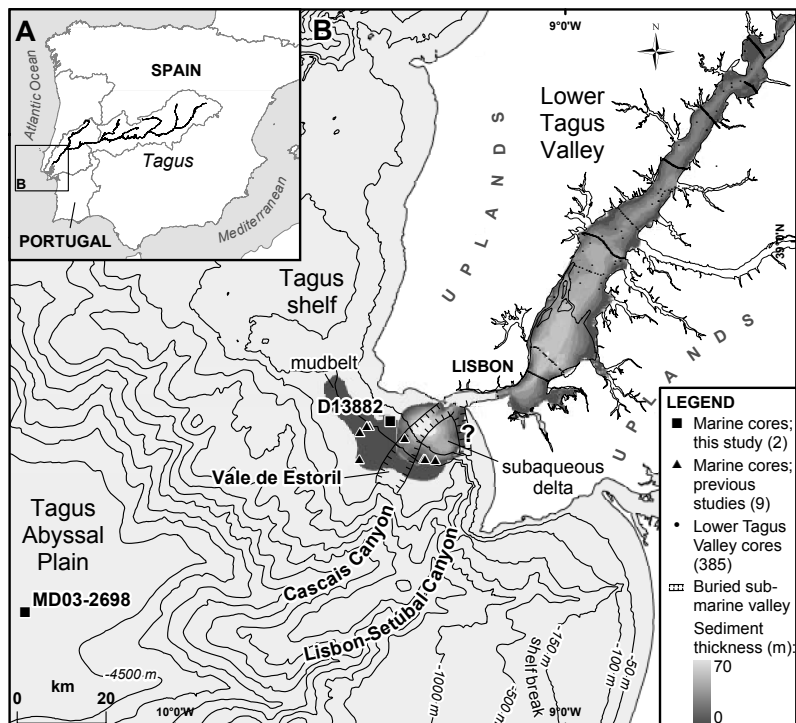
Figure 6.1 | Location map of the Lower Tagus Valley (LTV), Tagus shelf and Tagus Abyssal Plain: (A) Tagus catchment and study area on the Iberian Peninsula; (B) terrestrial and marine cores and isopach map of sediments deposited in the LTV and on the shelf since ~12,000 cal BP. The narrow bedrock-confined LTV enables robust sediment pathway and volumetric reconstructions. Buried submarine valleys from Mougenot (1985), bathymetry from IOC, IHO and BODC (2003) and INETI/DGM.

palaeogeography of the Lower Tagus Valley show an erosive system until ~14,000 cal BP, followed by a retrograding system until ~7000 cal BP. A maximum flooding surface was established followed by a prograding system. Sediment budgets across the Tagus fluvial-marine system were quantified for the last 12,000 cal BP, using the volume of fluvial and marine deposits. During the preceding period the shelf was exposed subaerialy due to the low RSL, and sediments were transferred to the deep sea, hampering volumetric calculations. The aridification since the mid Holocene may have caused changes in sediment production in the catchment.

6.2 METHODS

Sediment volumes were quantified using spatial models generated in Petrel 2008 software (Schlumberger Ltd.). Three-dimensional surfaces were modelled using convergent (geo-statistical) interpolation. For volumetric modelling, every 90 · 90 m grid cell was multiplied by the height between the upper and lower surface. Because the average carbonate and organic content of the sediments is below 5 %, no correction for volumetric calculation was made. Sediment volumes for the Tagus depocenters were converted to mass using dry bulk density. The sensitivity of storage rates to changes in dry bulk density of ± 0.1 t/m^3, reaches up to ± 8 %.

Terrestrial cores (385) and radiocarbon ages (86) from the Lower Tagus Valley (LTV), and detailed reconstructions of valley-fill history and palaeogeography, form the basis for the definition of terrestrial depocentre size and timing of deposition (De Mendonça, 1933; Van Leeuwaarden and Janssen, 1985; LUSOPONTE, 1995; Ramos *et al.*, 2002; Ramos Pereira *et al.*, 2002; BRISA, 2005; Azevêdo *et al.*, 2006; INETI, 2007; Van der Schriek *et al.*, 2007b; Chapters 3 and 4).

We used 11 marine cores and 41 marine radiocarbon ages (Labeyrie and Turon, 2005a, b; Segl and Alt-Epping, 2005a; Abrantes *et al.*, 2008). In this study we present one core recovered from the Tagus shelf (D13882) (Weaver, 2003) and one from the landward limit of the Tagus Abyssal Plain (TAP) (MD03-2698). The marine radiocarbon ages (Table 6.1) were calibrated using the program CALIB v5.0 (Stuiver and Reimer, 1993; Stuiver *et al.*, 2005) and the Marine04 age calibration data from Hughen *et al.* (2004). The marine calibration incorporates a time-dependent global ocean reservoir correction of about 400 years. Abrantes *et al.* (2005) proved that this is a good estimate for marine material off Portugal for the last ~110 years; however, older dated material may have been affected by different conditions. Therefore and to correct for local variations, the difference in reservoir age of the

Lab. Nr.	14C age yrs BP ± 1σ	dR ± SD (y)	Age cal. BP 2σ	Mean cal BP	Calibration curve	Coordinates (x-y/z) (m)	Sample depth (cm)	Core	Material	Source
KIA 27301	2920 ± 35	262 ± 164	2744-1944	2344	marine04.14c	460.591-4276.521/-87	464	D13882	Shells	This study
KIA 27302	4295 ± 40	262 ± 164	4510-3611	4061	marine04.14c	460.591-4276.521/-87	30	D13882	Shells	This study
KIA 27303	6120 ± 55	262 ± 164	6652-5894	6273	marine04.14c	460.591-4276.521/-87	632	D13882	Shells	This study
KIA 27304	10470 ± 70	262 ± 164	11876-10688	11282	marine04.14c	460.591-4276.521/-87	713	D13882	Shells	This study
KIA 27305	10470 ± 70	262 ± 164	11876-10688	11282	marine04.14c	460.591-4276.521/-87	759	D13882	Shells	This study
KIA 27307	10490 ± 70	262 ± 164	11908-10718	11313	marine04.14c	460.591-4276.521/-87	820	D13882	Shells	This study
KIA 27687	790 ± 25	262 ± 164	440-0	220	marine04.14c	378.451-4233.507/-4602	13-14	MD03-2698	mixed planktonics >250 µm	This study
KIA 27894	11735 ± 55	262 ± 164	13285-12793	13039	marine04.14c	378.451-4233.507/-4602	340-341	MD03-2698	mixed planktonics >250 µm	This study
KIA 29278	4830 ± 35	262 ± 164	5263-4357	4810	marine04.14c	378.451-4233.507/-4602	125-127	MD03-2698	G. inflata >250 µm	This study
KIA 29279	5935 ± 40	262 ± 164	6423-5689	6056	marine04.14c	378.451-4233.507/-4602	155-156	MD03-2698	mixed planktonics >250 µm	This study
KIA 29280	7820 ± 40	262 ± 164	8352-7683	8018	marine04.14c	378.451-4233.507/-4602	189-191	MD03-2698	G. inflata >315 µm	This study
KIA 29281	10540 ± 50	262 ± 164	11951-10795	11373	marine04.14c	378.451-4233.507/-4602	260-261	MD03-2698	G. inflata >250 µm	This study
KIA 29282	12240 ± 70	262 ± 164	13781-13118	13450	marine04.14c	378.451-4233.507/-4602	400-401	MD03-2698	mixed planktonics >150 µm	This study
KIA 29283	12895 ± 55	262 ± 164	14869-13762	14316	marine04.14c	378.451-4233.507/-4602	456.5-458.5	MD03-2698	mixed planktonics >150 µm	This study
KIA 29284	13800 ± 70	262 ± 164	16137-15034	15586	marine04.14c	378.451-4233.507/-4602	631-633	MD03-2698	G. bulloides >150 µm	This study
KIA 29285	15840 ± 70	262 ± 164	18838-18007	18423	marine04.14c	378.451-4233.507/-4602	1184.2-1186.2	MD03-2698	mixed planktonics >250 µm	This study
KIA 29728	9735 ± 55	262 ± 164	10717-9807	10262	marine04.14c	460.591-4276.521/-87	738	D13882	Shells	This study
KIA 29729	8215 ± 45	262 ± 164	8891-8049	8470	marine04.14c	460.591-4276.521/-87	699	D13882	Shells	This study
KIA 29730	3690 ± 30	262 ± 164	3688-2854	3271	marine04.14c	460.591-4276.521/-87	522	D13882	Shells	This study
KIA 29731	9440 ± 60	262 ± 164	10366-9511	9939	marine04.14c	460.591-4276.521/-87	62	D13882	Mollusc	This study
OS- 37706	1960 ±45	262 ± 164	1621-898	1260	marine04.14c	460.591-4276.521/-87	257	D13882	Shells	This study
OS- 37707	10450 ± 75	262 ± 164	11855-10650	11253	marine04.14c	460.591-4276.521/-87	798	D13882	Mollusc	This study
OS- 37708	11100 ± 50	262 ± 164	12819-11710	12265	marine04.14c	460.591-4276.521/-87	975	D13882	Mollusc	This study
OS- 37709	11500 ± 70	262 ± 164	13147-12325	12736	marine04.14c	460.591-4276.521/-87	1140	D13882	Mollusc	This study

Table 6.1 | Radiocarbon ages from cores D13882 and MD03-2698. Coordinates (X-Y) in European Datum 1950/UTM Zone 29N.

study area and the global ocean was determined ($\Delta R = 262 \pm 164$ y) using the marine reservoir correction database of Stuiver and Braziunas (1993). All mentioned radiocarbon dates are expressed as calibrated calendar ages (cal BP) with age spans at the 2σ range.

Grainsize was measured using a Fritsch A22 Laser Particle Sizer following the methods described by Konert and Vandenberghe (1997). The marine cores contained little opal; this opal was not removed. Grainsize samples of core D13882 (94) were taken every 5 cm in the upper 4 m and every 20 cm in the rest of the core. Grainsize samples in core MD03-2698 (40) were also taken at 20 cm intervals, avoiding turbiditic layers.

Pollen samples were prepared according to Faegri and Iversen (1975); clastic material was removed using a sodium polytungstate heavy liquid separation. Pollen concentrations were calculated based on added Lycopodium marker spore tablets (Stockmarr, 1971). The ratio of fossil pollen to marker spores was calculated using: $C = (T \cdot X_{TAB} \cdot P) / (X \cdot S)$ where: C is the concentration of fossil pollen grains/cm^3; T is the number of added tablets; X_{TAB} is the number of marker spores per tablet; P is the number of fossil pollen grains counted; and S is the volume of the sediment sample in cm^3. Pollen concentration was calculated based on all pollen and spores in a sample, excluding *Pinus* pollen.

From 11 sand samples from the LTV (ca. 100 cc), the heavy mineral composition (53-420 μm) was determined based on a minimum count of 100 transparent grains per sample.

6.3 DEPOCENTERS AND SEDIMENT VOLUMES

Tagus Abyssal Plain (TAP)

During low RSL, Tagus sediments bypassed the continental shelf and slope and were transported as turbidites through the Cascais and Lisbon-Setúbal Canyons to the vast Tagus Abyssal Plain (Fig. 6.1), where turbidite sediments alternate with pelagic beds (Lebreiro, 1995; Alves *et al.*, 2003). Although deposition of turbidites abruptly ended ~15,000 cal BP (Fig. 6.2a), the sedimentation rate remained relatively high on the abyssal plain until ~11,500 cal BP (~1.3 mm/y, Fig. 6.2d). This high rate reflects a continued strong supply of fluvially derived sediment to the abyssal plain due to efficient sediment bypassing through the canyons during low RSL, as also shown by the high pollen concentration (Fig. 6.2c). Because pollen grains behave as fine-grained sediment (Chmura and Eisma, 1995), the pollen concentration can be considered as a proxy for the ratio of terrestrial to marine sediment input. Pollen were mainly supplied by the Tagus River, and aeolian supply was limited (Naughton
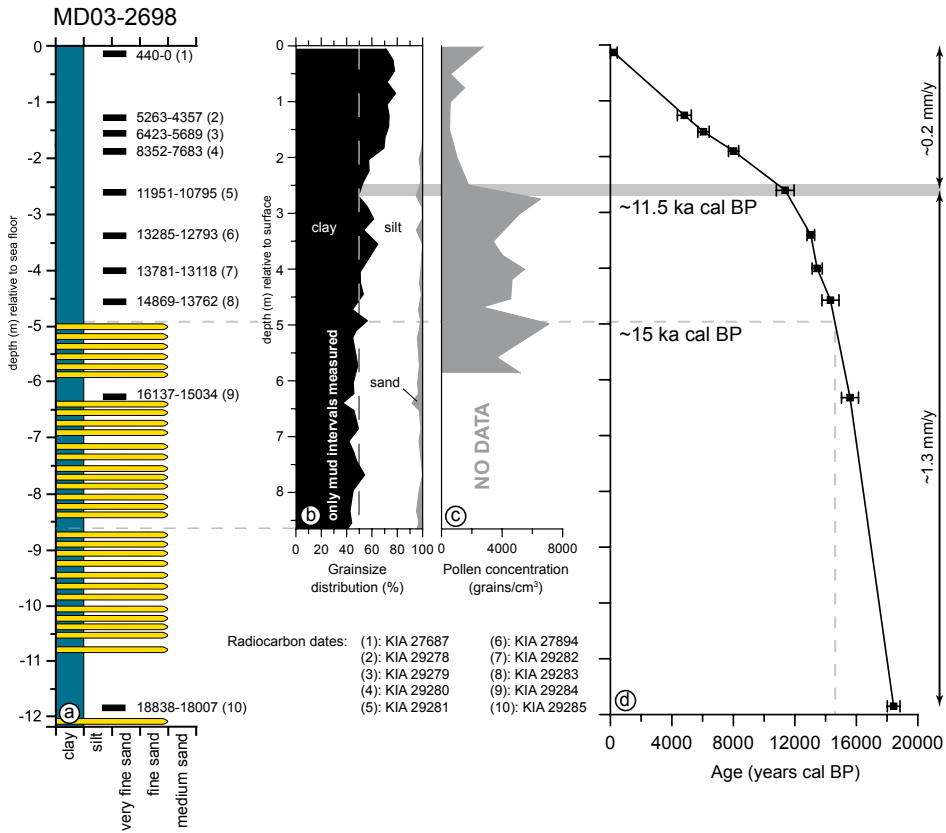
Figure 6.2 | Marine core MD03-2698 from the Tagus Abyssal Plain (-4602 m; 38°14' N - 10°23' W): a) lithology with calibrated radiocarbon ages (2σ); b) grainsize distribution; c) pollen concentration, high concentration = high sediment supply (analyses: Esther Bootsma); and d) average sedimentation rates. These sandy turbidites are mineralogically similar to LTV sands, confirming their fluvial origin (Duplaix *et al.*, 1965).

et al., 2007). Around 11,500 cal BP sediment bypassing came to a halt, resulting in a six fold decrease in sedimentation rate (from ~1.3 to ~0.2 mm/y). The pollen concentrations in the sediments are five times lower than during the preceding period and are carbonate-rich (40-70 %), implying little sediment transfer to the deep sea during rising and high RSL (Fig. 6.3).

Tagus shelf (subaqueous delta and mudbelt)

Sedimentation on the continental shelf started at ~13,500 cal BP with a high initial sedimentation rate (~2.6 mm/y) during the pre-Holocene period (Fig. 6.4d). A sandy interval which was deposited in the early stage of the Holocene (~10,500-5000 cal BP) coincides with the maximum flooding surface. This interval results from a period when fluvial mud was mainly trapped in the Lower Tagus Valley and mud supply to the shelf was low, making winnowing
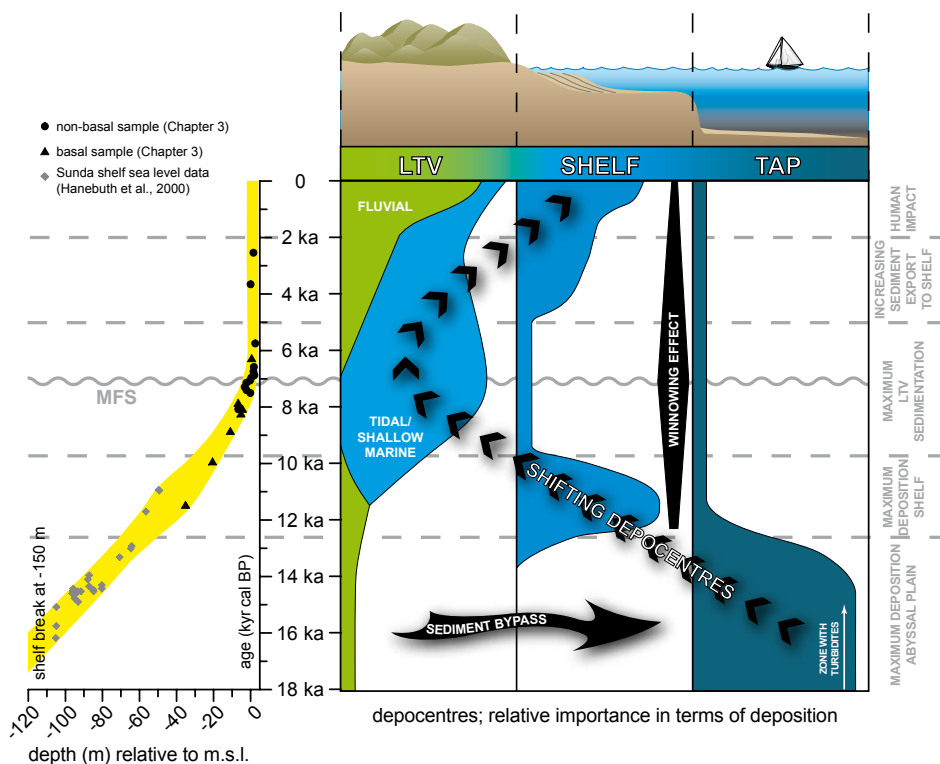
Figure 6.3 | Location of depocenters on the Iberian margin for the last 18,000 cal BP with respect to relative sea level (RSL). The main depocenter shifted due to RSL rise from the Tagus Abyssal Plain (TAP) to the Tagus shelf. Shortly after 12,000 cal BP, the landward shift to the Lower Tagus Valley (LTV) occurred and tidal, marine and fluvial sediments were deposited. The effect of winnowing on the shelf was strong when sediment supply was low (see text). After the end of RSL rise, the LTV progressively filled and export to the shelf started and was amplified during the last ~2000 cal BP by human land-use changes. MFS = maximum flooding surface.

by bottom currents relatively most effective relative to the preceding period (Chapter 4). This caused a low sedimentation rate on the shelf of ~0.3 mm/y (Fig. 6.4d). The low sedimentation rate and low fluvially derived mud input are also shown by the lowest pollen concentration (Fig. 6.4c). Around 5500 cal BP, the sedimentation rate increased (~1.2 mm/y) due to an enhanced supply of terrestrial material to the shelf, as shown also by an up to eightfold increase in pollen concentration. This reflects decreased sediment trapping in the Lower Tagus Valley, and mudbelt deposition on the shelf. The strong increase in sedimentation rate since ~2000 cal BP may reflect catchment deforestation.

The volume of sediment deposited on the Tagus shelf between 12,000 and 7000 cal BP is probably relatively small and much deposition on the shelf already occurred before 12,000 cal BP (Fig. 6.4a). Unfortunately, no data are
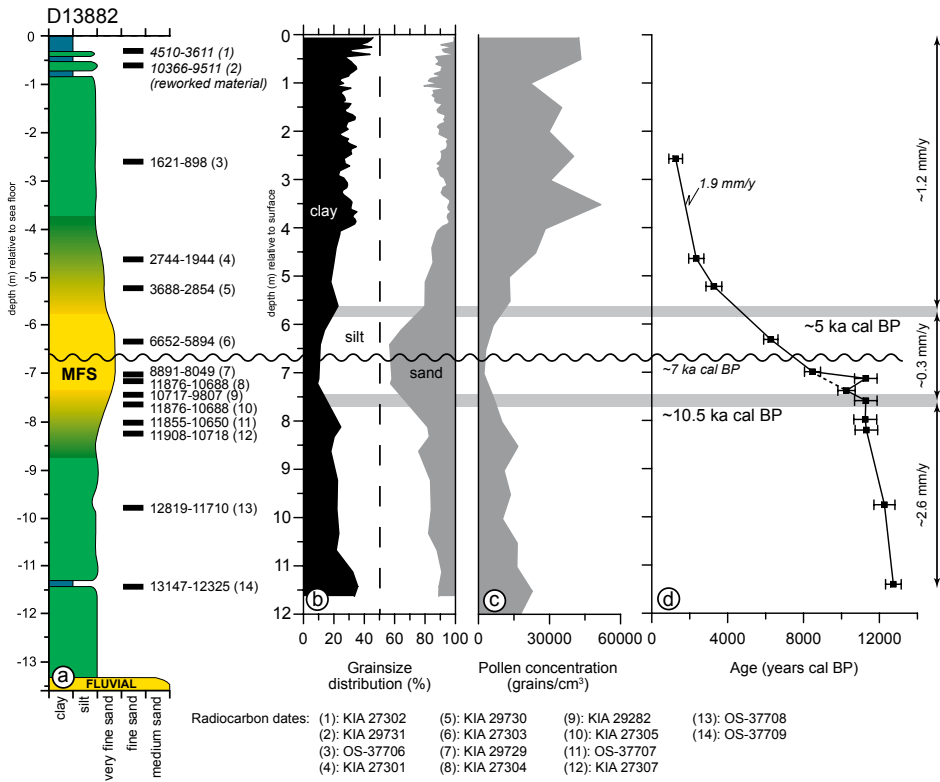
Figure 6.4 | Marine core D13882 from the Tagus shelf (-87 m; 38°38' N - 9°27' W): a) lithology with calibrated radiocarbon ages (2σ) (*italic* ages are considered too old due to reworking); b) grainsize distribution; c) pollen concentration, high concentration = high sediment supply (analyses: Martine Hagen); and d) average sedimentation rates. The sandy interval in the middle of the core is strongly winnowed. MFS = maximum flooding surface.

available to quantify the dimensions of the pre-7000 cal BP sediment body. Therefore, the volumetric calculations of the related shelf sediment body were performed for the period after 7000 cal BP, when the subaqueous delta (Fig. 6.1) and mudbelt had formed (Mougenot, 1985; Chapter 3). The subaqueous-delta volume was calculated using the reconstructed bathymetry of 7000 cal BP as the basal surface and by taking the present-day bathymetry as the upper surface. The mudbelt was considered to be an outward thinning, low-gradient ridge (cf. Jouanneau *et al.*, 1998). However, poorly constrained morphological boundaries and diffuse sediment dispersal in the marine realm complicate calculation of shelf volumes. Despite the narrow shelf, most sediment probably remained on the shelf (Jouanneau *et al.*, 1998), constraining the functioning of the post-7000 cal BP depocenter as a trap for fluvially derived sediment. Our calculations show that the subaqueous delta contains ~5.5 km³ of sediment and the mudbelt ~0.7 km³ (Fig. 6.1, Table 6.2). The relatively small

volume of mudbelt sediments shows that exclusion of the pre-7000 cal BP deposits has a minor impact on the sediment budget, although it may have caused a limited underestimate of the total 12,000-7000 cal BP sediment volume.
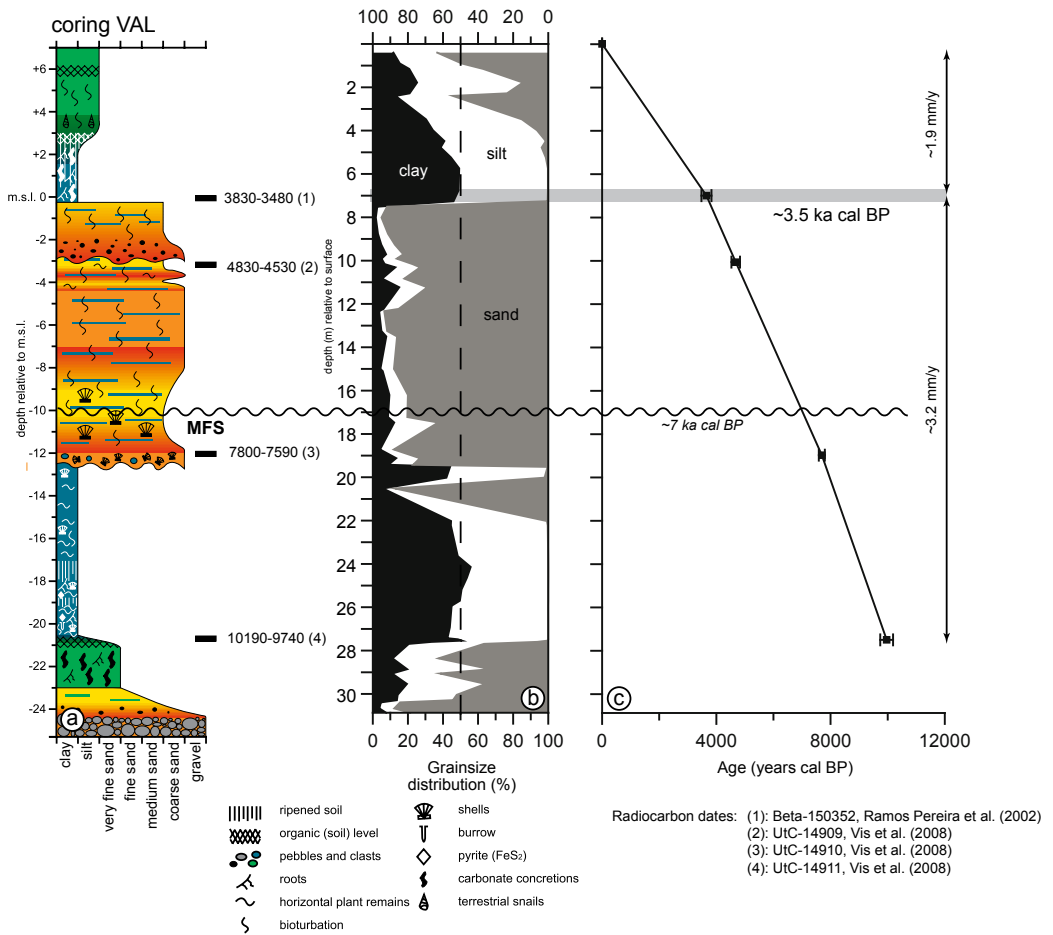
Lower Tagus Valley (LTV)

Since ~12,000 cal BP, rising RSL caused drowning of the deeply incised Lower Tagus Valley (Fig. 6.5), which accommodates up to 70 m of sediment. Heavy mineral analysis of Lower Tagus Valley sands confirms a fluvial provenance without a significant contribution of marine sediments (Fig. 6.6). The basal lowstand topography was dated at about 12,000 cal BP and is based on the study of 283 drilled cores and palaeogeographic interpretation (Chapter 3). The maximum flooding surface dates to 7000 cal BP based on 12 radiocarbon ages, and it's position is also based on palaeogeographic interpretation (Chapter 1). The upper surface equals the present-day topography. This shows that since 12,000 cal BP a total volume of ~20.4 km³ of sediment has accumulated in the Lower Tagus Valley (Fig. 6.1, Table 6.2).

The maximum flooding surface was used to calculate differences in sediment supply between the retrograding and prograding systems. In the north the Lower Tagus Valley is narrow and shallow and the maximum flooding surface is well defined. In contrast, further downstream the valley widens and deepens and less data are available to precisely locate the surface. Nonetheless, in the south a tidal basin was present with a relatively flat bottom, facilitating a careful and reliable interpolation of the maximum flooding surface. Our results show that about 13.9 km³ of sediment accumulated between the maximum flooding surface and the present-day topography. Subtracting this value from the total Lower Tagus Valley sediment volume (20.4 km³) reveals that the total volume deposited between 12,000 and 7000 cal BP is ~6.5 km³.

	Volume (km³)	DBD (t/m³)	Storage rate (t/y)
12-7 ka cal BP			
LTV	6.5	1.21*	**1.6x10⁶**
		~1.7x	
7-0 ka cal BP			
LTV	*13.9*	*1.37■*	*2.7x10⁶*
Subaq. delta	*5.5*	*1.50◊*	*1.2x10⁶*
Mudbelt	*0.7*	*1.15*	*0.1x10⁶*
Total	20.1		**4.0x10⁶**

(annotations: ~2.5x spanning from 1.6x10⁶ to 4.0x10⁶)

Table 6.2 | Sediment volumes, dry bulk densities (DBD) and storage rates of the Lower Tagus Valley (LTV), subaqueous delta and mudbelt. *Weighted average determined using a DBD of 1.70 t/m³ for sand and 1.15 t/m³ for mud and an estimated sand-mud ratio of 0.1-0.9, based on facies distributions. ■ Weighted average determined using an estimated 0.4-0.6 sand-mud ratio. ◊ Heterogeneous subaqueous delta (Goodbred and Kuehl, 2000).

Figure 6.5 | Terrestrial core VAL from the Lower Tagus Valley (+7 m; 39°09' N - 08°44' W): a) lithology with calibrated radiocarbon ages (2σ); b) grainsize distribution; and c) average sedimentation rates.

6.4 DISCUSSION AND CONCLUSION

Depocenter migration

During the Last Glacial Maximum, sedimentation in the Lower Tagus Valley and on the exposed shelf was limited. Although lowstand RSL remained ~30 m above the shelf break, fluvial sediments bypassed the shelf via incised valleys directly funnelling into the heads of marine canyons (Fig. 6.1). Bypassing of fluvial sediment to the deep sea resulted in high-frequency turbidite deposition (up to 10 turbidites per 500 y) near the Tagus Abyssal Plain between 20,000 and 15,000 cal BP (Fig. S1, Lebreiro *et al.*, in press). During low RSL conditions, turbidites delivered ~35 km³ of sediment to the Tagus Abyssal
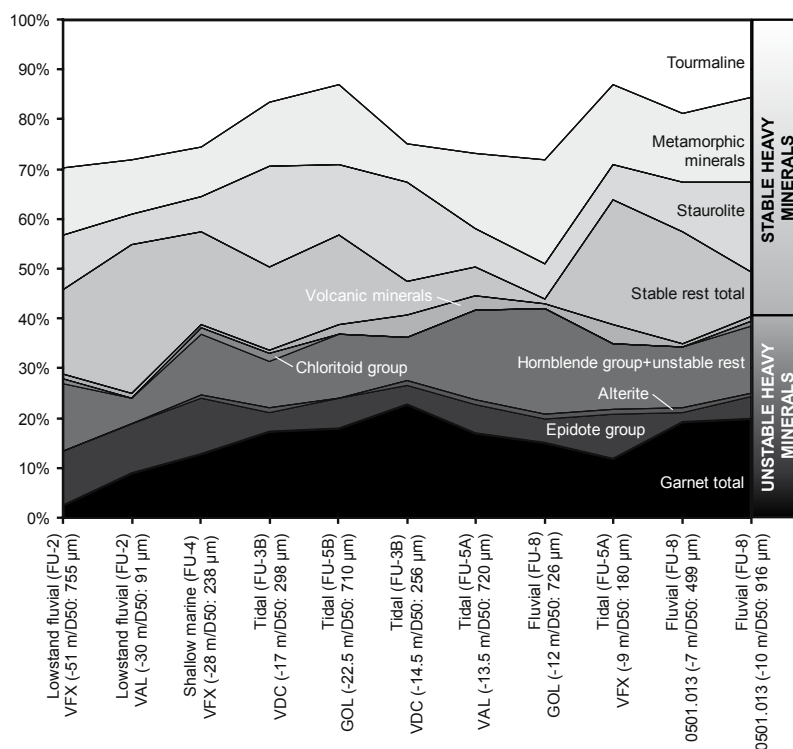
Figure 6.6 | Heavy mineral composition of 11 Lower Tagus Valley samples. Samples were taken from cores and are arranged from old (left) to young (right). FU-codes refer to facies units (Chapter 3) and depth is relative to surface. No large changes in heavy mineral composition are present, confirming a single upstream (fluvial) sediment source. The two oldest samples were taken from lowstand deposits and possibly suffered from long-term exposure and soil weathering.

Plain every 10,000 cal BP (Weaver *et al.*, 2000), which is considerably more than the total sediment volume deposited on the Tagus shelf and in the Lower Tagus Valley during the last 12,000 cal BP (26.6 km³, Table 6.2). This suggests that the Iberian terrestrial sediment flux during glacial periods with low RSL was noticeably higher than during interglacials.

The end of turbidite deposition at about 15,000 cal BP reflects the RSL rise after the Last Glacial Maximum (Fig. 6.3). Simultaneously, the Tagus changed from a braided into a single-channel river, due to climate change and increased production of fine-grained sediment. Until ~11,500 cal BP silici-clastic hemipelagic sedimentation on the Tagus Abyssal Plain caused a high sedimentation rate due to the continued supply of fluvially derived sediment. The final stage of rapid abyssal plain deposition (15,000-11,000 cal BP) co-incides with the onset of increased shelf sedimentation at 13,500 cal BP (Fig. 6.4). Deposition on the Tagus Abyssal Plain decreased strongly since ~11,500 cal BP, reflecting a landward depocenter shift (Fig. 6.3).

Rising RSL created accommodation space in the Lower Tagus Valley, which caused fluvial aggradation since ~12,000 cal BP, soon followed by transgressive tidal and shallow marine sedimentation (Figs. 6.3 and 6.5). Increasing sediment volumes were trapped in the Lower Tagus Valley, strongly reducing export to the shelf. Here, winnowing efficiently removed the finer-grained fractions, leaving a sandy unit deposited at ~7000 cal BP (Fig. 6.4). Until about 7000 cal BP, the depocenter shifted landward when Lower Tagus Valley accommodation space was maximal.

The end of RSL rise is marked by the maximum flooding surface, the onset of bayhead delta progradation in the Lower Tagus Valley, and the build-up of a fluvial wedge (Chapter 3). Around 7000 cal BP, the valley was filled to such an extent (6.5 km³, Table 6.2) that gradually sediment export increased again. This caused a progressive seaward build-up of the subaqueous delta and mudbelt and shift of the depocenter (Fig. 6.3). Since 7000 cal BP, the Lower Tagus Valley and shelf depocenters accommodated 20.1 km³ of sediment (Table 6.2). Increased deposition in the fluvial valley and on the shelf since ~2000 cal BP is likely to be caused by land-use changes in the Tagus catchment.

Our model of depocenter migration of a portion of the Iberian passive margin provides a unique example for comparative studies of Quaternary systems worldwide. Glacial sediment transfer to the abyssal plain was strong despite a RSL lowstand which remained ~30 m above the shelf break. This is in contrast to regions where the absence of incised valleys and canyons caused physical disconnection between continental and deep sea environments (Törnqvist *et al.*, 2006). During RSL highstand, sediment fluxes to the deep sea were strongly limited due to accommodation in fluvial and shallow marine depocenters. This strongly limited the offshore sediment export, despite a narrow continental shelf. Marine palynological studies on the Iberian margin (e.g. Hooghiemstra *et al.*, 1992) should therefore take migrating depocenters into account.

Calculation of sediment fluxes

Storage rates were calculated to identify changes in sediment flux (Table 6.2). Comparison of the total storage rates of $1.6 \cdot 10^6$ t/y (12-7 ka) and $4.0 \cdot 10^6$ t/y (7000-0 cal BP) shows that the latter is up to ~2.5 times higher. When comparing the storage rates of the Lower Tagus Valley deposits for the two above mentioned periods, the storage rate since 7000 cal BP is ~1.7 times higher than during the preceding period (Table 6.2), despite the omission of pre-7000 cal BP shelf sediments from the volumetric calculations. This supports a strong sediment-flux increase. Because some suspended sediment escaped from the system due to coastal and marine currents during both periods (as shown by the presence of clay in the Holocene section of the Tagus Abyssal Plain core),

the storage rates represent minimum values for Tagus sediment flux.

A climatic effect may explain the increased sediment flux. The African Humid Period (~11,500-5500 cal BP) ended due to the gradually decreasing summer insolation, leading to weakening of the African summer monsoon in the Mediterranean and North Africa (Claussen *et al.*, 1999; DeMenocal *et al.*, 2000). On the Iberian Peninsula this led to regional aridification and a progressively decreasing forest cover, resulting in increased herbaceous vegetation (Carrión *et al.*, 2007; Fletcher *et al.*, 2007). The more open vegetation cover increased vulnerability to soil erosion and thus Iberian fluvial sediment yields increased, leading to floodplain aggradation (Thorndycraft and Benito, 2006). The similar timing of the weakening of the summer monsoon, decreasing forest cover, increasing sediment yields, and up to ~2.5 times higher Lower Tagus Valley and shelf sediment fluxes, implies a causal relationship between the above observations.

Besides climate, a large part of the increased storage rate is the result of increased human impact during the last ~2000 cal BP, as tripled sedimentation rates are considered to be caused by land-use changes (Chapter 4). The ~2.5 times higher sediment flux is explained by a combination of climatic and human impact during the last 7000 cal BP, whereby during the last ~2000 cal BP climatic influence was overwhelmed by land-use changes.

Denudation rates and implications for future intensity of erosion

To validate the sediment volumes and to provide a starting point for future catchment erosion studies, we divided the total annual average sediment mass ($3.6 \cdot 10^{13}$ kg/12,000 y = $3.0 \cdot 10^9$ kg/y) deposited in the Lower Tagus Valley and shelf sediment depocenters by the Tagus catchment area (~$8 \cdot 10^4$ km^2), yielding ~$3.7 \cdot 10^4$ kg/km^2/y. Using an average rock density of 2700 kg/m^3, this specific sediment yield was converted into a net mechanical denudation rate of ~0.014 mm/y (cf. Hovius, 1998). This is a minimum estimate of catchment denudation rate, since a large fraction of sediment eroded on slopes is stored in colluvial, alluvial fan and fluvial deposits and currently does not reach the Lower Tagus Valley and shelf sediment depocenters. If we assume that 15 % of the sediment eroded on slopes in the catchment reaches the downstream depocenters, and recalculate mechanical denudation rate using an estimated total eroded catchment sediment mass of ~$20.0 \cdot 10^9$ kg/y, total mechanical denudation rate equals ~0.09 mm/y. This value is in agreement with long-term (10,000-40,000 years) erosion rates from middle European catchments, which range between 0.02 and 0.1 mm/y (Schaller *et al.*, 2001).

Although the average denudation rate is in agreement with those of other European rivers, the post-7000 cal BP denudation rate was up to ~2.5

times higher than during the pre-7000 cal BP period. Given the predicted tendency towards decreasing mean seasonal rainfall over the Iberian Peninsula (Goodess and Jones, 2002), and the increase of extreme events of flooding and drought in the next century (Lehner *et al.*, 2006), our study indicates that future erosion rates will intensify even further on the Iberian Peninsula.

CHAPTER 7

Synthesis

This chapter synthesises the sedimentary development and controls of the Tagus fluvial-marine

depositional system since the Last Glacial Maximum (~ 20,000 cal BP).

Photo: flood water in Paul do Boquilobo (Golegã).

7.1 PALAEOGEOGRAPHY AND DEPOCENTRES

Around 20,000 cal BP | lowstand relative sea level: incision

At around 20,000 cal BP relative sea-level lowstand (~120 m below present-day sea level) caused deep incision (~70 m near Lisbon) by the Tagus River (Chapter 2 and 3). The effect of incision was registered far inland (up to ~100 km). This is the result of a direct connection between the Lower Tagus Valley and the ocean across the narrow (~30 km) continental shelf. Despite the fact that lowstand sea level remained ~30 m above the shelf break, fluvial sediments were efficiently bypassing the largely exposed shelf via incised valleys directly funnelling into the heads of marine canyons and to the Tagus Abyssal Plain, where the main depocentre was located (Chapter 6). Bypassing of fluvial sediment to the deep sea resulted in strong turbidite deposition on the Tagus Abyssal Plain between 20,000 and 15,000 cal BP. Around that time, the Tagus was a braided, high-gradient (~60 cm/km) river which was probably a sediment conveyor-belt fluvial system, rather than an aggrading system, as testified by the relatively small thickness (10-15 m) and large width of the lowstand fluvial gravels (Chapters 2 and 3). The deep incision of the Lower Tagus Valley and the efficient sediment bypass, show that besides catchment size (upstream control) and sea level (downstream control) the width of the shelf is an important downstream control on incision depth and width through fluvial gradient and landward extent of regressive erosion.

20,000-12,000 cal BP | rapid sea-level rise: transgression

A gradually moister and warmer climate since ~20,000 cal BP caused the change from a braiding to a single-channel fluvial system at around 14,000 cal BP, which deposited fine-grained aggrading fluvial overbank deposits in the deeply incised Lower Tagus Valley (Chapter 2 and 3). Shortly after this (~12,000 cal BP), relative sea-level rise rapidly pushed the single-channel fluvial system inland, leading to upstream migration of the long profile crossover, creation of accommodation space and ultimately the drowning of the Lower Tagus Valley. The single-channel fluvial overbank deposits were found only locally, probably because they accumulated in a narrow, deeply incised valley, which was cut during the 30,000-20,000 cal BP relative sea-level drop within the broad fluvial plain (Chapter 2). The non-erosive transition to tidal deposits in the top of the fine-grained lowstand deposits indicates that the overbank deposits were preserved remarkably well. This is due to the rapid relative sea-level rise and transgression, precluding marine erosion. The lowstand braided and single-channel river deposits are part of the lowstand systems tract (Chapter 2).

On the Tagus Abyssal Plain rapid sedimentation continued until ~11,500 cal BP, because of a continued supply of fluvially derived sediment. The final stage of rapid abyssal plain deposition coincides with the onset of increased sedimentation on the shelf at around 13,500 cal BP, which continued until ~10,500 cal BP and reflects a landward depocentre shift caused by relative sea-level rise (Chapter 6).

12,000-7000 cal BP | final stage of sea-level rise: transgression

This period is characterized by the final stage of relative sea-level rise from 40 m below present-day sea level around 12,000 cal BP to present-day sea level at around 7000 cal BP (Chapter 3). As a result, the deeply incised lowstand valley was transgressed by tidal and marine environments and around 7000 cal BP the Lower Tagus Valley was completely drowned and occupied by a transgressive tidal environment which reached up to 100 km inland. This transgressive tidal environment reflects the transgressive systems tract (Chapter 2). The Lower Tagus Valley trapped increasing sediment volumes, which limited export to the shelf. This resulted in strongly decreased sedimentation on the shelf during the early stage of the Holocene (~10,500-5000 cal BP) (Chapter 6). Until around 7000 cal BP, the depocentre shifted landward because accommodation space was maximal in the Lower Tagus Valley. The morphology of the Lower Tagus Valley with its narrow exit created a sheltered inland basin upstream of Lisbon. The narrow exit strongly reduced the effect of storms and storm surges in the drowned valley, creating a relatively quiet environment on a wave-dominated Atlantic Coast. This quiet environment together with the depth of the incision facilitated deposition of fine-grained prodelta deposits and prohibited the import of coastal sand (Chapters 2 and 3).

7000-2000 cal BP | fluvial sediment supply: regression

Relative sea-level stability since 7000 cal BP resulted in regression marked by bayhead delta progradation and the build-up of a fluvial wedge in the Lower Tagus Valley, representing the highstand systems tract (Chapter 2). Around 5000 cal BP, the valley was filled to such an extent that gradually sediment export occurred again, and on the shelf a subaqueous delta and mudbelt built up, reflecting a seaward depocentre shift (Chapter 6). Due to continued fluvial sediment supply after the end of the relative sea-level rise (~7000 cal BP) combined with the protected setting, regression was mainly upstream controlled. The resulting fluvial sediment wedge prograded downstream and simultaneously the Holocene onlap point migrated upstream. The flooding history of the last ~6500 years in the Lower Tagus Valley was dominantly controlled by climatic changes during the period between 5500 and 1000 cal BP (Chapter 5).

2000-0 cal BP | human impact: increased fluvial-marine sedimentation

Since ~2000 cal BP an increasing sedimentary response of the Tagus fluvial-marine depositional system to land-use changes in the catchment was registered (Chapter 4). In the floodplain grainsize coarsened and sedimentation rate and magnetic susceptibility increased during this period. This is explained by increased erosion of catchment slopes due to deforestation and increasing agriculture, which led to an increased flooding frequency and/or intensity. On the Tagus shelf the mudbelt grainsize fined, together with a higher sedimentation rate and increased magnetic susceptibility. The fining grainsize is a consequence of an increased suspended sediment flux towards the shelf. The higher concentration of fine mud may have resulted in subdued winnowing and therefore a better preservation of fine-grained sediment. Four depositional phases linked with anthropogenic impact on the natural landscape in the Tagus catchment were identified (~2300/~1600/~1100/~670 cal BP), the latter two being the strongest ones. Since land-use changes like deforestation and agriculture in the Tagus catchment caused increased runoff, offshore proxy records should be interpreted with caution with respect to climatic changes for the last few thousand years.

7.2 CONTROLS

The multi-disciplinary and multi-proxy approach utilized in the present study has clearly demonstrated the shelf region—being at the confluence of terrestrial and marine processes—to be extremely sensitive to developments in the terrestrial and marine realms. The detailed study of sediment depocentres migrating from the deep-marine abyssal plain to the inland river valley and seaward again has shown to be of great value for the explanation of sedimentary successions on the continental shelf.

Sea-level change

Sea-level change has a strong control on shifting sediment depocentres. Depocentre movement and sea-level change play a large role in the situation of large sediment bodies such as fluvial channels and turbidites, which are potential hydrocarbon reservoirs. Depocentre movement and sea-level change also affect pollen concentrations in marine sediments. To deal with this, marine palynological studies should take into account palaeogeography and the position of sea level relative to the shelf break, to better understand the sediment and pollen source.

Configuration of the continental shelf

The configuration of the continental shelf (narrow, incised by a river valley) greatly affects sediment transport and bypass to the deep sea, thereby affecting depocentre location. A deeply incised inland river valley captures large sediment quantities during sea-level highstand, thereby limiting marine deposition. On the other hand, a deeply incised valley funnelling into the head of a submarine canyon efficiently bypasses sediment to the deep sea during sea-level lowstand.

Human impact

Using detailed sedimentological, chronological and historical data from the river valley and shelf, the effect of human impact in the river catchment could be traced from source-to-sink. The extensive human impact thereby shed light on the direction, scale and time of the response of a fluvial-marine depositional system to large-scale external forcing.

Tectonic activity

The studied region is known to be tectonically active, as illustrated by large historic earthquakes in 1531, 1755 and 1909 AD. Despite this historic tectonic activity, the horizontal relative sea-level curve since ~7000 cal BP proves that neotectonic uplift or subsidence were limited. Further, the present study has not identified sedimentological features in the fluvial-marine depositional system which could be clearly linked with earthquakes or tsunamis. The lowstand braided Tagus River deposits are relatively thin (up to 15 m thick) and directly overly Tertiary deposits in the Lower Tagus Valley. This implies that subsidence in the Lower Tagus Valley was absent during the Quaternary period and suggests that long-term tectonic uplift occurred, preventing the deposits from being lowered below the scour depth of younger fluvial systems.

Fluvial sediment supply and climate change

Relative sea-level stability since 7000 cal BP resulted in the increased relative importance of fluvial sediment supply, which controlled regression and fluvial progradation (Chapter 3). Quantitative estimates of sediment volume for the last ~12,000 years show a dramatically increased sediment flux and storage in the Tagus fluvial-marine depositional system after ~7000 cal BP, which was favoured by climate change. Since the end of the African Humid Period (~5500 cal BP) climate resulted in more arid conditions, followed by a progressive decrease of regional forest cover. Added to this are land-use changes during the last ~2000 years. These changes caused an increased vulnerability to soil erosion in the Tagus catchment and an up to a 2.5 times higher sediment flux to the Lower Tagus Valley and shelf, when compared to the pre-7000 cal BP

period (Chapter 6). It is striking that the increased sediment flux was not coinciding with a gradual increase in (peak) flood discharges during the last ~6000 years although three phases of increased fluvial activity were established in distal floodbasin settings (6500-5500, 4900-3500 and 1000-0 cal BP) (Chapter 5). Quantitative estimates of sediment volume deposited in the Tagus fluvial-marine depositional system have enabled calculation of the total mechanical denudation rate for the Tagus catchment, which equals ~0.09 mm/y (Chapter 6). This value is in agreement with long-term (10-40 ka) erosion rates from Central European catchments.

Sediment budgets at a passive continental margin

The present study uses for the first time a (semi-) quantitative approach to quantify sediment fluxes and budgets of a fluvial-marine depositional system. This study identified an increased flux and storage of sediment during the last ~7000 years, despite the fact that this was not identified by the analysis of the flooding history of the river using local observations (cores). This illustrates the advantage of a (semi-) quantitative approach using sediment budgets, because it provides a time-integrated three-dimensional reconstruction of sediment supply and deposition. Local differences in sedimentation which are inherent with different depositional environments have a limited effect on a reconstruction based on sediment budgets. Further, sediment budgets provide a powerful tool to link erosion with deposition, to identify changes in time and to link land and ocean depocentres. This is essential because changing external controls affect the complete depositional system. This underlines the importance of an integrated land-ocean study and the quantification of fluvial-marine sediment fluxes to identify effects of e.g. climate change and human impact on depositional systems.

7.3 FUTURE RESEARCH

Although this thesis contributes to a better understanding of fluvial and marine deposition on a passive continental margin, questions that remain to be answered are:

1. *How do fluvial and marine deposition on a passive continental margin develop on timescales of hundred thousands of years?* The present study only covers the last ~20,000 years, whereas sea level, climate, tectonics and sediment production on larger time-scales have varied considerably and probably interacted in much different ways. While marine records are known to represent millions of years, problematic for such a study will be the lack of terrestrial data due to erosion. Process-based catchment modelling under different scenarios of boundary conditions will be indispensable to understand developments occurring on land. Due

to the narrow exit near Lisbon, the Tagus River acts as a point-source of sediment, which together with the large sediment supply, makes this river well suited for this type of study.

2. *How are vegetation and sediment production affected by climatic aridification and what is the response of a fluvial system to this?* Although the present study suggests a relationship between the end of the African Humid Period, subsequent aridification and forest decline on the Iberian Peninsula and an increased sediment flux, the exact mechanisms linking climatic aridification to changing sediment fluxes in the fluvial and marine realm are unclear. For example, attention should be given to the buffering effect of colluvial, alluvial fan and inland fluvial basins.

3. *How have sediment fluxes and budgets evolved on smaller time-scales?* As the present first-order quantification of sediment volumes has highlighted major differences between the pre and post-7000 cal BP periods, a more detailed study would greatly add to the understanding of cause-and-effect relationships and response times. This requires a more detailed chronology, using radiocarbon dating.

4. *What is the detailed postglacial relative-sea level history in the southwest of the Iberian Peninsula and what were the local factors controlling relative sea-level change?* The relative sea-level reconstruction from the present study shows an early Holocene rising limb of the curve which plots above eustatic sea level reconstructions from tectonically stable regions elsewhere. At around 7000 cal BP relative sea-level rise reached the present-day level and remained stable since that time. This suggests at least early Holocene tectonic uplift, and possibly also uplift after 7000 cal BP. The resolution of the presented relative sea-level reconstruction limits the ability to answer this question and therefore a more detailed study of postglacial relative sea-level rise is needed.

5. *What is the applicability of magnetic susceptibility measurements for stratigraphic correlation in terrestrial-marine environments?* In this study the magnetic susceptibility signal has been used as a tool to correlate terrestrial and marine sediments. Increased magnetic susceptibility values have been interpreted as a proxy for soil erosion. Only the basic "volume-based magnetic susceptibility" was used and no magnetic measurements from catchment sediments and soils were done. Therefore a study of the value of the different magnetic properties that can be measured on terrestrial and marine sediments and their applicability in linking erosion from catchment slopes with downstream deposition is needed.

6. *What is the effect of future climate change on water and sediment discharge of the Tagus River?* For the next century a tendency towards

decreasing mean seasonal rainfall over the Iberian Peninsula and increasing extreme events of flooding and drought is predicted. Our study indicates that future erosion rates will intensify as a result of this. A study using detailed data of Holocene Tagus River flooding combined with detailed climate models and water and sediment discharge models would provide valuable new insight in the response of a major fluvial system in this climatically sensitive region.

References

Abrantes, F., Alt-Epping, U., Lebreiro, S.M., Voelker, A. and Schneider, R., 2008. Sedimentological record of tsunamis on shallow-shelf areas: The case of the 1969 AD and 1755 AD tsunamis on the Portuguese Shelf off Lisbon. Marine Geology 249, 283-293.

Abrantes, F., Baas, J., Haflidason, H., Rasmussen, T., Klitgaard, D., Loncaric, N. and Gaspar, L., 1998. Sediment fluxes along the northeastern European Margin: inferring hydrological changes between 20 and 8 kyr. Marine Geology 152, 7-23.

Abrantes, F., Lebreiro, S.M., Rodrigues, T., Gil, I., Bartels-Jónsdóttir, H., Oliveira, P., Kissel, C. and Grimalt, J.O., 2005. Shallow-marine sediment cores record climate variability and earthquake activity off Lisbon (Portugal) for the last 2000 years. Quaternary Science Reviews 24, 2477-2494.

Alday, M., Cearrata, A., Cachao, M., Freitas, M.C., Andrade, C. and Gama, C., 2006. Micropalaeontological record of Holocene estuarine and marine stages in the Corgo do Porto rivulet (Mira River, SW Portugal). Estuarine Coastal and Shelf Science 66, 532-543.

Allen, G.P., 1991. Sedimentary processes and facies in the Gironde estuary: a Recent model of macrotidal estuarine systems. In: Smith, G.D., Reinson, G.E., Zaitlin, B.A. and Rahmani, R.A. (Eds.), Clastic Tidal Sedimentology: Canadian Society of Petroleum Geologists Memoir 16. Canadian Society of Petroleum Geologists, pp. 29-40.

Allen, G.P. and Posamentier, H.W., 1993. Sequence Stratigraphy and Facies Model of an Incised Valley Fill - the Gironde Estuary, France. Journal of Sedimentary Petrology 63, 378-391.

Allen, J.R.L., 1990. The Severn Estuary in Southwest Britain - Its Retreat under Marine Transgression, and Fine-Sediment Regime. Sedimentary Geology 66, 13-28.

Allen, J.R.M., Huntley, B. and Watts, W.A., 1996. The vegetation and climate of northwest Iberia over the last 14000 yr. Journal of Quaternary Science 11, 125-147.

Allen, P.A. and Allen, J.R., 2005. Basin analysis: principles and applications. Blackwell Science Ltd, Oxford.

Alt-Epping, U., Stuut, J.-B.W., Hebbeln, D. and Schneider, R., 2009. Variations in sediment provenance during the past 3000 years off the Tagus River, Portugal. Marine Geology 261, 82-91.

Alves, T.M., Gawthorpe, R.L., Hunt, D.W. and Monteiro, J.H., 2003. Cenozoic tectono-sedimentary evolution of the western Iberian margin. Marine Geology 195, 75-108.

Amorosi, A., Colalongo, M.L., Pasini, G. and Preti, D., 1999. Sedimentary response to Late Quaternary sea-level changes in the Romagna coastal plain (northern Italy). Sedimentology 46, 99-121.

Amorosi, A., Colalongo, M.L., Fiorini, F., Fusco, F., Pasini, G., Vaiani, S.C. and Sarti, G., 2004. Palaeogeographic and palaeoclimatic evolution of the Po Plain from 150-ky core records. Global and Planetary Change 40, 55-78.

Andrade, A., Arroyo, T.M. and Zapata, B.R., 1990. Análisis palinológico de la cuenca alta del río Alberche (Ávila). Actas de Gredos. Boletín Universitario 10, 15-18.

Andrade, A., Zapata, B.R., Gil-García, M.J. and Fombella, M., 1996. Acción antrópica y su impacto sobre la vegetación, desde el tránsito Subatlántico-Subboreal, en la vertiente norte de la Sierra de Gredos (Ávila, España). Estudios Palinológicos 1996, 7-12.

Andréassian, V., 2004. Waters and forests: from historical controversy to scientific debate. Journal of Hydrology 291, 1-27.

Anonymous, 1800. A sketch of the River Tagus from the Bar of Alcaçova up to Coffin's Hole. Duckworth Collection.

Antoine, P., 1997. Lateglacial and Early Holocene evolution of valleys in northern France: new results. Comptes Rendus de l'Académie des Sciences. Serie II Fascicule A - Sciences de la Terre et des Planètes 325, 35-42.

Antoine, P., Munaut, A.V., Limondin-Lozouet, N., Ponel, P., Duperon, J. and Duperon, M., 2003. Response of the Selle river to climatic modifications during the Lateglacial and early Holocene (Somme Basin-Northern France). Quaternary Science Reviews 22, 2061-2076.

Arhan, M., Deverdiere, A.C. and Memery, L., 1994. The Eastern Boundary of the Subtropical North-Atlantic. Journal of Physical Oceanography 24, 1295-1316.

Arzola, R.G., Wynn, R.B., Lastras, G., Masson, D.G. and Weaver, P.P.E., 2008. Sedimentary features and processes in the Nazaré and Setúbal submarine canyons, west Iberian margin. Marine Geology 250, 64-88.

Atienza, M., Lobo, A.G. and Zapata, B.R., 1990. Estudio polínico de un depósito localizado en la Garganta del Trampal (Sierra de Béjar, Ávila). Actas de Gredos. Boletín Universitario 10, 19-23.

Atienza, M., Dorado, M. and Zapata, B.R., 1991. Palinología en el estudio de la acción antrópica. Aplicación de los depósitos localizados en la Sierra de Béjar y en la Sierra de Ávila (Ávila). Boletín Universitario 11, 31-38.

Azevêdo, M.T., 2001. A utilização dos dados históricos no estudo das cheias do Tejo. In: Estudos do Quaternário. APEQ, Lisboa, pp. 69-77.

Azevêdo, M.T., Favaretto, S., Miola, A., Mozzi, P., Nicosia, C., Nunes, E. and Sostizzo, I., 2006a. Palaeoenvironments of the Tagus valley during the last 15 ka: sedimentological, palynological and micromorphological evidence of the Entre Valas SEV coring (Santarém, Portugal). In: Tagus Floods '06 Workshop, Abstract Book 19-21 July 2006, Lisbon, Portugal 68-70.

Azevêdo, M.T., Ramos Pereira, A., Ramos, C., Nunes, E., Freitas, M.C., Andrade, A. and Pereira, D.I., 2007. Floodplain sediments of the Tagus River, Portugal: assessing avulsion, channel migration and human impact. In: Nichols, G., Williams, E. and Paola, C. (Eds.), Sedimentary processes, environments, and basins: a tribute to Peter Friend. International Association of Sedimentologists, Special publication 38. Blackwell Publishing Ltd., Oxford.

Azevêdo, T.M., Nunes, E. and Ramos, C., 2004. Some morphological aspects and hydrological characterization of the Tagus floods in the Santarem region, Portugal. Natural Hazards 31, 587-601.

Azevêdo, T.M., Ramos Pereira, A., Ramos, C., Nunes, E., Freitas, M.C., Andrade, C. and Pereira, D.I., 2006b. Role of the sedimentological and geomorphological analyses to identify the Middle Portuguese Tagus channel Holocene avulsions and shiftings. In: VII Congresso Nacional de Geologia, Livro de Resumos (Extended abstracts) 2, pp. 579-581.

Baas, J.H., Mienert, J., Abrantes, F. and Prins, M.A., 1997. Late Quaternary sedimentation on the Portuguese continental margin: Climate-related processes and products. Palaeogeography Palaeoclimatology Palaeoecology 130, 1-23.

Bao, R., Freitas, M.D. and Andrade, C., 1999. Separating eustatic from local environmental effects: a late-Holocene record of coastal change in Albufeira Lagoon, Portugal. Holocene 9, 341-352.

Bao, R., Alonso, A., Delgado, C. and Pages, J.L., 2007. Identification of the main driving mechanisms in the evolution of a small coastal wetland (Traba, Galicia, NW Spain) since its origin 5700 cal yr BP. Palaeogeography Palaeoclimatology Palaeoecology 247, 296-312.

Barbosa, B.P., 1995. Alostratigrafia e Litostratigrafia das Unidades Continentais da Bacia Terciária do Baixo Tejo. Relações com o Eustatismo e a Tectónica. Ph.D. thesis. University of Lisbon, Lisbon, 253 pp.

Barros, A.P., 1996. An evaluation of model parameterizations of sediment pathways: a case study for theTejo estuary. Continental Shelf Research 16, 1725-1749.

Bartels-Jónsdóttir, H.B., Knudsen, K.L., Abrantes, F., Lebreiro, S. and Eiríksson, J., 2006. Climate variability during the last 2000 years in the Tagus Prodelta, western Iberian Margin: Benthic foraminifera and stable isotopes. Marine Micropaleontology 59, 83-103.

Behre, K.E., 2004. Coastal development, sea-level change and settlement history during the later Holocene in the Clay District of Lower Saxony (Niedersachsen), northern Germany. Quaternary International 112, 37-53.

Benito, G., Sanchez-Moya, Y. and Sopena, A., 2003a. Sedimentology of high-stage flood deposits of the Tagus River, Central Spain. Sedimentary Geology 157, 107-132.

Benito, G., Diez-Herrero, A. and de Villalta, M.F., 2003b. Magnitude and frequency of flooding in the Tagus basin (Central Spain) over the last millennium. Climatic Change 58, 171-192.

Benito, G., Sopena, A., Sanchez-Moya, Y., Machado, M.J. and Perez-Gonzalez, A., 2003c. Palaeoflood record of the Tagus River (Central Spain) during the Late Pleistocene and Holocene. Quaternary Science Reviews 22, 1737-1756.

Benito, G., Thorndycraft, V.R., Rico, M., Sánchez-Moya, Y. and Sopeña, A., 2008. Palaeoflood and floodplain records from Spain: Evidence for long-term climate variability and environmental changes. Geomorphology 101, 68-77.

Berendsen, H.J.A. and Stouthamer, E., 2000. Late Weichselian and Holocene palaeogeography of the Rhine-Meuse delta, The Netherlands. Palaeogeography Palaeoclimatology Palaeoecology 161, 311-335.

Berendsen, H.J.A. and Stouthamer, E., 2001. The palaeogeographic development of the Rhine-Meuse delta, The Netherlands. Koninklijke Van Gorcum, Assen.

Berendsen, H.J.A., Hoek, W.Z. and Schorn, E.A., 1995. Late Weichselian and Holocene River Channel Changes of the Rivers Rhine and Meuse in the Central Netherlands (Land van Maas en Waal). In: Frenzel,B. (Ed.), European River Activity and Climatic Change during the Lateglacial and Early Holocene. Paläoklimaforschung (Paleoclimate Research) 14, 151-171. ESF project "European paleoclimate and man" (special issue 9).

Bettencourt, A. and Ramos, L., 2003. Estuários Portugueses. Instituto da Água. Ministério das Cidades, Ordenamento do Território e Ambiente. Direcção de Serviços de Planeamento, Lisboa.

Blott, S.J. and Pye, K., 2001. GRADISTAT: A grain size distribution and statistics package for the analysis of unconsolidated sediments. Earth Surface Processes and Landforms 26, 1237-1248.

Blum, M.D. and Törnqvist, T.E., 2000. Fluvial responses to climate and sea-level change: a review and look forward. Sedimentology 47, 2-48.

Blum, M.D. and Aslan, A., 2006. Signatures of climate vs. sea-level change within incised valley-fill successions: Quaternary examples from the Texas Gulf Coast. Sedimentary Geology 190, 177-211.

Borrego, J., Morales, J.A. and Pendon, J.G., 1995. Holocene estuarine facies along the mesotidal coast of Huelva, south-west Spain. Special Publications of the International Association of Sedimentologists 24, 151-170.

Borrego, J., Ruiz, F., Gonzalez-Regalado, M.L., Pendon, J.G. and Morales, J.A., 1999. The Holocene transgression into the estuarine central basin of the Odiel River mouth (Cadiz gulf, SW, Spain): lithology and faunal assemblages. Quaternary Science Reviews 18, 769-788.

Bosch, J.M. and Hewlett, J.D., 1982. A Review of Catchment Experiments to Determine the Effect of Vegetation Changes on Water Yield and Evapo-Transpiration. Journal of Hydrology 55, 3-23.

Boski, T., Moura, D., Veiga-Pires, C., Camacho, S., Duarte, D., Scott, D.B. and Fernandes, S.G., 2002. Postglacial sea-level rise and sedimentary response in the Guadiana Estuary, Portugal/Spain border. Sedimentary Geology 150, 103-122.

Boyd, R., Dalrymple, R.W. and Zaitlin, B.A., 2006. Estuary and incised valley facies models. In: Posamentier, H.W. and Walker, R.G. (Eds.), Facies Models Revisited. SEPM, Special Publication 84. Society for Sedimentary Geology, Tulsa, Oklahoma, pp. 171-234.

Bridge, J.S., 2003. Rivers and floodplains: forms, processes, and sedimentary record. Blackweel Science, Oxford.

Bridgland, D.R., Preece, R.C., Roe, H.M., Tipping, R.M., Coope, G.R., Field, M.H., Robinson, J.E., Schreve, D.C. and Crowe, K., 2001. Middle Pleistocene interglacial deposits at Barling, Essex, England: evidence for a longer chronology for the Thames terrace sequence. Journal of Quaternary Science 16, 813-840.

BRISA, 2005. A10 - Auto-estrada Bucelas/Carregado/IC3 sublanço Carregado (A1)-Benavente, travessia do Tejo no Carregado.

Bronk Ramsey, C., 1995. Radiocarbon Calibration and Analysis of Stratigraphy: The OxCal Program. Radiocarbon 37, 425-430.

Bronk Ramsey, C., 2001. Development of the Radiocarbon Program OxCal. Radiocarbon 43, 355-363.

Bronk Ramsey, C., 2005. OxCal v3.10 radiocarbon calibration software.

Bryant, M., Falk, P. and Paola, C., 1995. Experimental-Study of Avulsion Frequency and Rate of Deposition. Geology 23, 365-368.

Busschers, F.S., Kasse, C., van Balen, R.T., Vandenberghe, J., Cohen, K.M., Weerts, H.J.T., Wallinga, J., Johns, C., Cleveringa, P. and Bunnik, F.P.M., 2007. Late Pleistocene evolution of the Rhine-Meuse system in the southern North Sea basin: imprints of climate change, sea-level oscillation and glacio-isostacy. Quaternary Science Reviews 26, 3216-3248.

Cabral, J., 1995. Neotectónica em Portugal Continental. Memórias do Instituto Geológico e Mineiro 31.

Cabral, J., 2001. Paleoseismological Studies Near Lisbon: Holocene Thrusting or Landslide Activity? EOS Transactions, American Geophysical Union 82, 351-353.

Cabral, J. and Ribeiro, A., 1989. Carta Neotectónica de Portugal, Serviços Geológicos de Portugal, Scale 1:1.000.000, including Nota Explicativa, Lisboa.

Camoin, G.F., Montaggioni, L.F. and Braithwaite, C.J.R., 2004. Late glacial to post glacial sea levels in the Western Indian Ocean. Marine Geology 206, 119-146.

Carrión, J.S., 2002. Patterns and processes of Late Quaternary environmental change in a montane region of southwestern Europe. Quaternary Science Reviews 21, 2047-2066.

Carrión, J.S., Fuentes, N., González-Sampériz, P., Quirante, L.S., Finlayson, J.C., Fernández, S. and Andrade, A., 2007. Holocene environmental change in a montane region of southern Europe with a long history of human settlement. Quaternary Science Reviews 26, 1455-1475.

Carta Geológica do Concelho de Lisboa, 1985. Carta Geológica do Concelho de Lisboa, Folha 3. Direcção-geral de Geologia e Minas, Serviços Geológicos de Portugal, Lisboa.

Carvalho, A.M.F. and Almeida, F.J.N.d.S., 1996. Aspectos Económicos da Ocupação Romana na Foz do Tejo. Ocupação Romana dos Estuários do Tejo e do Sado - Actas das Primeiras Jornadas sobre Romanização dos Estuários do Tejo e do Sado, Seixal (1991). Câmara Municipal do Seixal/Publicações Dom Quixote, Lisboa, pp. 137-155.

Carvalho, J., Matias, H., Torres, L., Manupella, G., Pereira, R. and Mendes-Victor, L., 2005. The structural and sedimentary evolution of the Arruda and Lower Tagus sub-basins, Portugal. Marine and Petroleum Geology 22, 427-453.

Catuneanu, O., 2006. Principles of Sequence Stratigraphy. Elsevier, Oxford.

Chester, D.K., 2001. The 1755 Lisbon earthquake. Progress in Physical Geography 25, 363-383.

Chester, D.K. and James, P.A., 1991. Holocene Alluviation in the Algarve, Southern Portugal - the Case for an Anthropogenic Cause. Journal of Archaeological Science 18, 73-87.

Chmura, G.L. and Eisma, D., 1995. A palynological study of surface and suspended sediments on a tidal flat: implications for pollen transport and deposition in coastal waters. Marine Geology 128, 183-200.

Christie-Blick, N. and Driscoll, N.W., 1995. Sequence Stratigraphy. Annual Review of Earth and Planetary Sciences 23, 451-478.

Claussen, M., Kubatzki, C., Brovkin, V., Ganopolski, A., Hoelzmann, P. and Pachur, H.J., 1999. Simulation of an abrupt change in Saharan vegetation in the mid-Holocene. Geophysical Research Letters 26, 2037-2040.

Cohen, K.M., 2005. 3D Geostatistical interpolation and geological interpretation of paleo-groundwater rise in the Holocene coastal prism in The Netherlands. In: Giosan, L. and Bhattacharya, J.P. (Eds.), River Deltas-Concepts, Models, and examples. SEPM Special Publication 83, Society for Sedimentary Geology, Tulsa, Oklahoma, pp. 351-364.

Colman, S.M., Baucom, P.C., Bratton, J.F., Cronin, T.M., McGeehin, J.P., Willard, D., Zimmerman, A.R. and Vogt, P.R., 2002. Radiocarbon Dating, Chronologic Framework, and Changes in Accumulation Rates of Holocene Estuarine Sediments from Chesapeake Bay. Quaternary Research 57, 58-70.

Cunha, P.P., Martins, A.A., Daveau, S. and Friend, P.F., 2005. Tectonic control of the Tejo river fluvial incision during the late Cenozoic, in Rodao - central Portugal (Atlantic Iberian border). Geomorphology 64, 271-298.

Cunha, P.P., Martins, A.A., Huot, S., Murray, A. and Raposo, L., 2008. Dating the Tejo river lower terraces in the Rodao area (Portugal) to assess the role of tectonics and uplift. Geomorphology 102, 43-54.

Curtis, M.L., 1999. Structural and kinematic evolution of a Miocene to Recent sinistral restraining bend: the Montejunto massif, Portugal. Journal of Structural Geology 21, 39-54.

Dabrio, C.J., Zazo, C., Lario, J., Goy, J.L., Sierro, F.J., Borja, F., Gonzalez, J.A. and Flores, J.A., 1999. Sequence stratigraphy of Holocene incised-valley fills and coastal evolution in the Gulf of Cadiz (southern Spain). Geologie en Mijnbouw 77, 263-281.

Dabrio, C.J., Zazo, C., Goy, J.L., Sierro, F.J., Borja, F., Lario, J., Gonzalez, J.A. and Flores, J.A., 2000. Depositional history of estuarine infill during the last postglacial transgression (Gulf of Cadiz, Southern Spain). Marine Geology 162, 381-404.

Dalrymple, R.W., 2006. Incised valleys in time and space: introduction to the volume and an explanation of the controls on valley formation and filling. In: Dalrymple, R.W., Leckie, D.A. and Tillman, R. (Eds.), Incised valleys in time and space. SEPM Special Publication 51. Society for Sedimentary Geology, Tulsa, Oklahoma, p. 391.

Dalrymple, R.W. and Zaitlin, B.A., 1994. High-Resolution Sequence Stratigraphy of a Complex, Incised Valley Succession, Cobequid Bay - Salmon River Estuary, Bay of Fundy, Canada. Sedimentology 41, 1069-1091.

Dalrymple, R.W. and Choi, K., 2007. Morphologic and facies trends through the fluvial-marine transition in tide-dominated depositional systems: A schematic framework for environmental and sequence-stratigraphic interpretation. Earth-Science Reviews 81, 135-174.

Dalrymple, R.W., Zaitlin, B.A. and Boyd, R., 1992. Estuarine facies models: conceptual basis and stratigraphic implications. Journal of Sedimentary Petrology 62, 1130-1146.

Dalrymple, R.W., Boyd, R. and Zaitlin, B.A., 1994. Incised-valley systems: origin and sedimentary sequences. In: Dalrymple, R.W., Leckie, D.A. and Tillman, R. (Eds.), Incised valleys in time and space. SEPM Special Publication 51. Society for Sedimentary Geology, Tulsa, Oklahoma.

Dalrymple, R.W., Knight, R.J., Zaitlin, B.A. and Middleton, G.V., 1990. Dynamics and Facies Model of a Macrotidal Sand-Bar Complex, Cobequid Bay Salmon River Estuary (Bay of Fundy). Sedimentology 37, 577-612.

Daveau, S. and Gonçalves, V., 1985. A evolução holocénica do vale do Sorraia e as particularidades da sua antropização (Neolítico e Calcolítico). In: Actas I Reunião do Quaternário Ibérico 2, 187-197.

De Mendonça, A.F., 1933. Relatório das sondagens geológicas no leito do rio Tejo, entre o Beato e o Montijo. Annuário dos Serviços Hidráulicos Imprensa Nacional 1934, 73-84.

De Moor, J.J.W., Kasse, C., Van Balen, R., Vandenberghe, J. and Wallinga, J., 2008. Human and climate impact on catchment development during the Holocene - Geul River, the Netherlands. Geomorphology 98, 316-339.

Dearing, J.A., Morton, R.I., Price, T.W. and Foster, I.D.L., 1986. Tracing Movements of Topsoil by Magnetic Measurements - 2 Case-Studies. Physics of the Earth and Planetary Interiors 42, 93-104.

Delgado, M., 1981. Acerca da cerâmica da época Romana do Cabeço da Bruxa, Alpiarça. In: Separata da revista Portugália, nova série II/III, pp. 71-73.

DeMenocal, P., Ortiz, J., Guilderson, T., Adkins, J., Sarnthein, M., Baker, L. and Yarusinsky, M., 2000. Abrupt onset and termination of the African Humid Period: rapid climate responses to gradual insolation forcing. Quaternary Science Reviews 19, 347-361.

Denys, L. and Baeteman, C., 1995. Holocene Evolution of Relative Sea-Level and Local Mean High Water Spring Tides in Belgium - a First Assessment. Marine Geology 124, 1-19.

Dias, J.M.A., Boski, T., Rodrigues, A. and Magalhaes, F., 2000. Coast line evolution in Portugal since the Last Glacial Maximum until present - a synthesis. Marine Geology 170, 177-186.

Dinis, J.L., Henriques, V., Freitas, M.C., Andrade, C. and Costa, P., 2006. Natural to anthropogenic forcing in the Holocene, evolution of three coastal lagoons (Caldas da Rainha valley, western Portugal). Quaternary International 150, 41-51.

Doyle, P. and Bennet, M.R., 1998. Unlocking the Stratigraphical Record. Advances in Modern Stratigraphy. John Wiley & Sons, West Sussex.

Duplaix, S., Nesteroff, W.D. and Heezen, B.C., 1965. Minéralogie comparée des sédiments du Tage (Portugal) et de quelques sables profonds da la plaine abyssale correspondante. Deep-Sea Research 12, 211-217.

Emery, D. and Myers, K., 1996. Sequence Stratigraphy. Blackwell Science, Oxford.

Ethridge, F.G., Wood, L.J. and Schumm, S.A., 1998. Cyclic variables controlling fluvial sequence development: Problems and Perspectives. In: Shanley, K.J. and McCabe, P.J. (Eds.), Relative role of eustacy, climate and tectonism on continental rocks. SEPM Special Publication 59. Society for Sedimentary Geology, Tulsa, Oklahoma, pp. 17-29.

European Soil Portal, 2008. European Soil Data Center, 2008. European Commission, Joint Research Centre, Land Management & Natural Hazards Unit.

Faegri, K. and Iversen, J., 1975. Textbook of pollen analysis. Munksgaard, Copenhagen.

Faleh, A., Bouhlassa, S., Sadiki, A. and Garcia, C.C., 2005. Exploitation des mesures magnétiques dans l'identification des sources de sédiments: cas du bassin versant d'Abdelali (Rif oriental, Maroc). Zeitschrift für Geomorphologie 49, 309-320.

Faust, D., Zielhofer, C., Escudero, R.B. and del Olmo, F.D., 2004. High-resolution fluvial record of late Holocene geomorphic change in northern Tunisia: climate or human impact? Quaternary Science Reviews 23, 1757-1775.

Fernández-Salas, L.M., Lobo, F.J., Hernández-Molina, F.J., Somoza, L., Rodero, J., del Río, V.D. and Maldonado, A., 2003. High-resolution architecture of late Holocene highstand prodeltaic deposits from southern Spain: the imprint of high-frequency climatic and relative sea-level changes. Continental Shelf Research 23, 1037-1054.

Figueiral, I. and Carcaillet, C., 2005. A review of Late Pleistocene and Holocene biogeography of highland Mediterranean pines (Pinus type sylvestris) in Portugal, based on wood charcoal. Quaternary Science Reviews 24, 2466-2476.

FitzPatrick, E.A., 1983. Soils; their formation, classification and distribution. Longman, London and New York.

Fiúza, A.F.D., 1983. Upwelling patterns off Portugal. Coastal upwelling: its sediment record. Plenum Press, New York.

Fletcher, W.J., Boski, T. and Moura, D., 2007. Palynological evidence for environmental and climatic change in the lower Guadiana valley, Portugal, during the last 13 000 years. Holocene 17, 481-494.

Fonseca, J.F.B.D. and Vilanova, S.P., 2001. Reply on: Paleoseismological Studies Near Lisbon: Holocene Thrusting or Landslide Activity? EOS Transactions, American Geophysical Union 82, 351-353.

Fonseca, J.F.B.D., Bosi, V. and Vilanova, S.P., 2000. Investigations Unveil Holocene Thrusting for Onshore Portugal. EOS Transactions, American Geophysical Union 81, 412-413.

Fortunato, A.B., Oliveira, A. and Baptista, A.M., 1999. On the effect of tidal flats on the hydrodynamics of the Tagus estuary. Oceanologica Acta 22, 31-44.

Franco, F., García-Antón, M. and Sainz-Ollero, H., 1997. Impacto antrópico y dinámica de la vegetación durante los últimos 2000 años BP en la vertiente septentrional de la Sierra de Gredos: Navarredonda (Ávila, España). Revue de Paléobiologie de Genève 16, 29-45.

Freire, F.E., 1985. Inclusão de antigas restingas no delta interior do Tejo. In: Actas I Reunião do Quaternario Iberico 1, 311-322.

Freitas, M.C., Andrade, C., Moreno, J.C., Munha, J.M. and Cachao, M., 1999. The sedimentary record of recent (last 500 years) environmental changes in the Seixal Bay marsh, Tagus estuary, Portugal. Geologie en Mijnbouw 77, 283-293.

Frouin, R., Fiuza, A.F.G., Ambar, I. and Boyd, T.J., 1990. Observations of a Poleward Surface Current Off the Coasts of Portugal and Spain During Winter. Journal of Geophysical Research-Oceans 95, 679-691.

IOC, IHO and BODC, 2003. "Centenary Edition of the GEBCO Digital Atlas", published on CD-ROM on behalf of the Intergovernmental Oceanographic Commission and the International Hydrographic Organization as part of the General Bathymetric Chart of the Oceans. British Oceanographic Data Centre, Liverpool.

Gerli, E.M., 2003. Medieval Iberia: an encyclopedia. Routledge, New York.

Gil-Romera, G., Antón, M.G. and ACalleja, J.A., 2008. The late Holocene palaeoecological sequence of Serranía de las Villuercas (southern Meseta, western Spain). Vegetation History and Archaeobotany 17, 653-666.

Gil, I.M., Abrantes, F. and Hebbeln, D., 2006. The North Atlantic Oscillation forcing through the last 2000 years: Spatial variability as revealed by high-resolution marine diatom records from N and SW Europe. Marine Micropaleontology 60, 113-129.

Gil, I.M., Abrantes, F. and Hebbeln, D., 2007. Diatoms as upwelling and river discharge indicators along the Portuguese margin: instrumental data linked to proxy information. Holocene 17, 1245-1252.

Goodbred, S.L. and Kuehl, S.A., 2000. Enormous Ganges-Brahmaputra sediment discharge during strengthened early Holocene monsoon. Geology 28, 1083-1086.

Goodess, C. M., and Jones, P. D. 2002. Links between circulation and changes in the characteristics of Iberian rainfall. International Journal of Climatology 22, 1593-1615.

Goy, J.L., Zazo, C., Dabrio, C.J., Lario, J., Borja, F., Sierro, F.J. and Flores, J.A., 1996. Global and regional factors controlling changes of coastlines in Southern Iberia (Spain) during the Holocene. Quaternary Science Reviews 15, 773-780.

Granja, H.M., 1998. Evidence for Late Pleistocene and Holocene sea-level, neotectonic and climate control in the coastal zone of northwest Portugal. Geologie en Mijnbouw 77, 233-245.

Granja, H.M. and De Groot, T.A.M., 1996. Sea-level rise and neotectonism in a Holocene coastal environment at Cortegaca Beach (NW Portugal): A case study. Journal of Coastal Research 12, 160-170.

Grimley, D.A. and Arruda, N.K., 2007. Observations of magnetite dissolution in poorly drained soils. Soil Science 172, 968-982.

Guillén, J. and Palanques, A., 1997. A historical perspective of the morphological evolution in the lower Ebro river. Environmental Geology 30, 174-180.

Hanebuth, T., Stattegger, K. and Grootes, P.M., 2000. Rapid flooding of the Sunda Shelf: A late-glacial sea-level record. Science 288, 1033-1035.

Hanesch, M. and Scholger, R., 2005. The influence of soil type on the magnetic susceptibility measured throughout soil profiles. Geophysical Journal International 161, 50-56.

Hannon, G.E. and Gaillard, M.-J., 1997. The plant-macrofossil record of past lake-level changes. Journal of Paleolimnology 18, 15-28.

Haynes, R. and Barton, E.D., 1990. A Poleward Flow Along the Atlantic Coast of the Iberian Peninsula. Journal of Geophysical Research-Oceans 95, 11425-11441.

Heap, A.D. and Nichol, S.L., 1997. The influence of limited accommodation space on the stratigraphy of an incised-valley succession: Weiti River estuary, New Zealand. Marine Geology 144, 229-252.

Heller, P.L. and Paola, C., 1996. Downstream changes in alluvial architecture: An exploration of controls on channel-stacking patterns. Journal of Sedimentary Research 66, 297-306.

Holbrook, J.M., Willis, B.J. and Bhattacharya, J., 2003. The evolution of allocyclicity and autocyclicity as sedimentary concepts. AAPG Annual Meeting, Salt Lake City, Utah.

Hooghiemstra, H., Stalling, H., Agwu, C.O.C. and Dupont, L.M., 1992. Vegetational and Climatic Changes at the Northern Fringe of the Sahara 250,000-5000 Years Bp - Evidence from 4 Marine Pollen Records Located between Portugal and the Canary-Islands. Review of Palaeobotany and Palynology 74, 1-53.

Hornbeck, J.W., Adams, M.B., Corbett, E.S., Verry, E.S. and Lynch, J.A., 1993. Long-Term Impacts of Forest Treatments on Water Yield - a Summary for Northeastern USA. Journal of Hydrology 150, 323-344.

Hovius, N., 1998. Controls on sediment supply by large rivers. In: Shanley, K.W. and McCabe, P.J. (Eds.), Relative Role of Eustasy, Climate, and Tectonism in Continental Rocks. SEPM Special Publication 59. Society for Sedimentary Geology, Tulsa, Oklahoma.

Hughen, K.A., Baillie, M.G.L., Bard, E., Beck, J.W., Bertrand, C.J.H., Blackwell, P.G., Buck, C.E., Burr, G.S., Cutler, K.B., Damon, P.E., Edwards, R.L., Fairbanks, R.G., Friedrich, M., Guilderson, T.P., Kromer, B., McCormac, G., Manning, S., Ramsey, C.B., Reimer, P.J., Reimer, R.W., Remmele, S., Southon, J.R., Stuiver, M., Talamo, S., Taylor, F.W., van der Plicht, J. and Weyhenmeyer, C.E., 2004. Marine04 marine radiocarbon age calibration, 0-26 cal kyr BP. Radiocarbon 46, 1059-1086.

IGM/INETI, 2008. Carta Geológica de Portugal (1:50.000), Lisbon.

INETI, 1994. Relatório Final - Contrato de prospecção e pesquisa No. 5/94. Depósito de turfas da Goucha, Instituto Geológico e Mineiro (INETI).

INETI, 2007. INETI Library coring database. Different library entries.

Instituto Hidrográfico Portugal, 2008. Instituto Hidrográfico, Portugal. http://www.hidrografico.pt/.

Janssen, C.R., 1994. Palynological indications for the extent of the impact of man during Roman times in the western part of the Iberian Peninsula. In: Frenzel, B. (Ed.), Evaluation of land surfaces cleared from forests in the Mediterranean region during the time of the Roman empire. Palaeoclimate Research 10, 15-22.

Jarvis, A., Reuter, H.I., Nelson, A. and Guevara, E., 2006. Hole-filled seamless SRTM data V3. International Centre for Tropical Agriculture (CIAT).

Jelgersma, S., 1961. Holocene Sea-level changes in The Netherlands. Ph.D. thesis, Mededelingen Geologische Stichting, CVI-7, Leiden, 100 pp.

Jordan, G., van Rompaey, A., Szilassi, P., Csillag, G., Mannaerts, C. and Woldai, T., 2005. Historical land use changes and their impact on sediment fluxes in the Balaton basin (Hungary). Agriculture Ecosystems & Environment 108, 119-133.

Jorge, S.O., 1999. Domesticar a terra. As primeiras comunidades agrárias em território Português. Trajectos Portugueses 45. Gradiva Publicações, Lisboa.

Jouanneau, J.M., Garcia, C., Oliveira, A., Rodrigues, A., Dias, J.A. and Weber, O., 1998. Dispersal and deposition of suspended sediment on the shelf off the Tagus and Sado estuaries, SW Portugal. Progress in Oceanography 42, 233-257.

Kalb, P. and Höck, M., 1979. Cabeço da Bruxa, Alpiarça: relatório preliminar da escavação de Janeiro e Fevereiro de 1979 Separata da revista Portugália, nova série II/III, 61-69.

Kalb, P. and Höck, M., 1984. Moron: historisch und archäologisch. Madrider Mitteilungen 25, 91-102.

Kasse, C., Hoek, W.Z., Bohncke, S.J.P., Konert, M., Weijers, J.W.H., Cassee, M.L. and Van der Zee, R.M., 2005. Late Glacial fluvial response of the Niers-Rhine (western Germany) to climate and vegetation change. Journal of Quaternary Science 20, 377-394.

Kasse, K., Vandenberghe, J. and Bohncke, S., 1995. Climatic change and fluvial dynamics of the Maas during the late Weichselian and early Holocene. In: Frenzel,B. (Ed.), European River Activity and Climatic Change during the Lateglacial and Early Holocene. Paläoklimaforschung (Paleoclimate Research) 14, 151-171. ESF project "European paleoclimate and man" (special issue 9).

Kattenberg, A.E. and Aalbersberg, G., 2004. Archaeological prospection of the Dutch perimarine landscape by means of magnetic methods. Archaeological Prospection 11, 227-235.

Keesstra, S.D., 2007. Impact of natural reforestation on floodplain sedimentation in the Dragonja basin, SW Slovenia. Earth Surface Processes and Landforms 32, 49-65.

Kennett, J.P., 1982. Marine Geology. Prentice-Hall, Englewood-Cliffs, New Jersey.

Klein, J., 1920. The Mesta: a study in Spanish economic history: 1273-1836. Harvard economic studies, 21. Harvard U.P., Cambridge, Massachusetts.

Knox, J.C., 2000. Sensitivity of modern and Holocene floods to climate change. Quaternary Science Reviews 19, 439-457.

Knox, J.C., 2001. Agricultural influence on landscape sensitivity in the Upper Mississippi River Valley. Catena 42, 193-224.

Knox, J.C., 2006. Floodplain sedimentation in the Upper Mississippi Valley: Natural versus human accelerated. Geomorphology 79, 286-310.

Konert, M. and Vandenberghe, J., 1997. Comparison of laser grain size analysis with pipette and sieve analysis: A solution for the underestimation of the clay fraction. Sedimentology 44, 523-535.

Kranck, K., Smith, P.C. and Milligan, T.G., 1996a. Grain-size characteristics of fine-grained unflocculated sediments 1. 'One-round' distributions. Sedimentology 43, 589-596.

Kranck, K., Smith, P.C. and Milligan, T.G., 1996b. Grain-size characteristics of fine-grained unflocculated sediments 2. 'Multi-round' distributions. Sedimentology 43, 597-606.

Labeyrie, L. and Turon, J.-L., 2005a. Physical properties of sediment core MD99-2332. PANGAEA, Publishing Network for Geoscientific & Environmental Data.

Labeyrie, L. and Turon, J.-L., 2005b. Physical properties of sediment core MD99-2333. PANGAEA, Publishing Network for Geoscientific & Environmental Data.

Lang, A., Bork, H.R., Mackel, R., Preston, N., Wunderlich, E. and Dikau, R., 2003. Changes in sediment flux and storage within a fluvial system: some examples from the Rhine catchment. Hydrological Processes 17, 3321-3334.

Lario, J., Zazo, C., Goy, J.L., Dabrio, C.J., Borja, F., Silva, P.G., Sierro, F., Gonzalez, A., Soler, V. and Yll, E., 2002. Changes in sedimentation trends in SW Iberia Holocene estuaries (Spain). Quaternary International 93, 171-176.

Lastras, G., Arzola, R.G., Masson, D.G., Wynn, R.B., Huvenne, V.A.I., Hühnerbach, V. and Canals, M., 2008. Geomorphology and sedimentary features in the Central Portuguese submarine canyons, Western Iberian margin. Geomorphology 103, 310-329.

Le Pera, E. and Arribas, J., 2004. Sand composition in an Iberian passive-margin fluvial course: the Tajo River. Sedimentary Geology 171, 261-281.

Lebreiro, S., Voelker, A., Vizcaino, A., Abrantes, F., Alt-Epping, U., Jung, S., Thouveny, N. and Grácia, E., in press. Abrupt glacial climate changes destabilize continental slopes. Quaternary Science Reviews.

Lebreiro, S.M., 1995. Sedimentation history off Iberia: Tore seamount, Tagus and Horseshoe abyssal plains. Ph.D. thesis, University of Cambridge, Cambridge, United Kingdom, 192 pp.

Lebreiro, S.M., Francés, G., Abrantes, F.F.G., Diz, P., Bartels-Jónsdóttir, H.B., Stroynowski, Z.N., Gil, I.M., Pena, L.D., Rodrigues, T., Jones, P.D., Nombela, M.A., Alejo, I., Briffa, K.R., Harris, I. and Grimalt, J.O., 2006. Climate change and coastal hydrographic response along the Atlantic Iberian margin (Tagus Prodelta and Muros Ría) during the last two millennia. The Holocene 16, 1003-1015.

Lehner, B., Doll, P., Alcamo, J., Henrichs, T. and Kaspar, F., 2006. Estimating the impact of global change on flood and drought risks in Europe: A continental, integrated analysis. Climatic Change 75, 273-299.

Leira, M., 2005. Diatom responses to Holocene environmental changes in a small lake in northwest Spain. Quaternary International 140, 90-102.

Leithold, E.L., Perkey, D.W., Blair, N.E. and Creamer, T.N., 2005. Sedimentation and carbon burial on the northern California continental shelf: the signatures of land-use change. Continental Shelf Research 25, 349-371.

Lesueur, P., Tastet, J.P. and Marambat, L., 1996. Shelf mud fields formation within historical times: examples from offshore the Gironde estuary, France. Continental Shelf Research 16, 1849-1870.

Lesueur, P., Lesourd, S., Lefebvre, D., Garnaud, S. and Brun-Cottan, J.C., 2003. Holocene and modern sediments in the Seine Estuary (France): a synthesis. Journal of Quaternary Science 18, 339-349.

204

Lobo, F.J., Dias, J.M.A., Gonzalez, R., Hernandez-Molina, F.J., Morales, J.A. and Del Rio, V.D., 2003. High-resolution seismic stratigraphy of a narrow, bedrock-controlled estuary: The Guadiana estuarine system, SW Iberia. Journal of Sedimentary Research 73, 973-986.

LUSOPONTE, 1995. New road crossing of the Tagus in Lisbon (Main bridge geological and geotechnical study). Concessionária para a Travessia do Tejo S.A. (Ponte da Vasco Gama).

Mackey, S.D. and Bridge, J.S., 1995. 3-Dimensional Model of Alluvial Stratigraphy - Theory and Application. Journal of Sedimentary Research Section B-Stratigraphy and Global Studies 65, 7-31.

Macklin, M.G., Benito, G., Gregory, K.J., Johnstone, E., Lewin, J., Michczynska, D.J., Soja, R., Starkel, L. and Thomdycraft, V.R., 2006. Past hydrological events reflected in the Holocene fluvial record of Europe. Catena 66, 145-154.

Magny, M., Miramont, C. and Sivan, O., 2002. Assessment of the impact of climate and anthropogenic factors on Holocene Mediterranean vegetation in Europe on the basis of palaeohydrological records. Palaeogeography Palaeoclimatology Palaeoecology 186, 47-59.

Maher, B.A. and Thompson, R., 1991. Mineral Magnetic Record of the Chinese Loess and Paleosols. Geology 19, 3-6.

Maher, B.A. and Thompson, R., 1992. Paleoclimatic significance of the mineral magnetic record of the Chinese loess and paleosols. Quaternary Research 37, 155-170.

Makaske, B. and Nap, R.L., 1995. A Transition from a Braided to a Meandering Channel Facies, Showing Inclined Heterolithic Stratification (Late Weichselian, Central Netherlands). Geologie en Mijnbouw 74, 13-20.

Martins, A.A., 1999. Caracterização morfotectónica e morfossedimentar da Bacia do Baixo Tejo - pliocénico e quaternário. Ph.D. thesis, Universidade de Évora, Évora, 500 pp.

Masson, D.G. and Miles, P.R., 1984. Mesozoic seafloor spreading between Iberia, Europe and North America. Marine Geology 56, 279-287.

Mattheus, C.R., Rodriguez, A.B., Greene, D.L., Simms, A.R. and Anderson, J.B., 2007. Control of upstream variables on incised-valley dimension. Journal of Sedimentary Research 77, 213-224.

McCave, I.N., Manighetti, B. and Robinson, S.G., 1995. Sortable silt and fine sediment size composition slicing: parameters for palaeocurrent speed and palaeoceanography. Paleoceanography 10, 593-610.

Meckel, L.D., 1975. Holocene sand bodies in the Colorado delta, Salton Sea, Imperial County, California. In: Broussard, M.L. (Ed.), Deltas. Houston Geological Society, Houston, Texas, pp. 239-266.

Milliman, J.D. and Meade, R.H., 1983. World-Wide Delivery of River Sediment to the Oceans. Journal of Geology 91, 1-21.

Mohrig, D., Heller, P.L., Paola, C. and Lyons, W.J., 2000. Interpreting avulsion process from ancient alluvial sequences: Guadalope-Matarranya system (northern Spain) and Wasatch Formation (western Colorado). Geological Society of America Bulletin 112, 1787-1803.

Mol, J., Vandenberghe, J. and Kasse, C., 2000. River response to variations of periglacial climate in mid-latitude Europe. Geomorphology 33, 131-148.

Monteiro, J.H., Voelker, A., Ferreira, A., Mil-Homens, M., Nave, S., Magalhães, V., Salgueiro, E., Vaqueiro, S., Muiños, S. and Freitas, P., 2002. Report of the cruise PALEO I (PO287) on FS Poseidon (April 22-May 3, 2002), Instituto Geológico e Mineiro, Alfragide, Portugal.

Mougenot, D., 1985. Progradation on the Portuguese Continental-Margin - Interpretation of Seismic Facies. Marine Geology 69, 113-130.

Múgica, F.F., Anton, M.G. and Ollero, H.S., 1998. Vegetation dynamics and human impact in the Sierra de Guadarrama, Central System, Spain. Holocene 8, 69-82.

Naughton, F., Goni, M.F.S., Drago, T., Freitas, M.C. and Oliveira, A., 2007a. Holocene changes in the Douro estuary (Northwestern Iberia). Journal of Coastal Research 23, 711-720.

Naughton, F., Goni, M.F.S., Desprat, S., Turon, J.L., Duprat, J., Malaize, B., Joli, C., Cortijo, E., Drago, T. and Freitas, M.C., 2007b. Present-day and past (last 25 000 years) marine pollen signal off western Iberia. Marine Micropaleontology 62, 91-114.

Nichol, S.L., Boyd, R. and Penland, S., 1996. Sequence stratigraphy of a coastal-plain incised valley estuary: Lake Calcasieu, Louisiana. Journal of Sedimentary Research 66, 847-857.

Nichol, S.L., Zaitlin, B.A. and Thom, B.G., 1997. The upper Hawkesbury River, New South Wales, Australia: A Holocene example of an estuarine bayhead delta. Sedimentology 44, 263-286.

Nittrouer, C.A., Austin, J.A., Field, M.E., Kravitz, J.H., Syvitski, J.P.M. and Wiberg, P.L., 2007. Writing a Rosetta stone: insights into continental-margin sedimentary processes and strata. In: Nittrouer, C.A., Austin, J.A., Field, M.E., Kravitz, J.H., Syvitski, J.P.M. and Wiberg, P.L. (Eds.), Continental margin sedimentation: from sediment transport to sequence stratigraphy. Special Publication of the International Association of Sedimentologists 37. Blackwell Publishing Ltd., Oxford.

Oldfield, F., Maher, B.A., Donoghue, J. and Pierce, J., 1985. Particle-Size Related, Mineral Magnetic Source Sediment Linkages in the Rhode River Catchment, Maryland, USA. Journal of the Geological Society 142, 1035-1046.

Oldfield, F., Asioli, A., Accorsi, C.A., Mercuri, A.M., Juggins, S., Langone, L., Rolph, T., Trincardi, F., Wolff, G., Gibbs, Z., Vigliotti, L., Frignani, M., van der Post, K. and Branch, N., 2003. A high resolution late Holocene palaeo environmental record from the central Adriatic Sea. Quaternary Science Reviews 22, 319-342.

Peliz, A.J. and Fiúza, A.F.G., 1999. Temporal and spatial variability of CZCS-derived phytoplankton pigment concentrations off the western Iberian Peninsula. International Journal of Remote Sensing 20, 1363-1403.

Peltier, W.R. and Fairbanks, R.G., 2006. Global glacial ice volume and Last Glacial Maximum duration from an extended Barbados sea level record. Quaternary Science Reviews 25, 3322-3337.

Pons, L.J. and Schelling, J., 1951. De laatglaciale afzettingen van de Rijn en de Maas. Geologie en Mijnbouw 13, 293-297.

Pons, L.J. and Van Oosten, M.F., 1974. De bodem van Noordholland, Toelichting bij blad 5 van de bodemkaart van Nederland, schaal 1:200.000. Stichting voor bodemkartering (STIBOKA), Wageningen.

Portela, L.I. and Neves, R., 1994. Numerical modelling of suspended sediment transport in tidal estuaries: a comparison between the Tagus (Portugal) and the Scheldt (Belgium-The Netherlands). Netherlands Journal of Aquatic Ecology 28, 329-335.

Posamentier, H.W. and Allen, G.P., 1999. Siliciclastic sequence stratigraphy - concepts and applications. SEPM Concepts in Sedimentology and Paleontology 7. Society for Sedimentary Geology (SEPM), Tulsa, Oklahoma.

Pratson, L.F., Nittrouer, C.A., Wiberg, P.L., Steckler, M.S., Swenson, J.B., Cacchione, D.A., Karson, J.A., Murray, A.B., Wolinsky, M.A., Gerber, T.P., Mullenbach, B.L., Spinelli, G.A., Fulthorpe, C.S., O'Grady, D.B., Parker, G., Driscoll, N.W., Burger, R.L., Paola, C., Orange, D.L., Field, M.E., Friedrichs, C.T. and Fedele, J.J., 2007. Seascape evolution on clastic continental shelves and slopes. In: Nittrouer, C.A., Austin, J.A., Field, M.H., Kravitz, J.H., Syvitski, J.P.M. and Wiberg, P.L. (Eds.), Continental margin sedimentation: from sediment transport to sequence stratigraphy. Special Publication of the International Association of Sedimentologists 37. Blackwell Publishing Ltd., Oxford.

Psuty, N.P. and Moreira, M.E.S.A., 2000. Holocene sedimentation and sea level rise in the Sado Estuary, Portugal. Journal of Coastal Research 16, 125-138.

Ramos, C., Reis, E., Ramos Pereira, A., Azevêdo, T.M., Nunes, E., Freitas, M.C. and Andrade, C., 2002. Late Holocene evolution of the Lower Tagus alluvial plain and heavy metals content: preliminary results. Environmental Change and Water Sustainability, Instituto Pirenaico de Ecología, Zaragoza 167-182.

Ramos Pereira, A., Ramos, C., Reis, E., Azevêdo, T.M., Nunes, E., Freitas, M.C. and Andrade, C., 2002. A dinâmica da planície aluvial do Baixo Tejo no Holocénico recente: aplicação de métodos de análise geomorfológica e sedimentológica. Publicações da Associação Portuguesa de Geomorfólogos 1, 67-76.

Rasmussen, E.S., Lomholt, S., Andersen, C. and Vejbaek, O.V., 1998. Aspects of the structural evolution of the Lusitanian Basin in Portugal and the shelf and slope area offshore Portugal. Tectonophysics 300, 199-225.

Reading, H.G., 1998. Sedimentary Environments: Processes, Facies and Stratigraphy. Blackwell Science, Oxford.

Reimer, P.J., Baillie, M.G.L., Bard, E., Bayliss, A., Beck, J.W., Bertrand, C.J.H., Blackwell, P.G., Buck, C.E., Burr, G.S., Cutler, K.B., Damon, P.E., Edwards, R.L., Fairbanks, R.G., Friedrich, M., Guilderson, T.P., Hogg, A.G., Hughen, K.A., Kromer, B., McCormac, G., Manning, S., Ramsey, C.B., Reimer, R.W., Remmele, S., Southon, J.R., Stuiver, M., Talamo, S., Taylor, F.W., van der Plicht, J. and Weyhenmeyer, C.E., 2004. IntCal04 terrestrial radiocarbon age calibration, 0-26 cal kyr BP. Radiocarbon 46, 1029-1058.

Reineck, H.E. and Wunderlich, F., 1968. Classification and origin of flaser and lenticular bedding. Sedimentology 11, 99-104.

Renssen, H., Brovkin, V., Fichefet, T. and Goosse, H., 2006. Simulation of the Holocene climate evolution in Northern Africa: The termination of the African Humid Period. Quaternary International 150, 95-102.

Ribeiro, O., Teixeira, C., Gonçalves, F., Zbyszewski, G., Carreira de Deus, P. and Oliveira, J., 1977. Carta Geológica de Portugal, scale 1:50.000, sheet 27-D Abrantes. Direcção Geral de Minas e Serviços Geológicos, Serviços Geológicos de Portugal Lisboa.

Rocha, J.S., Fernandes, J.N. and Ferreira, G., 2005. Plano específico de gestão de extracção de inertes no domínio hídrico do Rio Tejo. Relatório 259/05-NRE, Laboratório Nacional de Engenharia Civil (LNEC), Departamento de Hidráulica e Ambiente, Núcleo de Recursos Hídricos e Estruturas e Ambiente, Lisboa.

Rodrigo, F.S., Esteban-Parra, M.J., Pozo-Vázquez, D. and Castro-Díez, Y., 1999. A 500-year precipitation record in Southern Spain. International Journal of Climatology 19, 1233-1253.

Rodríguez-Ramírez, A., Rodríguez-Vidal, J., Cáceres, L., Clemente, L., Belluomini, G., Manfra, L., Improta, S. and de Andrés, J.R., 1996. Recent coastal evolution of the Donana National Park (SW Spain). Quaternary Science Reviews 15, 803-809.

Rosina, P., 2004. Os terraços fluviais do Tejo e a fauna associada. Paleontologia e Arqueologia do Estuário do Tejo, Actas do I Seminário 4, 63-70.

Roucoux, K.H., De Abreu, L., Shackleton, N.J. and Tzedakis, P.C., 2005. The response of NW Iberian vegetation to North Atlantic climate oscillations during the last 65 kyr. Quaternary Science Reviews 24, 1637-1653.

Ruiz, F., Gonzalez-Regalado, M.L., Pendon, J.G., Abad, M., Olias, M. and Munoz, J.M., 2005. Correlation between foraminifera and sedimentary environments in recent estuaries of Southwestern Spain: Applications to Holocene reconstructions. Quaternary International 140, 21-36.

Sahin, V. and Hall, M.J., 1996. The effects of afforestation and deforestation on water yields. Journal of Hydrology 178, 293-309.

Sakai, T., Fujiwara, O. and Kamataki, T., 2006. Incised-valley-fill succession affected by rapid tectonic uplifts: An example from the upper-most Pleistocene to Holocene of the Isumi River lowland, central Boso Peninsula, Japan. Sedimentary Geology 185, 21-39.

Santos, L., Romani, J.R.V. and Jalut, G., 2000. History of vegetation during the Holocene in the Courel and Queixa Sierras, Galicia, northwest Iberian Peninsula. Journal of Quaternary Science 15, 621-632.

Savory, H.N., 1968. Spain and Portugal: The Prehistory of the Iberian Peninsula. Thames & Hudson, London.

Schaller, M., von Blanckenburg, F., Hovius, N. and Kubik, P.W., 2001. Large-scale erosion rates from in situ-produced cosmogenic nuclides in European river sediments. Earth and Planetary Science Letters 188, 441-458.

Schattner, T.G., 1998. Archäologischer Wegweiser durch Portugal. Philipp von Zabern, Mainz am Rhein.

Schumm, S.A., 1993. River Response to Baselevel Change - Implications for Sequence Stratigraphy. Journal of Geology 101, 279-294.

Secretaria d'Estado, 1784. Mappa do Tejo. Desde a Villa de Tancos ate a Villa Franca de Xira. Extracto tirado do Mappa Geral das Lezirias e Coutadas. In: Cardoso, J.L. (Ed.), Colecção de Obras Clássicas do Pensamento Económico Português. Memórias económicas da Academia Real das Ciências de Lisboa, para o adiantamento da agricultura, das artes, e da indústria em Portugal, e suas conquistas (1789-1815). Tomo II, 1. Banco de Portugal, Lisboa 1991.

Segl, M. and Alt-Epping, U., 2005a. Physical properties of sediment core GeoB8903-1, unpublished dataset #262003. PANGAEA, Publishing Network for Geoscientific & Environmental Data.

Segl, M. and Alt-Epping, U., 2005b. Physical properties of sediment core GeoB8904-1, unpublished dataset #262004. PANGAEA, Publishing Network for Geoscientific & Environmental Data.

Segl, M., Alt-Epping, U., deAbreu, L., Dimmler, W., Franke, P., Hüttich, D., Jung, S., Langer, J., Ratmeyer, V., Rodrigues, T. and Wunderlich, J., 2004. Report and preliminary results of Poseidon Cruise 304. Galway-Lisbon; 5-22 October 2003. Fachbereich Geowissenschaften 230, 27.

Slicher van Bath, B., 1960. De agrarische geschiedenis van West-Europa 500-1850. Het Spectrum, Utrecht/Antwerpen.

Slingerland, R. and Smith, N.D., 1998. Necessary conditions for a meandering-river avulsion. Geology 26, 435-438.

Slingerland, R. and Smith, N.D., 2004. River avulsions and their deposits. Annual Review of Earth and Planetary Sciences 32, 257-285.

Smith, C.D., 1979. Western Mediterranean Europe: a historical geography of Italy, Spain and southern France since the Neolithic. Academic Press, London.

Sommerfield, C.K. and Lee, H.J., 2004. Across-shelf sediment transport since the Last Glacial Maximum, southern California margin. Geology 32, 345-348.

Sommerfield, C.K. and Wheatcroft, R.A., 2007. Late Holocene sediment accumulation on the northern California shelf: Oceanic, fluvial, and anthropogenic influences. Geological Society of America Bulletin 119, 1120-1134.

Starkel, L., Gebica, P. and Superson, J., 2007. Last Glacial-Interglacial cycle in the evolution of river valleys in southern and central Poland. Quaternary Science Reviews 26, 2924-2936.

Stockmarr, J., 1971. Tablets with spores used in absolute pollen analysis. Pollen et Spores 13, 615-621.

Stouthamer, E. and Berendsen, H.J.A., 2007. Avulsion: The relative roles of autogenic and allogenic processes. Sedimentary Geology 198, 309-325.

Stuiver, M. and Braziunas, T.F., 1993. Modeling Atmospheric C-14 Influences and C-14 Ages of Marine Samples to 10,000 BC. Radiocarbon 35, 137-189.

Stuiver, M. and Reimer, P.J., 1993. Extended 14C database and revised CALIB radiocarbon calibration program. Radiocarbon 35, 215-230.

Stuiver, M., Reimer, P.J. and Reimer, R.W., 2005. CALIB 5.0. (internet program and documentation).

Syvitski, J.P.M., Peckham, S.D., Hilberman, R. and Mulder, T., 2003. Predicting the terrestrial flux of sediment to the global ocean: a planetary perspective. Sedimentary Geology 162, 5-24.

Talling, P.J., 1998. How and where do incised valleys form if sea level remains above the shelf edge? Geology 26, 87-90.

Thompson, R., Bloemendal, J., Dearing, J.A., Oldfield, F., Rummery, T.A., Stober, J.C. and Turner, G.M., 1980. Environmental Applications of Magnetic Measurements. Science 207, 481-486.

Thorndycraft, V.R. and Benito, G., 2006a. Late Holocene fluvial chronology of Spain: The role of climatic variability and human impact. Catena 66, 34-41.

Thorndycraft, V.R. and Benito, G., 2006b. The Holocene fluvial chronology of Spain: evidence from a newly compiled radiocarbon database. Quaternary Science Reviews 25, 223-234.

Thorndycraft, V.R., Benito, G., Rico, M., Sopena, A., Sanchez-Moya, Y. and Casas, A., 2005. A long-term flood discharge record derived from slackwater flood deposits of the Llobregat River, NE Spain. Journal of Hydrology 313, 16-31.

Tomaselli, R., 1977. Degradation of the Mediterranean maquis. In: Mediterranean Forests and Maquis: Ecology, Conservation and Management (MAB Technical Notes 2). UNESCO, Paris.

Törnqvist, T.E. and Van Dijk, G.J., 1993. Optimizing Sampling Strategy for Radiocarbon Dating of Holocene Fluvial Systems in a Vertically Aggrading Setting. Boreas 22, 129-145.

Törnqvist, T.E. and Bridge, J.S., 2002. Spatial variation of overbank aggradation rate and its influence on avulsion frequency. Sedimentology 49, 891-905.

Törnqvist, T.E., De Jong, A.F.M., Oosterbaan, W.A. and Vanderborg, K., 1992. Accurate Dating of Organic Deposits by Ams C-14 Measurement of Macrofossils. Radiocarbon 34, 566-577.

Törnqvist, T.E., van Ree, M.H.M., van 't Veer, R. and van Geel, B., 1998. Improving methodology for high-resolution reconstruction of sea-level rise and neotectonics by paleoecological analysis and AMS C-14 dating of basal peats. Quaternary Research 49, 72-85.

Törnqvist, T.E., Wortman, S.R., Mateo, Z.R.P., Milne, G.A. and Swenson, J.B., 2006. Did the last sea level lowstand always lead to cross-shelf valley formation and source-to-sink sediment flux? Journal of Geophysical Research-Earth Surface 111.

Toscano, M.A. and Macintyre, I.G., 2003. Corrected western Atlantic sea-level curve for the last 11,000 years based on calibrated C-14 dates from Acropora palmata framework and intertidal mangrove peat. Coral Reefs 22, 257-270.

Trigo, R.M., Pozo-Vazquez, D., Osborn, T.J., Castro-Diez, Y., Gamiz-Fortis, S. and Esteban-Parra, M.J., 2004. North Atlantic oscillation influence on precipitation, river flow and water resources in the Iberian Peninsula. International Journal of Climatology 24, 925-944.

Vale, C. and Sundby, B., 1987. Suspended Sediment Fluctuations in the Tagus Estuary on Semi-Diurnal and Fortnightly Time Scales. Estuarine Coastal and Shelf Science 25, 495-508.

Van de Meene, E.A., Van der Staay, J. and Hock, T.L., 1979. The Van der Staay suction-corer. A simple apparatus for drilling in sand below groundwater table. Rijks Geologische Dienst, The Netherlands.

Van de Plassche, O., 1981. Sea-level, Groundwater and Basal Peat Growth-a Reassessment of Data from The Netherlands. Geologie en Mijnbouw 60, 401-409.

Van den Berg, M.W., 1996. Fluvial sequences of the Meuse-a 10Ma record of neotectonics and climate change at various time-scales. Ph.D. thesis, Agricultural University Wageningen, Wageningen.

Van den Brink, L.M. and Janssen, C.R., 1985. The Effect of Human Activities During Cultural Phases on the Development of Montane Vegetation in the Serra da Estrêla, Portugal. Review of Palaeobotany and Palynology 44, 193-215.

Van der Knaap, W.O. and Van Leeuwen, J.F.N., 1995. Holocene vegetation succession and degradation as responses to climatic change and human activity in the Serra da Estrela, Portugal. Review of Palaeobotany and Palynology 89, 153-211.

Van der Schriek, T., Passmore, D.G., Rolao, J. and Stevenson, A.C., 2007a. Estuarine-fluvial floodplain formation in the Holocene Lower Tagus valley (Central Portugal) and implications for Quaternary fluvial system evolution. Quaternary Science Reviews 26, 2937-2957.

Van der Schriek, T., Passmore, D.G., Stevenson, A.C. and Rolao, J., 2007b. The palaeogeography of Mesolithic settlement-subsistence and shell midden formation in the Muge valley, Lower Tagus Basin, Portugal. The Holocene 17, 369-385.

Van der Spek, A.J.F., 1997. Tidal asymmetry and long-term evolution of Holocene tidal basins in The Netherlands: simulation of palaeo-tides in the Schelde estuary. Marine Geology 141, 71-90.

Van der Woude, J.D., 1981. Holocene Paleoenvironmental Evolution of a Perimarine Fluviatile Area. Ph.D. thesis, Vrije Universiteit Amsterdam, Amsterdam, 112 pp.

Van Dijk, G.J., Berendsen, H.J.A. and Roeleveld, W., 1991. Holocene Water Level Development in the Netherlands River Area - Implications for Sea-Level Reconstruction. Geologie en Mijnbouw 70, 311-326.

Van Geel, B., Buurman, J. and Waterbolk, H.T., 1996. Archaeological and palaeoecological indications of an abrupt climate change in The Netherlands, and evidence for climatological teleconnections around 2650 BP. Journal of Quaternary Science 11, 451-460.

Van Huissteden, J. and Kasse, C., 2001. Detection of rapid climate change in Last Glacial fluvial successions in The Netherlands. Global and Planetary Change 28, 319-339.

Van Leeuwaarden, W. and Janssen, C.R., 1985. A preliminary palynological study of peat deposits near an oppidum in the Lower Tagus Valley, Portugal. Reunião do Quaternario Iberico 2, 226-236.

Van Rompaey, A.J.J., Govers, G. and Puttemans, C., 2002. Modelling land use changes and their impact on soil erosion and sediment supply to rivers. Earth Surface Processes and Landforms 27, 481-494.

Van Staalduinen, C.J., 1979. Toelichting bij de geologische kaart van Nederland, Blad Rotterdam West (37W), schaal 1:50.000. Rijks Geologische Dienst (TNO), Haarlem.

Van Wagoner, J.C., Posamentier, H.W., Mitchum, R.M., Vail, P.R., Sarg, J.F., Loutit, T.S. and Hardenbol, J., 1988. An overview of the fundamentals of sequence stratigraphy and key definitions. In: Wilgus, C.K., Hastings, B.S., Kendall, C.G.S.C., Posamentier, H.W., Ross, C.A. and Van Wagoner, J.C. (Eds.), Sea-Level Changes: An Integrated Approach. Special Publication. Society of Economic Paleontologists and Mineralogists, Tulsa, Oklahoma.

Vandenberghe, J. and Woo, M.K., 2002. Modern and ancient periglacial river types. Progress in Physical Geography 26, 479-506.

Vandenberghe, J., Kasse, C., Bohncke, S. and Kozarski, S., 1994. Climate-Related River Activity at the Weichselian Holocene Transition - a Comparative-Study of the Warta and Maas Rivers. Terra Nova 6, 476-485.

Vanney, J.-R. and Mougenot, D., 1981. La plate-forme continentale du Portugal et les provinces adjacentes: analyse geomorphologique. Memórias dos Serviços Geológicos de Portugal 28. IGM/INETI, Lisboa.

Vilanova, S.P. and Fonseca, J., 2004. Seismic hazard impact of the Lower Tagus Valley Fault Zone (SW Iberia). Journal of Seismology 8, 331-345.

Vis, G.-J. and Kasse, C., 2009. Late Quaternary valley-fill succession of the Lower Tagus Valley, Portugal. Sedimentary Geology, doi:10.1016/j.sedgeo.2009.07.010.

Vis, G.-J., Kasse, C. and Vandenberghe, J., 2008. Late Pleistocene and Holocene palaeogeography of the Lower Tagus Valley (Portugal): effects of relative sea level, valley morphology and sediment supply. Quaternary Science Reviews 27, 1682-1709, doi: 10.1016/j.quascirev.2008.07.003.

Waelbroeck, C., Labeyrie, L., Michel, E., Duplessy, J.C., McManus, J.F., Lambeck, K., Balbon, E. and Labracherie, M., 2002. Sea-level and deep water temperature changes derived from benthic foraminifera isotopic records. Quaternary Science Reviews 21, 295-305.

Ward, P.J., Renssen, H., Aerts, J.C.J.H., van Balen, R.T. and Vandenberghe, J., 2008. Strong increases in flood frequency and discharge of the River Meuse over the late Holocene: impacts of long-term anthropogenic land use change and climate variability. Hydrology and Earth System Sciences 12, 159-175.

Weaver, P.P.E., 2003. Discovery Cruise 249, 19 Aug-10 Sep 2000. History of Sedimentation in the Gulf of Cadiz: investigations with the SOC giant piston corer, Southampton Oceanography Centre, Southampton, UK.

Weaver, P.P.E., Wynn, R.B., Kenyon, N.H. and Evan, J., 2000. Continental margin sedimentation, with special reference to the north-east Atlantic margin. Sedimentology 47, 239-256.

Weerts, H.J.T. and Berendsen, H.J.A., 1995. Late Weichselian and Holocene fluvial palaeogeography of the southern Rhine–Meuse delta (The Netherlands). Geologie en Mijnbouw 74, 199-212.

Weston, D.G., 2002. Soil and susceptibility: aspects of thermally induced magnetism within the dynamic pedological system. Archaeological Prospection 9, 207-215.

Williams, M., 2000. Dark ages and dark areas: global deforestation in the deep past. Journal of Historical Geography 26, 28-46.

Zaitlin, B.A., Dalrymple, R.W. and Boyd, R., 1994. The stratigraphic organization of incised-valley systems associated with relative sea-level change. In: Dalrymple, R.W., Boyd, R. and Zaitlin, B.A. (Eds.), Incised-valley systems: origin and sedimentary sequences. SEPM Special Publication 51. Society for Sedimentary Geology, Tulsa, Oklahoma, pp. 45-60.

Zazo, C., Goy, J.L., Somoza, L., Dabrio, C.J., Belluomini, G., Improta, S., Lario, J., Bardaji, T. and Silva, P.G., 1994. Holocene Sequence of Sea-Level Fluctuations in Relation to Climatic Trends in the Atlantic-Mediterranean Linkage Coast. Journal of Coastal Research 10, 933-945.

Zbyszewski, G., 1969. Carta Geológica do Quaternário de Portugal. Serviços Geológicos de Portugal, Direcção Geral de Minas e Serviços Geológicos, Lisboa.

Zheng, H., Oldfield, F., Yu, L., Shaw, J. and An, Z., 1991. The magnetic properties of particle-sized samples from the Luo Chuan loess section: evidence for pedogenesis. Physics of the Earth and Planetary Interiors 68, 250-258.

Zielhofer, C. and Faust, D., 2008. Mid- and late Holocene fluvial chronology of Tunisia. Quaternary Science Reviews 27, 580-588.

SUMMARY

Changing global climate as a result of strong human impact on system earth, is receiving much scientific, political and public attention. For a thorough understanding of the effects of global climatic changes, a look at the geological past provides valuable insights. Geological records in sediments of coastal zones bear traces of both terrestrial and marine processes. Coasts with a narrow continental shelf (up to 200 m water depth) and a steep continental slope enable robust geological reconstructions because of the high sediment accumulation rates and well-defined sediment pathways. At *passive continental margins*, thick sediment layers with high resolution geological archives are present due to a large fluvial sediment supply. Furthermore, disturbances by volcanoes and large earthquakes are absent, making passive continental margins well suited to improve the fundamental understanding of sedimentary processes on continental margins.

Most studies of continental margins either focus on the terrestrial part or on the marine part of the system. To improve the understanding of sedimentary processes and to unravel the controls on terrestrial and marine sedimentation, an integrated palaeoenvironmental reconstruction of a passive margin including the delta, coast, continental shelf and slope, and the deep sea abyssal plain is needed. Special emphasis should be given to the significant influence of transport and sedimentation processes under varying climates. For this purpose the collaborative research project SEDPORT was initiated within the European Science Foundation (ESF) EUROCORES EUROMARGINS framework. The general aims of this project are:

1. To better determine the influence of terrestrial and marine sediment transport mechanisms on the composition and physical properties of the last glacial to Holocene margin sediment cover with respect to modern environmental conditions;
2. To investigate how sedimentation processes have changed under varying climate conditions affecting ocean circulation, sea level, continental weathering, vegetation and precipitation since the last glacial into the Holocene.

The Iberian passive margin near the Lower Tagus Valley is well suited for such a study. Due to the narrow exit of the valley southwest of Lisbon, the Tagus River acts as a point source of sediment. The narrow and deep bedrock-confined Lower Tagus Valley is an efficient trap for fluvial, tidal and marine deposits and enables robust sediment pathway and volumetric reconstructions. During sea-level lowstand the narrow continental shelf caused efficient sediment bypassing to the Tagus Abyssal Plain while during highstand sea

215

level, sediments were efficiently trapped in the Lower Tagus Valley and on the narrow shelf.

The general aims of this study are elaborated through a series of specific aims, which resulted in two intermingled lines of research which have the correlation of land and sea records as a common background:

1. Reconstructing the *palaeogeographic evolution and fluvial-marine sediment budget of the Tagus depositional system* using facies, sedimentary architecture, sequence-stratigraphy and timing of sediment deposition;

2. Identifying the *controls* on the nature and architecture of incised-valley successions, changing sediment fluxes and fluvial-marine depocenter migrations.

To achieve these aims, a large dataset was created for the Tagus depositional system, consisting of hand and mechanical cores from the Lower Tagus Valley floodplain and three marine cores; two from the continental shelf (D13882 and GeoB-8903-1) and one from the Tagus Abyssal Plain (MD03-2698). Samples from these cores were used for multi-proxy measurements (radiocarbon age, grainsize, and heavy mineral, organic matter, carbonate, floral, and faunal content). Additionally, lithological and sedimentological information from 284 cone penetration tests, and continuous and discontinuous geological cores used for geotechnical studies was used. Geological cross sections and palaeogeographic maps were constructed to facilitate the calculation of sediment budgets.

The palaeogeographic evolution and fluvial-marine sediment budget of the Tagus depositional system

Around 20,000 years ago | lowstand sea level: incision
Lowstand sea level (120 m lower than at present) and a direct connection between the Lower Tagus Valley and the ocean across the narrow (~30 km) continental shelf caused incision of a deep valley (~70 m near Lisbon) by the Tagus River which reached up to ~100 km inland. Fluvial sediments were efficiently bypassing the largely exposed shelf via incised valleys directly funnelling into the heads of marine canyons and to the deep sea (4000-5000 m depth; Tagus Abyssal Plain), where the main depocentre was located. Bypassing of fluvial sediment resulted in high-frequency turbidite deposition on the Tagus Abyssal Plain between 20,000 and 15,000 years ago. The Tagus was a braided, and since ~14,000 years ago a single-channel river. The deep incision of the valley prevented large-scale erosion by a transgressive marine system. Consequently a thick *lowstand systems tract* has been preserved. The deep incision of the Lower Tagus Valley and the efficient sediment bypass, show that besides catchment

size and sea level, the width of the shelf is an important downstream control on incision dimension by means of fluvial gradient and landward extent of regressive erosion.

20,000-12,000 years ago | rapid relative sea-level rise: transgression
Since ~20,000 years ago relative sea level rose rapidly and at ~12,000 years ago, the rising sea level pushed the Tagus fluvial system far inland, creating accommodation space and ultimately drowning the Lower Tagus Valley. On the Tagus Abyssal Plain rapid sedimentation continued until ~11,500 years ago because of a continued supply of fluvially derived sediment. The final stage of rapid deep-sea deposition coincides with the onset of increased sedimentation on the shelf at ~13,500 years ago, which continued until ~10,500 years ago and reflects a landward depocentre shift caused by relative sea-level rise.

12,000-7000 years ago | final stage of relative sea-level rise: transgression
The final stage of relative sea-level rise from ~40 m below present-day sea level at ~12,000 years ago to present-day sea level at ~7000 years ago resulted in transgression in the deeply incised lowstand valley (*transgressive systems tract*). Because of this transgression, the accommodation space was maximal in the Lower Tagus Valley and the depocentre shifted landward. The morphology of the valley with its narrow exit created a sheltered inland basin upstream of Lisbon, strongly reducing the effect of storms and storm surges in the drowned valley. Since ~7000 years ago the Lower Tagus Valley was completely drowned and occupied by tidal and marine environments which reached up to 100 km inland. The valley trapped increasing sediment volumes, which limited export to the shelf. Therefore, sedimentation on the shelf strongly decreased during the early stage of the Holocene (~10,500-5000 years ago).

7000-2000 years ago | fluvial sediment supply: regression
A stable relative sea level since ~7000 years ago resulted in regression marked by bayhead delta progradation and the build-up of a fluvial wedge in the Lower Tagus Valley (*highstand systems tract*). Around 5000 years ago, the valley was filled to such an extent that gradually sediment export occurred again, and on the shelf a subaqueous delta and mudbelt built up, reflecting a seaward depocentre shift. After ~7000 years ago a continued fluvial sediment supply combined with the protected setting of the valley resulted in mainly upstream controlled regression. The fluvial sediment wedge prograded downstream and simultaneously the Holocene onlap point migrated upstream. Between ~5500-1000 years ago the flooding history of the Lower Tagus Valley was dominantly controlled by climatic variability.

2000-0 years ago | human impact: increased fluvial-marine sedimentation
Since ~2000 years ago the Tagus fluvial-marine depositional system increasingly reflects land-use changes in the catchment. In the floodplain grainsize coarsened and sedimentation rate increased. This is explained by an increased flooding frequency and/or intensity. On the Tagus shelf the mudbelt grainsize fined, together with a higher sedimentation rate. The fining grainsize is a consequence of a strongly increased suspended sediment flux towards the shelf. The higher concentration of fine mud may have resulted in subdued winnowing and therefore a better preservation of fine-grained sediment. The observed changes are interpreted as the result of increased erosion of catchment slopes due to deforestation and increasing agriculture. Four depositional phases related with human impact on the natural landscape in the Tagus catchment were identified (~2300/~1600/~1100/~670 years ago), the latter two being strongest.

Sediment budgets at a passive continental margin
Using a (semi-) quantitative approach to quantify sediment fluxes and budgets of the fluvial-marine depositional system, an up to 2.5 times higher flux and storage of sediment during the last ~7000 years was identified. This increased flux was favoured by more arid climate conditions and land-use changes. The analysis of the fluvial flooding history using local observations (cores) did not identify the increased flux. This illustrates the advantage of a (semi-) quantitative approach using sediment budgets, because it provides a time-integrated three-dimensional reconstruction of sediment supply and deposition. It underlines the importance of an integrated land-ocean study and the quantification of fluvial-marine sediment fluxes to identify effects of climate change and human impact on depositional systems.

Controls

The multi-disciplinary and multi-proxy approach utilized in the present study has clearly demonstrated the shelf region—situated at the confluence of terrestrial and marine processes—to be extremely sensitive to developments in the terrestrial and marine realms. The main controls responsible for sedimentary changes on the studied passive continental margin are:

- **Sea-level change:** this has a strong control on shifting sediment depocentres. Depocentre movement and sea-level change play a large role in the situation of large sediment bodies such as fluvial channels and turbidites, which are potential hydrocarbon reservoirs.
- **Configuration of the continental shelf:** the configuration of the continental shelf (narrow, incised by a river valley) greatly affects sediment transport and bypass to the deep sea, thereby affecting depocentre

location. A deeply incised inland river valley captures large sediment quantities during sea-level highstand, thereby limiting marine deposition. On the other hand, a deeply incised valley funnelling into the head of a submarine canyon efficiently bypasses sediment to the deep sea during sea-level lowstand.

- **Human impact:** using detailed sedimentological, chronological and historical data from the river valley, catchment and shelf, the effect of human impact in the river catchment could be traced from source-to-sink. Extensive human impact thereby sheds light on the direction, scale and timing of the response of the fluvial-marine depositional system to large-scale external forcing.

- *Tectonic activity:* despite historic tectonic activity (large earthquakes in 1531, 1755 and 1909 AD) the horizontal relative sea-level curve since ~7000 years ago suggests that neotectonic uplift or subsidence were limited. Further, the present study has not identified sedimentological features in the fluvial-marine depositional system which could be clearly linked with earthquakes or tsunamis. The relatively thin lowstand braided Tagus River deposits directly overly Tertiary deposits, implying that subsidence in the Lower Tagus Valley was absent during the Quaternary period. Long-term tectonic uplift prevailed, preventing the deposits from being lowered below the scour depth of younger fluvial systems.

- *Fluvial sediment supply and climate change:* a stable sea level during the last 7000 years resulted in the increased relative importance of fluvial sediment supply, which controlled regression and fluvial progradation. Quantitative estimates of sediment volume for the last ~12,000 years show a drastically increased sediment flux and storage in the Tagus fluvial-marine depositional system after ~7000 years ago, which was favoured by climate change. Since the end of the African Humid Period (~5,500 years ago) regional climate resulted in more arid conditions and regional forest-cover decreased. Land-use changes since ~2000 years ago were added to that causing an increased vulnerability to soil erosion which resulted in an up to a 2.5 times higher sediment flux to the Lower Tagus Valley and shelf. The increased sediment flux did not coincide with a gradual increase in (peak) flood discharges during the last ~6000 years, although three phases of increased fluvial activity were established in distal floodbasin settings (6500-5500, 4900-3500 and 1000-0 years ago). Quantitative estimates of sediment volume deposited by the Tagus depositional system have enabled calculation of the total mechanical denudation rate for the Tagus catchment, which equals ~0.09 mm/y. This value is in agreement with long-term (10-40 ka) erosion rates from Central European catchments.

RESUMO

As alterações climáticas como resultado do forte impacto humano na Terra, tem recebido uma importante atenção por parte da comunidade científica bem como do poder político e da população em geral. Para um conhecimento detalhado dos efeitos das alterações climáticas globais, é necessário um olhar sobre o registo geológico, pois fornece um entendimento valioso. Os registos geológicos nos sedimentos das zonas costeiras contêm marcas de processos terrestres e marinhos.

As zonas costeiras com uma plataforma continental estreita (até 200 m de profundidade) e com uma encosta íngreme permitem reconstruções geológicas robustas, devido às elevadas taxas de acumulação de sedimentos e vias de transporte de sedimentação bem definidas. Nas *margens passivas continentais*, as camadas espessas com registos geológicos de alta resolução existem devido ao elevado fornecimento de sedimentos fluviais. Adicionalmente, devido a ausência de perturbações por parte de vulcões ou de sismos de grande intensidade, as margens passivas continentais são adequadas para uma melhoria no entendimento fundamental dos processos sedimentares nas margens continentais.

A maior parte dos estudos das margens continentais incide ou na componente terrestre ou na componente marinha do sistema. De modo a melhorar o entendimento dos processos sedimentares e para desvendar quais os controlos da sedimentação terrestre e marinha, é necessária uma reconstrução paleoambiental integrada de uma margem passiva que inclua a parte deltaica, costeira, plataforma e talude continentais, e planície abissal profunda. Uma ênfase especial deve ser dada aos processos de transporte e sedimentação sujeitos a climas variados desde a zona mais distante da costa até ao oceano. Por esta razão, iniciou-se dentro da estrutura da European Science Foundation (ESF) EUROCORES EUROMARGINS o projecto de investigação conjunta SEDPORT. Os objectivos gerais do projecto são:

1. Melhorar a compreensão dos mecanismos de transporte terrestre e marinho na composição e propriedades físicas da cobertura sedimentar que vai da última glaciação até ao Holocénico (de há 20.000 anos até à actualidade), com atenção às condições ambientais actuais em geral;

2. Averiguar como os processos de sedimentação mudaram quando sujeitos a condições climatéricas diversas que tiveram influência na circulação oceânica, no nível do mar, na meteorização continental, na vegetação e precipitação desde a última era glaciar até ao Holocénico.

Para este estudo, a margem passiva Ibérica junto ao Vale Inferior do Tejo é adequada. Devido à saída estreita do vale a sudoeste de Lisboa, o Rio Tejo actua

como fonte de sedimentos. O Vale Inferior do Tejo que é estreito e confinado por um soco rochoso profundo, é uma armadilha eficiente para depósitos, fluviais, tidais e marinhos e permite uma reconstrução robusta dos percursos e volumes sedimentares. Durante um nível do mar baixo devido à estreita plataforma continental, os sedimentos atravessam/passam de um forma eficiente para a Planicie Abissal do Tejo (5000 m de profundidade), no entanto, durante um nível do mar alto os sedimentos ficam retidos no Vale Inferior do Tejo ou na estreita plataforma.

Os objectivos gerais deste estudo foram elaborados através de uma série de objectivos mais específicos, que resultou em duas linhas de investigação interligadas, que têm como fundo comum a correlação entre os registos terrestres e marinhos:

1. Reconstruir a *evolução paleogeográfica e a provisão sedimentar marinho-fluvial no sistema deposicional do Tejo*, utilizando fáceis, arquitectura sedimentar, sequência-estratigráfica e período de deposição sedimentar;
2. Identificar os *controlos* na natureza e arquitectura das sucessões de vales encaixados modificando os fluxos sedimentares e as migrações dos depocentros marinho-fluviais.

Para atingir estes objectivos, foi compilado um grande volume de dados para o sistema deposicional do Tejo, com sondagens manuais e mecânicas na planície de inundação do Vale Inferior do Tejo e três sondagens de pistão, dois na plataforma continental (D13882 e GeoB-8903-1) e um da Planície Abissal do Tejo (MD03-2698). Amostras destes testemunhos de sondagens foram utilizados para medições de multi-indicadores (datações radiocarbono, granulometria, minerais pesados, matéria orgânica, carbonatos, flora e fauna). Adicionalmente, foram utilizados dados geotécnicos com a informação litológica e sedimentológica de 284 testes de penetração e testemunhos de sondagem geológicos contínuos e descontínuos. De modo a facilitar o cálculo do balanço sedimentológico foram elaborados perfis geológicos e mapas paleogeográficos.

A evolução paleogeográfica e a provisão sedimentológica fluvial-marinha no sistema deposicional do Tejo

Aproximadamente 20.000 anos atrás | nível do mar baixo: encaixamento

O nível do mar baixo (120 m abaixo do actual) e a ligação directa entre o Vale Inferior do Tejo e o oceano através da estreita (~30 km) plataforma continental o Rio Tejo causou o encaixe de um vale profundo (~70 m junto a Lisboa) que se estendeu até 100 km para o interior. Os sedimentos fluviais foram eficientemente transportados passando a plataforma exposta por vales submarinos

e canalizando estes sedimentos directamente para as cabeceiras dos canhões submarinos e em direcção à planície abissal (4000-5000 m de profundidade, Planície Abissal do Tejo), onde estava localizado o principal depocentro. Este transporte de sedimentos fluviais resultou numa deposição turbidítica de alta-frequência na Planície Abissal do Tejo a 20.000 e 15.000 anos atrás. O Tejo caracterizava-se pelas várias ramificações e há cerca de ~14.000 anos passou a ser um rio de canal único. Os vales profundos encaixados impediram uma erosão a larga escala por um sistema transgressivo marinho. Consequentemente ficou registada uma camada espessa do período de mar baixo (*lowstand systems tract*). O forte encaixe do Vale Inferior do Tejo e o transporte eficiente dos sedimentos, mostra que apesar do tamanho da captura e o nível do mar, a largura da plataforma é um importante controlo a jusante da largura do encaixe, na inclinação fluvial e na extensão para o interior da erosão regressiva.

20.000 a 12.000 anos atrás | aumento súbito do nível do mar: inundação do vale

Por volta de há 20.000 anos atrás houve uma subida rápida do nível do mar, e à aproximadamente 12.000 anos o mar empurrou o sistema fluvial do Tejo para o interior, criando um espaço de acomodação e por fim submergido o Vale Inferior do Tejo. Na Planície Abissal a sedimentação efectuou-se a um ritmo acelerado até ~11.500 anos atrás devido a um fornecimento constante de sedimentos fluviais. A etapa final da deposição em oceano profundo coincide com a crescente sedimentação na plataforma, por volta de 13.500 anos atrás, processo que continuou até ~10.500 anos atrás e reflecte a migração do depocentro para o interior por influência de um aumento relativo do nível do mar.

12.000 a 7000 anos atrás | etapa final da subida relativa do nível do mar: submersão completa do vale

A etapa final da subida relativa do nível do mar de ~40 m abaixo do actual nível do mar à cerca de 12.000 anos atrás, até ao nível do mar actual há ~7000 anos, resultou numa transgressão do vale profundo (*transgressive systems tract*). Devido a esta transgressão, o espaço de acomodação foi máximo no Vale Inferior do Tejo e o depocentro migrou para terra. A morfologia do vale com uma saída estreita criou uma bacia terrestre abrigada a montante de Lisboa, que reduziu grandemente o efeito de tempestades no vale submerso. Desde há ~7000 anos atrás o Vale Inferior do Tejo foi completamente submerso e foi ocupado até 100 km para o interior por ambientes tidais e marinhos. O vale encurralado aumentou o volume de sedimentação, o que limitou a carga sedimentar para a plataforma. Deste modo, a sedimentação na plataforma diminuiu grandemente no início do Holocénico (~10.500-5000 anos atrás).

7000 a 2000 anos atrás | fornecimento fluvial de sedimentos: estabelecimento do delta

Um nível do mar estável há ~7000 anos atrás resultou numa regressão marcada por uma progradação deltaica e a constituição de uma cunha fluvial no Vale Inferior do Tejo (*highstand systems tract*). Há 5000 anos atrás, o vale foi preenchido numa extensão tal que teve que ocorrer um reinício do transporte de sedimentos, e na plataforma formaram-se um delta subaquático e uma faixa lodosa, reflectindo uma migração do depocentro em direcção ao mar. Depois, há ~7000 anos atrás um fornecimento continuo de sedimentos combinado com a localização protegida do vale resultou numa regressão controlada a montante. A cunha de sedimentos fluviais progradou para jusante e simultaneamente o ponto *onlap* do Holocénico migrou a montante. Por volta de ~5500-1000 anos atrás a história de inundações do Vale Inferior do Tejo foi dominantemente controlada por alterações climáticas.

2000 a 0 anos atrás | impacto humano: um aumento de sedimentação fluvio-marinha

Há 2000 anos atrás há um reflexo na mudança de utilização da terra na captura, no sistema fluvio-marinho deposicional do Tejo. Na planície de inundação a granulometria da sedimentação tornou-se mais grosseira. Na plataforma do Tejo a granulometria da faixa lodosa tornou-se mais fina, juntamente com um aumento da taxa de sedimentação. A diminuição da granulometria é uma consequência do aumento do fluxo de sedimentos que chega à plataforma. A alta concentração de argila fina poderá ter resultado numa melhor preservação dos sedimentos de granulometria fina (*subdued winnowing*). Estes mudanças podem ser explicadas pelo aumento da erosão dos declives de captura devido à desflorestação e aumento da actividade agrícola, o que resultou num aumento intensidade e/ou frequência de cheias. Foram identificadas quatro fases de deposição relacionadas com o impacto antropogénico na paisagem natural da captura do Tejo (~2300/~1600/~1100/~670 anos atrás), sendo as duas últimas foram as mais intensas.

O balanço sedimentar numa margem passiva continental

Utilizando uma abordagem (semi-) quantitativa para quantificar os fluxos e provisões de sedimentação num sistema deposicional fluvio-marinho, foi identificado um fluxo e armazenamento sedimentar 2,5 vezes superior nos últimos ~7000 anos. Este aumento do fluxo foi favorecido por condições de clima mais árido e uma mudança da utilização da terra. Da análise da história de inundações fluviais utilizando observações locais (testemunhos de sondagem) não foram identificados aumentos de fluxo. Isto ilustra a vantagem de uma abordagem (semi-) quantitativa utilizando balanços sedimentares, porque

proporciona reconstrução da produção e deposição sedimentar tridimensional e integrada no tempo. Sublinha a importância de um estudo integrado terra-oceano e da quantificação dos fluxos sedimentares fluvio-marinhos para iden-tificar os efeitos das mudanças climáticas e o impacto do homem nos sistemas deposicionais.

Controlos

A abordagem multi-disciplinar e recorrendo a multi-indicadores utilizada no presente estudo mostrou claramente que a região da plataforma, situada na confluência dos processos marinhos e terrestres, é extremamente sensível a desenvolvimentos nos domínios terrestre e marinho. Os principais controlos responsáveis pelas alterações sedimentares na margem passiva estudada são:

- Variação do nível do mar: esta variação tem um forte controlo no desloca-mento dos depocentros sedimentares. O movimento dos depocentros e a variação do nível do mar desempenham um papel importante em grandes corpos sedimentares como canais fluviais e turbiditos, que poderão ser potenciais reservatórios de hidrocarbonetos.
- Configuração da plataforma continental: a configuração da plataforma continental (estreita, encaixada por um vale de rio) afecta grandemente o transporte sedimentar para o grandes profundidades, afectando deste modo a localização de depocentros. Um vale fluvial encaixado captura grandes quantidades de sedimentos durante períodos de nível do mar alto, limitando assim a deposição marinha. Por outro lado, durante períodos de nível do mar baixo um vale submarino profundo canaliza para a cabeceira de um canhão submarino e transporta eficazmente os sedimentos para mar profundo.
- Impacto humano: utilizando dados sedimentológicos, cronológicos e históricos detalhados do vale do rio, na captura e na plataforma, o efeito do impacto humano na captura do rio, pode ser seguida desde a origem até à profundidade (planícies abissais). Desta forma, o impacto humano extensivo demonstra a direcção, escala e tempo de resposta de uma força externa no sistema deposicional fluvio-marinho a uma escala alargada.
- Actividade tectónica: Apesar da actividade tectónica histórica (sismos de grande intensidade em 1531, 1755 e 1909) a curva de forma horizontal relativa aos últimos ~7000 anos sugere que o levantamento neotectónico ou subsidência são incipientes. Além disso, o estudo não identificou carac-terísticas sedimentológicas no sistema deposicional marinho-fluvial que possam ser claramente relacionados com sismos ou tsunamis. Os depósitos relativamente fino e ramificado do Rio Tejo situado directamente sobre o Terciário, implicam que durante o período Quaternário (últimos 2,5 milhões de anos) a subsidência no Vale Inferior do Tejo não existiu. Preva-

leceu durante um período longo, um levantamento tectónico impedindo que os depósitos baixassem a um nível inferior relativamente à profundidade do encaixe dos sistemas fluviais recentes.

- Fornecimento fluvial de sedimentos e alterações climáticas: um nível do mar estável durante os últimos 7000 anos resultou no aumento da importância relativa do fornecimento de sedimentos fluviais, que controlou a regressão e a progradação fluvial. Estimativas quantitativas do volume de sedimentos dos últimos ~12000 anos demonstraram um fluxo sedimentar crescente e a deposição no sistema fluvio-marinho do Tejo a aproximadamente 7000 anos atrás, que foi favorecida pelas alterações climáticas. Desde o fim do Período Húmido Africano (aproximadamente 5500 anos atrás) as condições climatéricas regionais tornaram-se mais áridas. A diminuição da cobertura florestal e a mudança da utilização do solo contribuiu para um aumento da vulnerabilidade do solo à erosão, que resultou num fluxo de sedimentação no Vale Inferior do Tejo e na plataforma 2,5 vezes superior. Este aumento de fluxo de sedimentação não coincidiu com um aumento gradual das inundações durante os últimos ~6000 anos, apesar de três fases de aumento de actividade fluvial se terem fixado numa bacia de inundação mais distal (6500-5500, 4900-3500 e 1000-0 anos atrás). Estimativas quantitativas sobre volume de sedimentos depositados no sistema deposicional do Tejo, permitiram o cálculo da taxa total de denudação mecânica para a captura do Tejo, cujo total é de cerca de 0,09 mm/ano. Verifica-se que este valor está concordante com as taxas de erosão a longo prazo (10.000-40.000 anos) para as capturas na Europa Central.

SAMENVATTING

De huidige klimaatverandering heeft grote gevolgen voor de aarde en krijgt daarom veel wetenschappelijke, politieke en maatschappelijke aandacht. Door veranderende weersystemen wordt het op sommige plaatsen droger en op andere plaatsen natter. Ook zullen extreme weersgebeurtenissen, zoals langdurige droogtes en hevige regenbuien, vaker voorkomen. Daarbovenop komt nog de zeespiegelstijging, veroorzaakt door het opwarmen en uitzetten van zeewater en door het smelten van landijs. Vooral in laaggelegen kustgebieden neemt de kans op overstromingen toe en juist daar woont het grootste gedeelte van de wereldbevolking.

Om de gevoeligheid voor klimaatverandering beter te begrijpen, kijkt deze studie naar de geologische geschiedenis van kustgebieden. Het samenspel tussen land- en zeeprocessen leidt tot het afwisselend afzetten en eroderen van grote hoeveelheden zand en klei. Deze processen bepalen of de zee terrein wint ten opzichte van het land of andersom en ze worden sterk beïnvloed door klimaatverandering. Grote rivierdelta's zoals die van de Mississippi en lange estuaria zoals die van de Westerschelde zijn bijvoorbeeld ontstaan door verschillende combinaties van aanvoer van zand en klei, getijde en zeespiegelstand.

Door de ontstaansgeschiedenis van bestaande kustgebieden te reconstrueren, kan worden onderzocht hoe het transport en de afzetting van sedimenten zijn beïnvloed door klimaatveranderingen in het verleden. Met deze kennis kunnen we beter voorspellen wat de gevolgen van de huidige klimaatverandering zullen zijn; *the past is the key to the present*. De routes waarlangs de sedimenten (zand en klei) ooit zijn getransporteerd, zijn vaak nog goed te herkennen, vooral in kustgebieden waar het continentaal plat (waterdieptes tot 200 m, vergelijkbaar met de Noordzee) slechts enkele tientallen kilometers breed is en de helling naar de diepzee steil is. Rivieren die hier in zee uitkomen, voeren grote hoeveelheden sediment aan, wat in dikke lagen wordt afgezet op de zeebodem. Wanneer kustgebieden niet worden verstoord door vulkanen en grote aardbevingen (zogenaamde *passieve continentranden*), kan rustige afzetting plaatsvinden van het door de rivieren aangevoerde sediment. Dit maakt het makkelijker om transport en afzetting van sediment te bestuderen om zo de reactie van sedimentaire processen op klimaatveranderingen in het verleden beter te begrijpen.

De meeste studies van continentranden beperken zich tot het landgedeelte of het zeegedeelte, terwijl dit onderzoek juist naar de continentrand als *geheel* kijkt. Om alle processen die sturend zijn voor land- en zeesedimentatie te ontrafelen, is het nodig om zowel de rivierdelta, de kust, het continentaal plat, de helling naar de diepzee als de diepzee zelf (ca. 5000 m waterdiepte) te bestuderen. Om het onderzoek naar de effecten van klimaatverander-

ing op sedimenttransport en sedimentatie grootschalig aan te pakken is het Europese onderzoeksproject SEDPORT opgezet binnen het EUROCORES EUROMARGINS programma van de European Science Foundation (ESF). De algemene doelstellingen van dit project zijn om voor de periode sinds het maximum van de laatste ijstijd (ca. 20.000 jaar geleden):

1. Beter inzicht te krijgen in het samenspel tussen rivier- en zeeprocessen wat bepaalt waar wanneer welke sedimenten langs de continentrand afgezet worden;
2. Te bepalen hoe deze processen worden beïnvloed door veranderingen op het land (neerslag, vegetatie, erosie) en in zee (zeespiegelstand, stromingen) die het gevolg zijn van de klimaatverandering.

De passieve continentrand aan de westkant van het Iberische Schiereiland nabij Lissabon (Portugal) is zeer geschikt voor een dergelijke studie. De Taag heeft een groot achterland (met 1008 km lengte is het de twaalfde rivier van Europa) en stroomt van het warme en droge binnenland van Spanje naar de koelere nattere Atlantische kust van Portugal. Hierdoor levert de rivier veel sediment en is het riviersysteem gevoelig voor klimaatveranderingen. Door de smalle verbinding van het Beneden Taagdal met de oceaan is de Taag een puntbron van sediment; dat is behulpzaam voor de reconstructie van sedimenttransportroutes. Het smalle en diep ingesneden Beneden Taagdal wordt omgeven door ouder gesteente waardoor het een zeldzame beschutte ligging heeft. Hierdoor hebben duizenden jaren lang rivier-, getijde- en zeesedimenten het dal in alle rust kunnen opvullen. Het Taagdal is hierdoor een prachtig geologisch archief aan de hand waarvan sedimenttransportroutes en -volumes kunnen worden gereconstrueerd.

De algemene doelstellingen van het SEDPORT project zijn vertaald naar een aantal specifiekere doelstellingen voor het bestuderen van het Beneden Taagdal in deze studie. Deze specifiekere doelstellingen kunnen worden ondergebracht in de volgende twee verweven onderzoekslijnen, die de correlatie van land- en zeesedimenten als gemeenschappelijk doel hebben:

1. Het uitzoeken van *wat er met de Taag is gebeurd* gedurende de laatste 20.000 jaar, daarbij lettend op waar en wanneer op land en in zee wat voor sedimenten werden afgezet en hoeveel dat was;
2. Het bepalen wat de *oorzaken* waren van de waargenomen veranderingen.

Om deze doelen te bereiken is een grote hoeveelheid gegevens verzameld in het sedimentatiesysteem van de Taag. Deze gegevens bestonden uit hand- en mechanische boringen in het Beneden Taagdal, en uit zeeboringen. Twee zeeboringen zijn gedaan op de bodem van het continentaal plat en één op

de bodem van de diepzee. De monsters die uit de land- en zeeboringen zijn genomen, werden gebruikt voor het bepalen van ouderdom, korrelgrootte, zware mineralen samenstelling, organisch materiaal- en kalkgehalte, en plant- en dierfossielen. Daarnaast werd informatie uit 284 sonderingen en geologische boringen uit geotechnische studies gebruikt. Aan de hand van al deze gegevens werden dwarsdoorsneden en kaarten gemaakt, waarmee vervolgens het transport en de sedimentatie van zand en klei konden worden gereconstrueerd. De volumes sediment die in de loop der tijd door de Taag zijn afgezet, zijn berekend met behulp van 3D computersoftware. Deze volumes zijn ook vergeleken met de hoeveelheden sediment die door de eeuwen heen uit het achterland verdwenen zijn in een zogenaamd *sediment budget*.

Wat is er met de Taag gebeurd tijdens de laatste 20.000 jaar?

Circa 20.000 jaar geleden | lage zeespiegelstand: dalvorming
Ongeveer 20.000 jaar geleden stond de zeespiegel 120 meter lager dan tegenwoordig en bestond er een directe verbinding tussen het Beneden Taagdal en de oceaan via een diep dal in het ~30 km smalle continentaal plat. Hierdoor werd het Beneden Taagdal tot 70 m diep en 100 km landinwaarts ingesneden. Bijna al het riviersediment werd efficiënt afgevoerd naar de bodem van de diepzee via rivierdalen en onderzeese canyons. De doorvoer van sediment naar de diepzee resulteerde in veel troebelheidsstromen (onderzeese aardverschuivingen) die tussen 20.000 en 15.000 jaar geleden veel van het sedimenttransport naar de diepzee voor hun rekening namen.

Tot 14.000 jaar geleden was de Taag een vlechtende rivier met veel zandbanken. Daarna concentreerde het water zich onder invloed van klimaat- en vegetatieverandering in één geul. Het Beneden Taagdal was diep en steil. Toen de zeespiegel begon te stijgen, liep het dal zo snel onder water dat de oudere rivierafzettingen werden bedekt met zeeklei en heel goed bewaard bleven. Door de combinatie van de lage zeespiegel tijdens de ijstijd en het smalle continentale plat, is de Taag één van de diepst en verst landinwaarts ingesneden rivierdalen langs de Europese kust.

20.000-12.000 jaar geleden | snelle zeespiegelstijging: eerste overstroming
Vanaf 20.000 jaar geleden steeg de zeespiegel snel (ca. 1 meter per eeuw) en rond 12.000 jaar geleden had de stijgende zeespiegel een deel van het Beneden Taagdal verdronken en de rivier landinwaarts geduwd. In het ondergelopen Beneden Taagdal ontstond steeds meer ruimte om sediment in te vangen. Doordat steeds meer sediment in het Beneden Taagdal werd afgezet, nam het sedimenttransport naar de diepzee geleidelijk af. De laatste periode van snelle sedimentatie in de diepzee valt dan ook samen met het begin van de sedimentatie op het continentaal plat rond 13.500 jaar geleden. De snelle sedimentatie

op het continentaal plat eindigde ongeveer 10.500 jaar geleden. Deze veranderingen weerspiegelen een landwaartse verplaatsing van het zwaartepunt van sedimentatie als gevolg van zeespiegelstijging.

12.000-7000 jaar geleden | het laatste stadium van zeespiegelstijging: verdrinking

Van 12.000-7000 jaar geleden steeg de zeespiegel nog 40 meter tot aan het huidige niveau. Gedurende dit laatste stadium van zeespiegelstijging verdronk het Beneden Taagdal helemaal. De vorm van het dal met zijn smalle uitgang, zorgde voor een beschutte baai ten oosten van het huidige Lissabon waarin golven en golfwerking beperkt waren. In het begin stond het Beneden Taagdal geheel onder water tot wel 100 km landinwaarts. Getijdenstroming en golfwerking domineerden de sedimentatie- en erosieprocessen. Het verdronken dal ving steeds meer sediment in, waardoor er steeds minder sediment naar zee werd afgevoerd. De zeespiegelstijging zorgde voor een verdere landwaartse verschuiving van het zwaartepunt van sedimentatie.

7000-2000 jaar geleden | fluviatiele sedimentaanvoer: deltavorming

Een min of meer stabiele zeespiegel tijdens de afgelopen ca. 7000 jaar en een constante aanvoer van sediment door de Taag zorgden voor de vorming van een delta. De delta bouwde zich stroomafwaarts uit en vormde een steeds dikker wordende laag riviersediment in het Beneden Taagdal. Rond 5000 jaar geleden was het Beneden Taagdal al zo ver opgevuld met sediment, dat er langzaam weer sediment werd doorgevoerd naar zee. Hierdoor ontstonden op het continentaal plat een onderwaterdelta en slibafzettingen. Dit omslagmoment weerspiegelt een zeewaartse verplaatsing van het zwaartepunt van sedimentatie. Door de beschermde ligging van het dal werd de uitbouw van de delta niet tegengewerkt door zeestromingen en golferosie. De delta bleef zich stroomafwaarts uitbouwen en tegelijkertijd werden bovenstroomse gebieden ook langzaam gevuld met sediment. In de opbouw van de sedimentlagen zijn de gevolgen van klimaat- en vegetatieveranderingen in het stroomgebied goed herkenbaar.

2000 jaar geleden tot nu | menselijke invloed: toegenomen land- en zeesedimentatie

Gedurende de laatste ca. 2000 jaar werd sedimentatie in het land-zee bereik van het Taag-systeem in toenemende mate beïnvloed door veranderend landgebruik in het stroomgebied. Vooral tijdens de Middeleeuwen begon grootschalige ontbossing, wat zorgde voor grote hoeveelheden sediment die via de rivieren naar de delta en de zee werden getransporteerd. In de delta namen de korrelgrootte en sedimentatiesnelheid van het overstromingssediment

toe. Op het continentaal plat werden de slibafzettingen echter fijner, terwijl ook hier de sedimentatiesnelheid toenam. De verfijning van de korrelgrootte is het gevolg van een sterk toegenomen aanvoer van fijn sediment. De oceaanstromingen waren niet sterk genoeg om deze grote hoeveelheid fijn sediment af te voeren, waardoor meer fijn sediment de zeebodem bereikte en bewaard bleef. De waargenomen veranderingen werden verklaard door toegenomen erosie vanaf hellingen in het stroomgebied. Dit werd veroorzaakt door ontbossing en toenemend landgebruik, waardoor overstromingen van de Taag vaker voorkwamen en intensiever waren.

Er zijn vier afzettingsfasen onderscheiden op land en in zee die zijn toegeschreven aan ontbossing en toenemend landgebruik in het stroomgebied van de Taag. Deze fasen vonden plaats rond ca. 2300, 1600, 1100 en 670 jaar geleden, waarbij de laatste twee fasen het sterkst waren.

Sedimentbudget van een passieve continentrand

Dit is een van de eerste studies die heeft berekend hoeveel sediment er in een sedimentatiesysteem zowel op land als in zee is afgezet. Door de volumes sediment die zijn afgezet in de periodes 12.000-7000 en 7000-0 jaar geleden met elkaar te vergelijken, blijkt dat tijdens de laatste 7000 jaar ongeveer twee en een half keer zoveel sediment is afgezet dan in de periode daarvoor. Deze toegenomen sedimentatie werd veroorzaakt door een grotere sedimentaanvoer als gevolg van drogere klimaatomstandigheden en ontbossing, waardoor meer erosie optrad. Het voordeel van een grootschalige land-zee aanpak is dat lokale variatie in sedimentatie in ruimte en tijd een kleine rol speelt. Bovendien wordt bij een land-zee aanpak ook het naar zee afgevoerde sediment in de volumebepaling meegenomen. Dit sediment wordt bij een puur op landgegevens gebaseerde studie buiten beschouwing gelaten.

Wat waren de oorzaken van de waargenomen veranderingen?

Deze studie hanteert een aanpak met gebruikmaking en vergelijking van verschillende gegevensbronnen. Hierdoor kon duidelijk worden aangetoond dat het continentaal plat, gelegen op het raakvlak van land- en zeeprocessen, erg gevoelig is voor de gevolgen van klimaatverandering. De belangrijkste sturende factoren voor sedimentaire veranderingen van de passieve continentrand zijn:

- **Zeespiegelverandering:** dit heeft veel invloed op de ligging van het zwaartepunt van sedimentatie. De verplaatsing van dit zwaartepunt en de verandering van de zeespiegel spelen een grote rol in de ligging van grote sedimentlichamen zoals rivergeulen en afzettingen van onderzeese troebelheidsstromen, welke bijvoorbeeld potentiële olie- en gasreservoirs zijn.
- **De vorm van het continentaal plat:** verschillende vormen (smal, in-

gesneden door een rivier) hebben veel invloed op sedimenttransport en sedimentdoorvoer naar de diepzee, en mede daardoor ook op de ligging van het zwaartepunt van sedimentatie. Een diep en ver landinwaarts ingesneden rivierdal vangt veel sediment in tijdens een hoge zeespiegel, waardoor sedimentatie in zee wordt beperkt. Aan de andere kant zorgt een diep ingesneden dal dat is verbonden met een onderzeese canyon voor efficiënte afvoer van sediment naar de diepzee gedurende een lage zeespiegel.

- **Menselijke invloed:** door gebruik te maken van gedetailleerde sedimentologische, chronologische en historische gegevens van zowel het stroomgebied, het rivierdal als het continentaal plat is het gevolg van menselijk handelen in het stroomgebied gereconstrueerd. Grootschalige menselijke invloed zorgt als het ware voor een mega-experiment dat laat zien hoe het sedimenttransport reageert op een verstoring.

- **Tektonische activiteit:** ondanks het feit dat grote aardbevingen in het recente verleden hebben plaatsgevonden (1531, 1755 en 1909 AD), suggereert de vlakke curve van de zeespiegelreconstructie voor de laatste 7000 jaar dat tektonische opheffing of daling beperkt waren. Tijdens deze studie zijn dan ook geen sedimentologische kenmerken aangetroffen die duidelijk het gevolg zijn van aardbevingen of tsunamis. De relatief dunne riviersedimenten die zijn afgezet tijdens de lage zeespiegelstand, liggen direct op oudere (Tertiaire) afzettingen. Dit toont aan dat er geen daling van het Beneden Taagdal heeft plaatsgevonden gedurende de laatste 2,5 miljoen jaar. Langdurige opheffing had de overhand, waardoor de oude riviersedimenten werden opgeruimd door erosie door jongere riviersystemen. Dit in tegenstelling tot het dalende Nederland, waar de op elkaar gestapelde rivierafzettingen van de laatste miljoenen jaren wel bewaard zijn gebleven.

- **Sedimentaanvoer en klimaatverandering:** door een stabiele zeespiegel gedurende de laatste 7000 jaar, was de invloed van sedimentaanvoer door de rivier op sedimentatie relatief groot en vormde zich een delta. Bepalingen van het sedimentvolume laten een drastisch toegenomen sedimentaanvoer zien in het land-zee afzettingssysteem gedurende de laatste 7000 jaar. Dit kwam doordat er in deze periode veel bossen verdwenen waardoor de bodem gevoeliger werd voor erosie. Het verdwijnen van de bossen was het gevolg van het steeds droger wordende klimaat op het Iberische Schiereiland. Gedurende de laatste 2000 jaar kwam de mens daar nog bij met een groot aandeel in de ontbossing. Door deze veranderingen werd tot wel twee en een half keer meer sediment naar het Beneden Taagdal en het continentaal plat gevoerd.

Appendices

APPENDIX 1
Lower Tagus Valley boreholes

Borehole Nr.	Date	X-coordinate (km)	Y-coordinate (km)	Elevation relative to m.s.l. (m)	End depth (cm)
0401.001	5-10-2004	542.966	4360.878	14.87	560
0401.002	5-10-2004	542.899	4360.935	16.23	640
0401.003	6-10-2004	543.033	4360.799	16.50	780
0401.004	6-10-2004	542.275	4361.616	16.69	850
0401.005	6-10-2004	542.554	4361.317	16.74	660
0401.006	7-10-2004	541.907	4362.034	16.00	820
0401.007	7-10-2004	541.729	4362.252	15.76	730
0401.008	8-10-2004	543.575	4360.182	14.82	730
0401.009	8-10-2004	544.711	4358.476	17.60	850
0401.010	11-10-2004	543.531	4360.236	16.12	480
0401.011	11-10-2004	543.619	4360.131	15.91	700
0401.012	12-10-2004	544.480	4358.836	17.27	550
0401.013	12-10-2004	544.533	4358.745	16.63	450
0401.014	12-10-2004	544.925	4358.383	13.00	390
0401.015	14-10-2004	541.504	4352.118	13.22	990
0401.016	14-10-2004	541.583	4352.086	16.65	600
0401.017	14-10-2004	541.374	4352.170	15.77	520
0401.018	15-10-2004	542.958	4350.452	11.06	1310
0401.019	18-10-2004	541.157	4362.880	14.24	970
0401.020	19-10-2004	541.306	4362.679	14.90	940
0401.021	19-10-2004	541.501	4362.494	14.30	870
0401.022	20-10-2004	544.335	4359.068	17.52	420
0401.023	20-10-2004	544.267	4359.182	16.84	620
0401.024	20-10-2004	543.934	4359.658	16.83	730
0401.025	21-10-2004	543.749	4359.993	16.09	870
0401.026	21-10-2004	543.254	4360.562	15.43	550
0401.027	21-10-2004	544.076	4359.453	17.17	1020
0401.028	21-10-2004	548.999	4364.324	20.00	330
0401.029	22-10-2004	542.691	4351.035	13.39	1280
0401.030	22-10-2004	542.482	4351.315	14.00	870
0401.031	25-10-2004	543.094	4350.798	12.00	270
0401.032	26-10-2004	542.962	4350.648	11.43	1320
0401.033	26-10-2004	541.958	4351.879	15.26	530
0401.034	26-10-2004	542.158	4351.790	15.15	600
0401.035	29-10-2004	541.199	4352.347	15.74	370
0401.036	29-10-2004	540.965	4352.463	15.44	670
0401.037	30-10-2004	540.387	4352.823	16.26	780
0401.038	30-10-2004	542.596	4351.157	13.48	890
0401.039	3-11-2004	542.834	4350.820	12.03	1660
0401.040	4-11-2004	543.013	4350.856	11.40	470
0401.101	12-10-2004	544.448	4358.894	16.80	550
0401.102	29-10-2004	541.046	4352.409	14.67	660
0401.103	29-10-2004	540.912	4352.497	15.25	660
0401.104	30-10-2004	540.649	4352.679	15.68	710
0401.105	30-10-2004	542.349	4351.529	14.30	700
0401.106	1-11-2004	541.584	4352.084	16.65	500
0401.107	1-11-2004	548.067	4363.257	19.00	610
0401.201	23-5-2004	503.024	4310.105	2.00	550
0401.202	25-5-2004	534.045	4346.350	10.50	190
0401.203	25-5-2004	531.812	4342.025	8.00	800
0401.204	26-5-2004	543.060	4350.655	11.43	550
0401.205	26-5-2004	541.750	4352.000	15.96	340
0401.302	4-11-2004	542.943	4350.667	12.73	1930
0401.304	12-11-2004	544.750	4358.375	17.40	2380
0501.001	19-9-2005	534.571	4342.667	16.61	250
0501.002	19-9-2005	534.375	4342.900	13.55	200
0501.003	19-9-2005	534.163	4343.100	11.32	100
0501.004	19-9-2005	533.963	4343.325	10.50	420
0501.005	20-9-2005	533.775	4343.550	11.15	350
0501.006	20-9-2005	533.538	4343.743	10.57	350
0501.007	20-9-2005	533.375	4344.025	10.38	1660
0501.008	23-9-2005	533.175	4344.225	11.27	1120
0501.009	26-9-2005	532.532	4344.941	11.62	680
0501.010	22-9-2005	532.125	4345.496	6.81	720
0501.011	23-9-2005	532.975	4344.465	11.94	940
0501.012	23-9-2005	532.750	4344.700	12.55	980

0501.013	26-9-2005	531.726	4345.914	11.07	1080
0501.014	26-9-2005	531.535	4346.165	12.05	1110
0501.015	27-9-2005	531.299	4346.352	10.61	1060
0501.016	30-9-2005	531.088	4346.563	11.38	2310
0501.017	28-9-2005	530.881	4346.811	11.17	900
0501.018	30-9-2005	532.401	4345.262	6.30	880
0501.019	5-10-2005	530.690	4347.012	11.20	1430
0501.020	5-10-2005	531.864	4345.684	12.61	1300
0501.021	10-10-2005	527.253	4333.159	8.71	300
0501.022	10-10-2005	526.939	4333.270	5.22	500
0501.023	10-10-2005	526.632	4333.363	5.13	600
0501.024	10-10-2005	526.387	4333.357	5.68	780
0501.025	11-10-2005	526.038	4333.421	7.42	1330
0501.026	11-10-2005	525.799	4333.449	7.62	1450
0501.027	12-10-2005	525.370	4333.540	8.05	1150
0501.028	12-10-2005	525.075	4333.660	6.53	960
0501.029	13-10-2005	540.407	4359.849	12.00	1250
0501.030	15-10-2005	524.799	4333.804	7.60	900
0501.031	16-10-2005	502.911	4298.545	1.00	430
0501.032	18-10-2005	524.604	4333.900	7.94	1230
0501.033	18-10-2005	524.315	4334.031	5.90	880
0501.034	19-10-2005	524.091	4334.210	7.00	930
0501.035	19-10-2005	523.852	4334.353	6.75	1050
0501.036	19-10-2005	523.585	4334.509	6.63	1010
0501.037	19-10-2005	523.372	4334.720	6.58	820
0501.038	20-10-2005	523.086	4334.848	6.28	940
0501.039	20-10-2005	522.855	4335.011	5.61	780
0501.040	20-10-2005	522.607	4335.187	5.35	670
0501.041	20-10-2005	522.373	4335.353	4.30	1390
0501.042	21-10-2005	522.094	4335.448	3.94	910
0501.043	24-10-2005	515.102	4320.951	4.00	810
0501.044	24-10-2005	514.940	4321.160	4.00	1490
0501.045	24-10-2005	514.577	4321.581	4.00	720
0501.046	25-10-2005	514.140	4321.972	4.00	350
0501.047	25-10-2005	513.813	4322.330	4.00	420
0501.048	25-10-2005	513.496	4322.696	4.00	460
0501.049	28-10-2005	513.132	4323.090	3.00	1250
0501.050	27-10-2005	514.130	4322.014	4.00	930
0501.051	28-10-2005	512.824	4323.436	3.00	630
0501.052	28-10-2005	512.474	4323.832	3.00	1620
0501.053	28-10-2005	512.191	4324.241	2.00	580
0501.054	31-10-2005	516.677	4319.229	17.00	400
0501.055	31-10-2005	516.605	4319.334	4.00	560
0501.056	31-10-2005	516.325	4319.718	3.00	650
0501.057	31-10-2005	515.963	4320.157	3.00	620
0501.058	1-11-2005	511.908	4324.462	2.00	1430
0501.059	2-11-2005	525.406	4333.520	8.27	1400
0501.060	7-11-2005	509.252	4308.798	2.00	500
0501.061	7-11-2005	507.972	4309.303	1.50	830
0501.062	8-11-2005	507.294	4309.538	1.00	530
0501.063	8-11-2005	506.685	4309.884	2.00	550
0501.064	9-11-2005	505.838	4310.140	2.50	880
0501.065	9-11-2005	506.029	4311.621	2.00	760
0501.066	9-11-2005	503.908	4311.005	1.00	530
0501.067	10-11-2005	502.491	4311.456	1.00	790
0501.068	10-11-2005	503.169	4311.226	1.00	560
0501.069	10-11-2005	502.074	4311.678	1.00	710
0501.070	11-11-2005	532.679	4344.768	8.53	1150
0501.071	14-11-2005	504.812	4310.535	2.00	630
0501.072	16-11-2005	515.190	4320.840	1.00	860
0501.401	1-1-2004	530.589	4347.131	11.15	1940
0601.001	14-7-2006	535.961	4343.054	6.00	800
0601.002	8-7-2006	526.420	4333.197	5.50	650
0601.003	14-7-2006	541.163	4348.836	11.00	800
0601.301	14-2-2006	523.321	4334.600	7.00	3220
0601.302	14-2-2006	505.439	4310.324	2.00	5000
0701.001	24-5-2007	534.306	4344.205	9.00	1550
0701.003	25-5-1907	535.216	4343.538	6.00	900
0701.004	25-5-2007	535.237	4343.634	6.50	700

235

0701.005	25-5-2007	535.742	4343.157	6.10	750
0701.006	25-5-2007	536.088	4342.933	6.50	1270
0701.007	26-5-2007	536.855	4342.491	8.20	880
0701.008	28-5-2007	536.464	4342.696	7.00	410
0701.009	28-5-2007	537.424	4342.607	10.50	460
0701.010	28-5-2007	537.865	4342.852	13.00	160
0701.011	28-5-2007	536.497	4342.765	7.00	1060
0701.012	29-5-2007	535.898	4343.027	6.00	670
0701.013	16-7-2007	536.277	4342.851	6.60	790
0701.014	29-5-2007	535.469	4343.385	5.60	680
0701.015	30-5-2007	535.375	4343.207	6.00	670
0701.016	31-5-2007	535.831	4343.082	6.00	840
0701.017	25-5-2007	534.878	4343.854	9.50	1210

236

APPENDIX 2
Lower Tagus Valley previously published radiocarbon dates

^{14}C age yrs BP ± 1σ	Age cal. BP 2σ	Midpoint	Coordinates (x-y/z) (m)	Sample depth (cm)	Borehole nr.	Site

Appendix 2 *(continued)*

Material	Significance	¹⁴C type	Remarks
peat/wood	?	?	Azevêdo et al, 2006a
peat/wood	?	?	Azevêdo et al, unpublished
peat/wood	?	?	Azevêdo et al, 2006a
peat/wood	?	?	Azevêdo et al, 2006a
peat/wood	?	?	Azevêdo et al, 2006a
peat/wood	?	?	Azevêdo et al, 2006a
peat/wood	?	?	Azevêdo et al, 2006a
peat/wood	?	?	Azevêdo et al, 2006a
?	?	?	Azevêdo et al, unpublished
?	?	bulk	Van Leeuwaarden & Janssen, 1985
?	?	bulk	Van Leeuwaarden & Janssen, 1985
?	?	bulk	Van Leeuwaarden & Janssen, 1985
?	?	bulk	Van Leeuwaarden & Janssen, 1985
?	?	?	Ramos Pereira et al, 2002
?	?	?	Ramos Pereira et al, 2002
?	?	?	Ramos Pereira et al, 2002
?	?	?	Ramos Pereira et al, 2002
?	?	?	Ramos et al, 2002
?	?	?	Ramos et al, 2002
?	?	?	Ramos et al, 2002
bulk, peaty silt	last soil formation	radiometric	Van der Schriek et al., 2007b
bulk, clayey silt	range-finder	radiometric	Van der Schriek et al., 2007b
Scrobicularia fragments	start saltwater + fine sedime	AMS	Van der Schriek et al., 2007b (marine calibration, Calib Rev. 5.0.2)
plant fragments	start saltwater + fine sedime	AMS	Van der Schriek et al., 2007b
plant & wood frgs.	start saltwater + fine sedime	AMS	Van der Schriek et al., 2007b
plant fragments	max. tidal influence	AMS	Van der Schriek et al., 2007b
bulk,organic clayey silt	end saltwater pollen	AMS	Van der Schriek et al., 2007b
wood fragments	start soil and alder pollen	AMS	Van der Schriek et al., 2007b
plant fragments	start fine sedimentation	AMS	Van der Schriek et al., 2007b
plant fragments	start fine sedimentation	AMS	Van der Schriek et al., 2007b
plant fragments	start fine sedimentation	AMS	Van der Schriek et al., 2007b
bulk, peat	start local peat formation	radiometric	Van der Schriek et al., 2007b
bulk, peat	end peat formation	radiometric	Van der Schriek et al., 2007b
plant fragments	end peat formation	AMS	Van der Schriek et al., 2007b

APPENDIX 3
Lower Tagus Valley radiocarbon dates from this study

Lab. Nr.	¹⁴C age yrs BP ± 1σ	Age cal. BP 2σ	Midpoint	δ¹³C	Coordinates (x-y/z) (m)	Sample depth (cm)	Borehole nr.	Sample name
GrA-27234	5530 +/- 45	6410-6210	6310	-27.98	531.812-4342.025/+8	740-741	0401.003/203	Almeirim 1
GrA-27236	2005 +/- 35	2050-1870	1960	-25.73	543.112-4350.825/+9	300-310	0401.004/204	Vale de Cavalos 1
GrA-29205	1390 +/- 35	1360-1265	1313	-28.75	541.501-4362.494/+14.3	366-370	0401.021	Golega 1
GrA-29447	1510 +/- 40	1520-1310	1415	-27.12	541.501-4362.494/+14.3	366-370	0401.021	Golega 1
GrA-29214	3850 +/-40	4410-4150	4280	-24.28	541.501-4362.494/+14.3	506-508	0401.021	Golega 2
GrA-29215	3610 +/- 60	4090-3720	3905	-24.85	541.501-4362.494/+14.3	506-508	0401.021	Golega 2
GrA-29216	4215 +/- 40	4860-4610	4735	-24.44	541.501-4362.494/+14.3	554-556	0401.021	Golega 3
GrA-29218	3945 +/- 40	4520-4240	4380	-25.82	541.501-4362.494/+14.3	554-556	0401.021	Golega 3
GrA-29220	545 +/- 35	650-510	580	-25.36	544.533-4358.745/+16.63	370-380	0401.013	Golega 4
GrA-29221	200 +/- 35	310-0	155	-25.42	540.649-4352.679/+15.68	370-380	0401.104	Vale de Cavalos 2
GrA-29530	930 +/- 35	930-760	845	-23.5	542.899-4360.935/+16.23	260-270	0401.002	Golega 5
GrA-29843	65 +/- 40	270-0	135	-27.11	541.504-4352.118/+13.22	540-550	0401.015	Vale de Cavalos 3
GrA-29535	2490 +/- 40	2730-2360	2545	-27.32	541.504-4352.118/+13.22	840-850	0401.015	Vale de Cavalos 4
GrA-29538	335 +/- 35	490-300	395	-27.21	540.649-4352.679/+15.68	610-620	0401.104	Vale de Cavalos 5
GrA-29539	1095 +/- 55	1070-930	1000	-25.55	541.584-4352.084/+16.65	300-310	0401.106	Vale de Cavalos 6
GrA-30616	4485 +/- 35	5300-4970	5135	-24.6	542.943-4350.667/+12.73	923-926	0401.302/S2	Vale de Cavalos 7
GrA-31005	6500 +/- 50	7510-7300	7405	-26.1	542.943-4350.667/+12.73	1491-1495	0401.302/S2	Vale de Cavalos 8
GrA-30961	6360 +/- 45	7420-7170	7295	-28.65	542.943-4350.667/+12.73	1588-1590	0401.302/S2	Vale de Cavalos 9
GrA-30615	5790 +/- 40	6680-6480	6580	-27.18	540.407-4359.849/+12	1024-1029	0501.029	Boquilobo 1
GrA-31004	5900 +/- 45	6860-6630	6745	-25.49	540.407-4359.849/+12	1046-1050	0501.029	Boquilobo 2
GrA-30860	325 +/- 30	480-300	390	-25.13	548.938-4364.435/+25	110-120	--	Morro da Serra 1
GrA-32584	8030 +/- 40	9030-8750	8890	-29.18	531.088-4346.563/+11.38	2230-2240	0501.016	Almeirim 2
GrA-32586	2440 +/- 30	2710-2350	2530	-26.71	531.726-4345.914/+11.07	820-830	0501.013	Almeirim 3
GrA-32647	2480 +/- 30	2720-2360	2540	-25.49	522.094-4335.448/+3.94	240-250	0501.042	Benfica 1
GrA-33637	5640 +/- 45	6510-6300	6405	-29.31	522.373-4335.353/+4.30	1160-1170	0501.041	Benfica 2
GrA-32650	600 +/- 25	660-540	600	-25.65	524.799-4333.804/+7.60	690-700	0501.030	Benfica 4
GrA-32651	6165 +/- 35	7170-6950	7060	-24.81	526.038-4333.421/+7.42	770-780	0501.025	Benfica 5
GrA-32654	7440 +/- 40	8360-8180	8270	-28.04	526.038-4333.421/+7.42	1260-1270	0501.025	Benfica 6
GrA-32587	2625 +/- 30	2785-2720	2753	-23.51	514.130-4322.014/+4	860-880	0501.050	Azambuja 1
GrA-32644	450 +/- 30	540-470	505	-28.86	512.824-4323.436/+3	360-370	0501.051	Azambuja 2
GrA-33636	101,91 +/- 0,4%	0	0	-12.57	512.474-4323.832/+3	1590-1610	0501.052	Azambuja 3
GrA-32645	2555 +/- 30	2760-2500	2630	-26.09	514.940-4321.160/+4	1440-1450	0501.044	Azambuja 4
GrA-32646	5010 +/- 35	5900-5650	5775	-28.13	512.474-4323.832/+3	860-870	0501.052	Azambuja 5
GrA-32656	1765 +/- 30	1820-1570	1695	-27.3	504.812-4310.535/+2	440-480	0501.071	Vila Franca 1
GrA-32655	6265 +/- 35	7270-7020	7145	-27.43	544.750-4358.375/+17.40	1967-1974	0401.304/S4	Golega 6
UtC-14746	2530 +/- 60	2760-2360	2560	-26,00	540.407-4359.849/+12	516-520	0501.029	Boquilobo 3
UtC-14747	3089 +/- 38	3390-3210	3300	-25.2	540.407-4359.849/+12	604-607	0501.029	Boquilobo 4
UtC-14748	4129 +/- 42	4830-4520	4675	-23.3	540.407-4359.849/+12	711-712	0501.029	Boquilobo 5
UtC-14749	1022 +/- 37	1060-790	925	-28.4	540.407-4359.849/+12	331-334	0501.029	Boquilobo 6
UtC-14750	1136 +/- 38	1180-960	1070	-27,00	540.407-4359.849/+12	331-334	0501.029	Boquilobo 7
UtC-14744	1630 +/- 35	1610-1410	1510	-26,00	526.420-4333.197/+5	140-150	0601.002	Benfica 7
UtC-14745	3849 +/- 47	4420-4100	4260	-26,00	526.420-4333.197/+5	280-290	0601.002	Benfica 8
UtC-14909	4145 +/- 42	4830-4530	4680	-26.8	523.321-4334.600/+7	1004-1010	0601.301	VALADA 1
UtC-14910	6860 +/- 50	7800-7590	7695	-26.7	523.321-4334.600/+7	1898	0601.301	VALADA 2
UtC-14911	8880 +/- 60	10190-9740	9965	-28.9	523.321-4334.600/+7	2748-2753	0601.301	VALADA 3
UtC-14904	3647 +/- 41	4090-3850	3970	-27.3	505.439-4310.324/+2	1281	0601.302	VFDEXIRA 1
UtC-14905	6247 +/- 46	7270-7010	7140	-27.8	505.439-4310.324/+2	2192-2196	0601.302	VFDEXIRA 2
UtC-14906	8900 +/- 50	10200-9780	9990	-26.2	505.439-4310.324/+2	2842-2848	0601.302	VFDEXIRA 3
UtC-14907	9990 +/- 70	11800-11200	11500	-27.5	505.439-4310.324/+2	3710-3716	0601.302	VFDEXIRA 4
UtC-14908	12160 +/- 90	14260-13780	14020	-29.1	505.439-4310.324/+2	4919-4925	0601.302	VFDEXIRA 5
UtC-1983	6040 ± 50	7010-6740	6875	-28.1	536.620-4342.720/+7.5	761-760	Alpiarça III	ALP-III/A
UtC-1984	5670 ± 40	6560-6320	6440	-28.3	536.620-4342.720/+7.5	752-751	Alpiarça III	ALP-III/B
UtC-1985	3660 ± 40	4410-3870	4005	-29.2	536.620-4342.720/+7.5	502-501	Alpiarça III	ALP-III/C
UtC-1986	2200 ± 40	2340-2120	2230	-29.5	536.620-4342.720/+7.5	301-299	Alpiarça III	ALP-III/D

Appendix 3 *(continued)*

Material	Significance	^{14}C type	Weight (g)	Remarks
peat	GW-level	bulk AMS	9,75	-
peat/bark	res. channel	AMS	-	-
humic clay	start sedimentation	AMS	-	loogextract
humic clay	start sedimentation	AMS	-	residue
humic clay	end sedimentation	AMS	-	loogextract
humic clay	end sedimentation	AMS	-	residue
humic clay	end sedimentation	AMS	-	loogextract
humic clay	end sedimentation	AMS	-	residue
charcoal	active Tagus	AMS	-	charcoal (AAA)
charcoal	active Tagus	AMS	-	charcoal (AAA)
terrestrial botanical macrofossils(+charcoal?)	soil formation	AMS	-	Sieved at 250 & 125 μm
terrestrial botanical macrofossils	active Tagus	AMS	-	Sieved at 250 μm
terrestrial botanical macrofossils	active Tagus	AMS	-	Sieved at 250 & 125 μm
terrestrial botanical macrofossils	end sedimentation	AMS	-	Sieved at 250 μm
terrestrial botanical macrofossils	soil formation	AMS	-	Sieved at 250 & 125 μm
terrestrial botanical macrofossils	top valley fill	AMS	-	Sieved at 125 μm
terrestrial botanical macrofossils	active channel	AMS	-	Sieved at 125 μm
terrestrial botanical macrofossils	active channel	AMS	-	Sieved at 125 μm
terrestrial botanical macrofossils	start sedimentation	AMS	-	Sieved at 200 μm
terrestrial botanical macrofossils	end sedimentation	AMS	-	Sieved at 200 μm
charcoal	active dune	AMS	-	charcoal
Iris pseudacorus seed	drowning	AMS	-	Sieved at 63 μm
terrestrial botanical macrofossils	estuarine c.	AMS	-	Sieved at 125 μm
non-rounded wood pieces	soil formation	AMS	-	Sieved at 125 μm
deciduous leaf remains	marsh sedimentation	AMS	-	Sieved at 63 μm
twig with bud	active Tagus	AMS	-	Sieved at 125 μm
oxidized organic plant remains	marsh sedimentation	AMS	-	Sieved at 63 μm
terrestrial botanical macrofossils	start sedimentation	AMS	-	Sieved at 63 μm
seed/berry	start sedimentation	AMS	-	Sieved at 125 μm
terrestrial botanical macrofossils	marsh sedimentation	AMS	-	Sieved at 63 μm
terrestrial botanical macrofossils	marsh sedimentation	AMS	-	Sieved at 63 μm
terrestrial botanical macrofossils	mouth bar	AMS	-	Sieved at 125 μm
terrestrial botanical macrofossils	marsh sedimentation	AMS	-	Sieved at 63 μm
terrestrial botanical macrofossils	marsh sedimentation	AMS	-	Sieved at 63 μm
undifferentiated plant remains	clay layer	AMS	-	Sieved at 63 μm
terrestrial botanical macrofossils	max. wet	AMS	-	Sieved at 125 μm
terrestrial botanical macrofossils	trans dry-wet	AMS	-	Sieved at 125 μm
terrestrial botanical macrofossils	trans dry-wet	AMS	-	Sieved at 125 μm
total organic fraction < 125 μm	start sedimentation	AMS	total = 3,75 g	Sieved at 125 μm
roots of fraction > 125 μm	start sedimentation	AMS	total = 3,75 g	Sieved at 125 μm
bulk clay	soil formation	AMS	440 g	-
bulk clay	soil formation	AMS	425 g	-
terrestrial botanical macrofossils	active sedimentation	AMS	-	Sieved at 63 μm
terrestrial botanical macrofossils	start sedimentation	AMS	-	Sieved at 63 μm
terrestrial botanical macrofossils	start sedimentation	AMS	-	Sieved at 63 μm
terrestrial botanical macrofossils	start sedimentation	AMS	-	Sieved at 63 μm
terrestrial botanical macrofossils	start sedimentation	AMS	-	Sieved at 63 μm
terrestrial botanical macrofossils+root-like	marsh sedimentation	AMS	-	Sieved at 63 μm
terrestrial botanical macrofossils	start marsh sd.	AMS	-	Sieved at 63 μm
root+small branch-like pieces	start floodplain	AMS	-	Sieved at 63 μm
peat	end Chenopodiaceae	bulk	-	Van Leeuwaarden & Janssen, unpublished
peat	end Pinus decline	bulk	-	Van Leeuwaarden & Janssen, unpublished
peat	many herbs	bulk	-	Van Leeuwaarden & Janssen, unpublished
peat	start Olea	bulk	-	Van Leeuwaarden & Janssen, unpublished

APPENDIX 4
Marine radiocarbon dates used in this study

| Lab. Nr.	¹⁴C age yrs BP ± 1σ	Age cal. BP 2σ	Midpoint	δ¹³C (‰)	Coordinates (x-y) (m)	Waterdepth (m)	Sample depth (cm)	N. Latitude
KIA 30888	< 0	0	0	-1.24 ± 0.32	455.895-4275.498	102	8-12	38° 37'30"
KIA 28966	610 ± 35	0	0	-	455.895-4275.498	102	51-53	38° 37'30"
KIA 30890	735 ± 55	418-0	209	-4.21 ± 0.20	455.895-4275.498	102	65-70	38° 37'30"
KIA 28967	760 ± 25	423-0	212	-	455.895-4275.498	102	139-141	38° 37'30"
KIA 28968	685 ± 30	0	0	-	455.895-4275.498	102	171-173	38° 37'30"
KIA27064	760 ± 45	428-0	214	4.01 ± 0.54	455.895-4275.498	102	198	38° 37'30"
KIA 27065	1035 ± 30	650-0	325	0.94 ± 0.49	455.895-4275.498	102	248	38° 37'30"
KIA 27066	1660 ± 35	1272-649	961	3.03 ± 0.49	455.895-4275.498	102	333	38° 37'30"
KIA 27067	2000 ± 40	1661-935	1298	-0.10 ± 0.65	455.895-4275.498	102	413	38° 37'30"
KIA 27320	2885 ± 40	2724-1913	2319	-9.73 ± 0.21	455.895-4275.498	102	493	38° 37'30"
KIA 27302	4295 ± 40	4510-3611	4061	2.05 ± 0.17	460.591-4276.521	87	30	38° 38'04"
KIA 29731	9440 ± 60	10366-9511	9939	-7.55 ± 0.22	460.591-4276.521	87	62	38° 38'04"
OS- 37706	1960 ±45	1621-898	1260	2.6	460.591-4276.521	87	257	38° 38'04"
KIA 27301	2920 ± 35	2744-1944	2344	-4.98 ± 0.59	460.591-4276.521	87	464	38° 38'04"
KIA 29730	3690 ± 30	3688-2854	3271	-1.24 ± 0.19	460.591-4276.521	87	522	38° 38'04"
KIA 27303	6120 ± 55	6652-5894	6273	1.47 ± 0.19	460.591-4276.521	87	632	38° 38'04"
KIA 29729	8215 ± 45	8891-8049	8470	-1.20 ± 0.25	460.591-4276.521	87	699	38° 38'04"
KIA 27304	10470 ± 70	11876-10688	11282	0.67 ± 0.39	460.591-4276.521	87	713	38° 38'04"
KIA 29728	9735 ± 55	10717-9807	10262	-1.61 ± 0.25	460.591-4276.521	87	738	38° 38'04"
KIA 27305	10470 ± 70	11876-10688	11282	-1.11 ± 0.40	460.591-4276.521	87	759	38° 38'04"
OS- 37707	10450 ± 75	11855-10650	11253	2.42	460.591-4276.521	87	798	38° 38'04"
KIA 27307	10490 ± 70	11908-10718	11313	-6.22 ± 0.49	460.591-4276.521	87	820	38° 38'04"
OS- 37708	11100 ± 50	12819-11710	12265	-2.72	460.591-4276.521	87	975	38° 38'04"
OS- 37709	11500 ± 70	13147-12325	12736	-1.12	460.591-4276.521	87	1140	38° 38'04"
KIA 27687	790 ± 25	440-0	220	0.68 ± 0.27	378.451-4233.507	4602	13-14	38° 14'22"
KIA 29278	4830 ± 35	5263-4357	4810	0.54 ± 0.08	378.451-4233.507	4602	125-127	38° 14'22"
KIA 29279	5935 ± 40	6423-5689	6056	0.02 ± 0.06	378.451-4233.507	4602	155-156	38° 14'22"
KIA 29280	7820 ± 40	8352-7683	8018	-1.59 ± 0.34	378.451-4233.507	4602	189-191	38° 14'22"
KIA 29281	10540 ± 50	11951-10795	11373	-1.75 ± 0.15	378.451-4233.507	4602	260-261	38° 14'22"
KIA 27894	11735 ± 55	13285-12793	13039	0.35 ± 0.11	378.451-4233.507	4602	340-341	38° 14'22"
KIA 29282	12240 ± 70	13781-13118	13450	-4.15 ± 0.22	378.451-4233.507	4602	400-401	38° 14'22"
KIA 29283	12895 ± 55	14869-13762	14316	-3.73 ± 0.13	378.451-4233.507	4602	456.5-458.5	38° 14'22"
KIA 29284	13800 ± 70	16137-15034	15586	-1.05 ± 0.13	378.451-4233.507	4602	631-633	38° 14'22"
KIA 29285	15840 ± 70	18838-18007	18423	0.43 ± 0.11	378.451-4233.507	4602	1184.2-1186.2	38° 14'22"

Appendix 4 *(continued)*

W. Longitude	Borehole nr.	Material	Weight (mg)	Source	Remarks
9° 30'29"	GeoB-8903-1	plankt. forams (*G. bulloides*)	3,9	Abrantes et al. (2008)	prepared in Kiel
9° 30'29"	GeoB-8903-1	plankt. forams (*G. bulloides*)	-	Abrantes et al. (2008)	-
9° 30'29"	GeoB-8903-1	plankt. forams (*G. bulloides*)	3,6	Abrantes et al. (2008)	prepared in Kiel
9° 30'29"	GeoB-8903-1	plankt. forams (*G. bulloides*)	-	Abrantes et al. (2008)	-
9° 30'29"	GeoB-8903-1	plankt. forams (*G. bulloides*)	-	Abrantes et al. (2008)	-
9° 30'29"	GeoB-8903-1	plankt. forams (*G. bulloides*)	-	Abrantes et al. (2008)	prepared in Kiel
9° 30'29"	GeoB-8903-1	plankt. forams (*G. bulloides*)	-	Abrantes et al. (2008)	prepared in Kiel
9° 30'29"	GeoB-8903-1	plankt. forams (*G. bulloides*)	-	Abrantes et al. (2008)	prepared in Kiel
9° 30'29"	GeoB-8903-1	plankt. forams (*G. bulloides*)	-	Abrantes et al. (2008)	prepared in Kiel
9° 30'29"	GeoB-8903-1	plankt. forams (*G. bulloides*)	-	Abrantes et al. (2008)	prepared in Kiel
9° 27'15"	D13882	shells	-	This study (Chapter 6)	age reversal/ reworked
9° 27'15"	D13882	Mollusc	-	This study (Chapter 6)	age reversal/ reworked
9° 27'15"	D13882	shells	-	This study (Chapter 6)	-
9° 27'15"	D13882	shells	-	This study (Chapter 6)	-
9° 27'15"	D13882	shells	-	This study (Chapter 6)	-
9° 27'15"	D13882	shells	-	This study (Chapter 6)	-
9° 27'15"	D13882	shells	-	This study (Chapter 6)	-
9° 27'15"	D13882	shells	-	This study (Chapter 6)	age reversal/ reworked
9° 27'15"	D13882	shells	-	This study (Chapter 6)	-
9° 27'15"	D13882	shells	-	This study (Chapter 6)	instant sedimentation?/ reworked?/ 14C plateau
9° 27'15"	D13882	Mollusc	-	This study (Chapter 6)	instant sedimentation?/ reworked?/ 14C plateau
9° 27'15"	D13882	shells	-	This study (Chapter 6)	-
9° 27'15"	D13882	Mollusc	-	This study (Chapter 6)	-
9° 27'15"	D13882	Mollusc	-	This study (Chapter 6)	-
10° 23'25"	MD03-2698	mixed planktonics >250µm	3,8	This study (Chapter 6)	prepared in Kiel
10° 23'25"	MD03-2698	*G. inflata* >250µm	21,2	This study (Chapter 6)	prepared in Kiel
10° 23'25"	MD03-2698	mixed planktonics >250µm	16,4	This study (Chapter 6)	prepared in Kiel
10° 23'25"	MD03-2698	*G. inflata* >315µm	15,2	This study (Chapter 6)	prepared in Kiel
10° 23'25"	MD03-2698	*G. inflata* >250µm	10,5	This study (Chapter 6)	prepared in Kiel
10° 23'25"	MD03-2698	mixed planktonics >250µm	9,9	This study (Chapter 6)	prepared in Kiel
10° 23'25"	MD03-2698	mixed planktonics >150µm	6,6	This study (Chapter 6)	prepared in Kiel
10° 23'25"	MD03-2698	*G. inflata, G. bulloides, O. universa, G. ruber* white, *G. truncatulinoides* >150µm	7,6	This study (Chapter 6)	prepared in Kiel
10° 23'25"	MD03-2698	*G. bulloides* >150µm	5,3	This study (Chapter 6)	prepared in Kiel
10° 23'25"	MD03-2698	*G. inflata, G. aequilateralis, G. calida, G. bulloides* >250µm	12,5	This study (Chapter 6)	prepared in Kiel

APPENDIX 5

Pollen diagram from marine core D13882 (-87 m)

Only calibrated radiocarbon-date midpoints are given; see Chapter 6 and Appendix 4 for details.
Note that pollen sum includes *Pinus* pollen.

APPENDIX 6

Pollen diagram from marine core MD03-2698 (-4602 m)

Only calibrated radiocarbon-date midpoints are given; see Chapter 6 and Appendix 4 for details.
Note that pollen sum includes *Pinus* pollen.
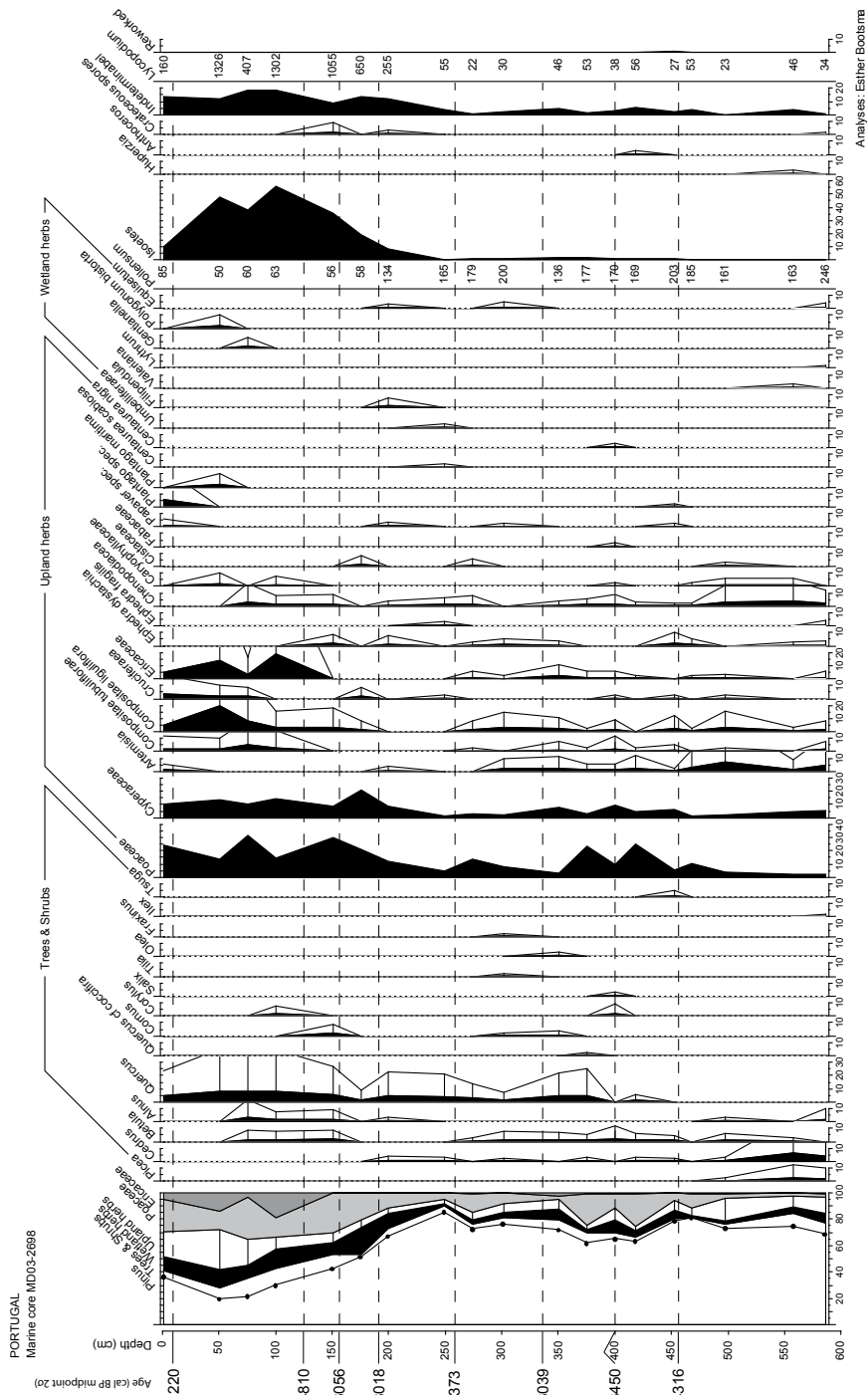
CURRICULUM VITAE

Geert-Jan Vis was born on September 9, 1979 in Reeuwijk (the Netherlands). He finished secondary school at the Coenecoop College in Waddinxveen in 1997, and in September of the same year he started studying Physical Geography at Utrecht University. He specialized in Quaternary geology and fluvial sedimentology. He wrote his M.Sc. thesis together with Thijs Nales about the palaeogeographic evolution of the Old Rhine channel belt, west of the city of Utrecht. He did an internship with Alessandro Fontana from the Università degli Studi di Padova, where he studied the quaternary geology of a spring river in northeast Italy, also together with Thijs Nales. After graduation in 2003, he worked as junior project manager prospective research with archaeological consultancy company BAAC B.V. in Deventer.

In January 2004 he started his Ph.D. research at the Department of Climate Change and Landscape Dynamics of the Faculty of Earth and Life Sciences at VU University Amsterdam. He conducted fieldwork in the Lower Tagus Valley in Portugal in 2004 - 2007. During his time at VU University he supervised many students during different fieldworks, excursions and B.Sc. and M.Sc. projects. He organized several discussion meetings on River Systems Research and was member of the Netherlands Centre for Geo-ecological Research (ICG) Ph.D. Committee with Femke Tonneijk and Gilles Erkens. Among the courses followed are oral presentation skills and scientific writing. He presented the results of this work at many international meetings. The Ph.D. thesis will eventually result in five publications in international peer-reviewed journals, of which two have already been published.

Since October 2008, he is employed at TNO *Geological Survey of the Netherlands*, where he works for the Advisory Board of the Ministry of Economic Affairs.
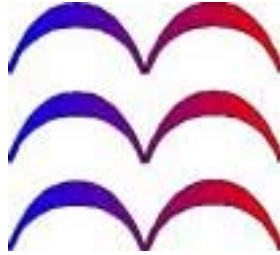
Fluvial Archives Group Biennial meeting 2010 in Portugal

September 6-10th 2010

The meeting will be held in Vila Velha de Ródão, a small town located on the north bank of the Tagus River, close to the Portuguese / Spanish border.

Two days of oral presentations (6th & 7th September) will take place in Ródão followed by a 3-day field excursion (8-10th September) that will showcase the long-term drainage record of the Tagus River and includes several stops in the Lower Tagus Valley.

COLOFON

Fluvial and marine sedimentation at a passive continental margin:
The late Quaternary Tagus depositional system
[Ph.D. dissertation]

In Dutch: Fluviatiele en mariene sedimentatie op een passieve continentrand:
Het laat Kwartaire Taag afzettingssysteem
[Academisch proefschrift]

Graphic design, cartography and figures: Geert-Jan Vis

Cover: hill-shaded digital elevation model based on NASA Space Shuttle data (Jarvis *et al.*, 2006)
Fokke & Sukke cartoon (page 7) used with kind permission of the authors

Fonts: Garamond Premier Pro and Myriad Pro
Paper: 100-gram matt MC

Copies: 350

GEOLOGICAL CROSS SECTIONS OF THE LOWER TAGUS VALLEY
(Chapters 2 & 3)

LEGEND

Facies Units

- FU-1A: fluvial terrace deposits
- FU-1B: high-gradient fluvial channels
- FU-2: aggrading fluvial overbank
- FU-3A: brackish water marshes and tidal flats
- FU-3B: intertidal and subtidal flats
- FU-4: shallow-marine prodelta
- FU-5A: distributary mouth tidal bars with shells
- FU-5B: fluvially influenced tidal channels without shells
- FU-6A: condensed fluvial floodbasins
- FU-6B: fluvial floodbasins
- FU-7: natural levees and crevasses
- FU-8: fluvial channels
- peat-dominated deposits (FU-6B)

Lithology in cores

- peat
- humic clay
- clay
- (silty) clay loam
- silt loam
- loam
- sandy loam
- fine & medium sand
- coarse & very coarse sand
- gravel
- humic sand
- clay pebbles
- ripened soil
- organic soil level
- dike

Golegã cross section

1A: 1360-1265* cal BP (GrA-29205)
1B: 1520-1310* cal BP (GrA-29447)
2A: 4410-4150* cal BP (GrA-29214)
2B: 4090-3720* cal BP (GrA-29215)
3A: 4860-4610* cal BP (GrA-29216)
3B: 4520-4240* cal BP (GrA-29218)
4: 930-760 cal BP (GrA-29530)
5: 650-510 cal BP (GrA-29220)
6: 7270-7020 cal BP (GrA-32655)
Pottery 1: 1st-5th Century AD (1950-1550 cal BP)
Pottery 2: Roman (2250-1650 cal BP)
[*: bulk date]

Benfica do Ribatejo cross section

1: 2720-2360 cal BP (GrA-32647)
2: 6510-6300 cal BP (GrA-33637)
3: 3830-3480 cal BP (Beta-150352), Ramos Pereira et al.(2002)
4: 4830-4530 cal BP (UtC-14909)
5: 7800-7590 cal BP (UtC-14910)
6: 10190-9740 cal BP (UtC-14911)
7: 660-540 cal BP (GrA-32650)
8: 7170-6950 cal BP (GrA-32651)
9: 8360-8180 cal BP (GrA-32654)
10: 1610-1410* cal BP (UtC-14744)
11: 4420-4100* cal BP (UtC-14745)
Pottery 1: Late-Roman (1950-1650 cal BP)
Pottery 2: Roman (2250-1650 cal BP)
[*: bulk date]

Chamusca cross section

1: 310-0 cal BP (GrA-29221)
2: 490-300 cal BP (GrA-29538)
3: 270-0 cal BP (GrA-29843)
4: 2730-2360 cal BP (GrA-29535)
5: 1070-930 cal BP (GrA-29539)
6: 2050-1870 cal BP (GrA-27236)
7: 5300-4970 cal BP (GrA-30616)
8: 7510-7300 cal BP (GrA-31005)
9: 7420-7170 cal BP (GrA-30961)

Azambuja cross section

1: 5900-5650 cal BP (GrA-32646)
2: 101.91 +/- 0.4%* (GrA-33636)
3: 540-470 cal BP (GrA-32644)
4: 2785-2720 cal BP (GrA-32587)
5: 2760-2500 cal BP (GrA-32645)
Pottery 1: Bronze/Iron Age (3950-2250 cal BP)
[*: recent; probably polluted]

Almeirim - Vale de Atela cross section

1: 816 cal BP (Azevêdo et al. 2006)
2: 3086 cal BP (Azevêdo et al. 2006)
3: 3550 cal BP (Azevêdo et al. 2006)
4: 6960 cal BP (Azevêdo et al. 2006)
5: 8097 cal BP (Azevêdo et al. 2006)
6: 9030-8750 cal BP (GrA-32584)
7: 2710-2350 cal BP (GrA-32586)
8: 2340-2120 cal BP (UtC-1986)
9: 4080-3770 cal BP (UtC-1985)
10: 6560-6320 cal BP (UtC-1984)
11: 7010-6740 cal BP (UtC-1983)
Pottery 1: ~Early Middle Ages (1650-1550 cal BP)
Pottery 2: Roman (2250-1650 cal BP)

Map Legend

- Water
- Land
- Tagus channel belt
- Floodplain
- Cities & villages
- Cross section
- Coring

European Datum 1950/UTM Zone 29N

PORTUGAL

Golegã, GOL, Santarém, Alpiarça, VAL, RIVER TAGUS, Vila Franca de Xira, VFX

0501.016
0501.044

Vila Franca de Xira cross section

NNW — SSE

borehole numbers

0501.069 0501.067 0501.068 0501.066 0501.071 0501.065 0501.302 = coring VFX 0501.064 0501.063 0501.062 0501.061 0501.060

Tagus River Sorraia River

elevation (m) relative to m.s.l.

-15,5 m

FU-3A FU-3B FU-5A FU-5B FU-1A FU-4 FU-5A FU-2 FU-1B

⑥

1: 1820-1570 cal BP (GrA-32656)
2: 4090-3850 cal BP (UtC-14904)
3: 7270-7010 cal BP (UtC-14905)
4: 10200-9780 cal BP (UtC-14906)
5: 11800-11200 cal BP (UtC-14907)
6: 14260-13780 cal BP (UtC-14908)

3 km

LEGEND

Facies Units
- FU-1A: fluvial terrace deposits
- FU-1B: high-gradient fluvial channels
- FU-2: aggrading fluvial overbank
- FU-3A: brackish water marshes and tidal flats
- FU-3B: intertidal and subtidal flats
- FU-4: shallow-marine prodelta
- FU-5A: distributary mouth tidal bars with shells
- FU-5B: fluvially influenced tidal channels without shells
- FU-6A: condensed fluvial floodbasins
- FU-6B: fluvial floodbasins
- FU-7: natural levees and crevasses
- FU-8: fluvial channels
- peat-dominated deposits (FU-6B)

Lithology in cores
- peat
- humic clay
- clay
- (silty) clay loam
- silt loam
- loam
- sandy loam
- fine & medium sand
- coarse & very coarse sand
- gravel
- humic sand
- clay pebbles

Sedimentary logs
- cross bedding
- ripples
- ripened soil
- organic soil level
- pebbles and clasts
- roots
- horizontal plant remains
- bioturbation
- shells
- burrow
- pyrite (FeS2)
- carbonate concretions
- terrestrial snails
- dike

Longitudinal cross section

NE — SW

core GOL (0401.304) + core ST3 (INETI report 4946)
Golegã cross section

Almeirim/Santarém NOT IN VALLEY AXIS core 0501.016

Benfica do Ribatejo cross section core VAL (0601.301)

Azambuja core 0501.044

Vila Franca de Xira core VFX (0601.302)

elevation (m) relative to m.s.l.
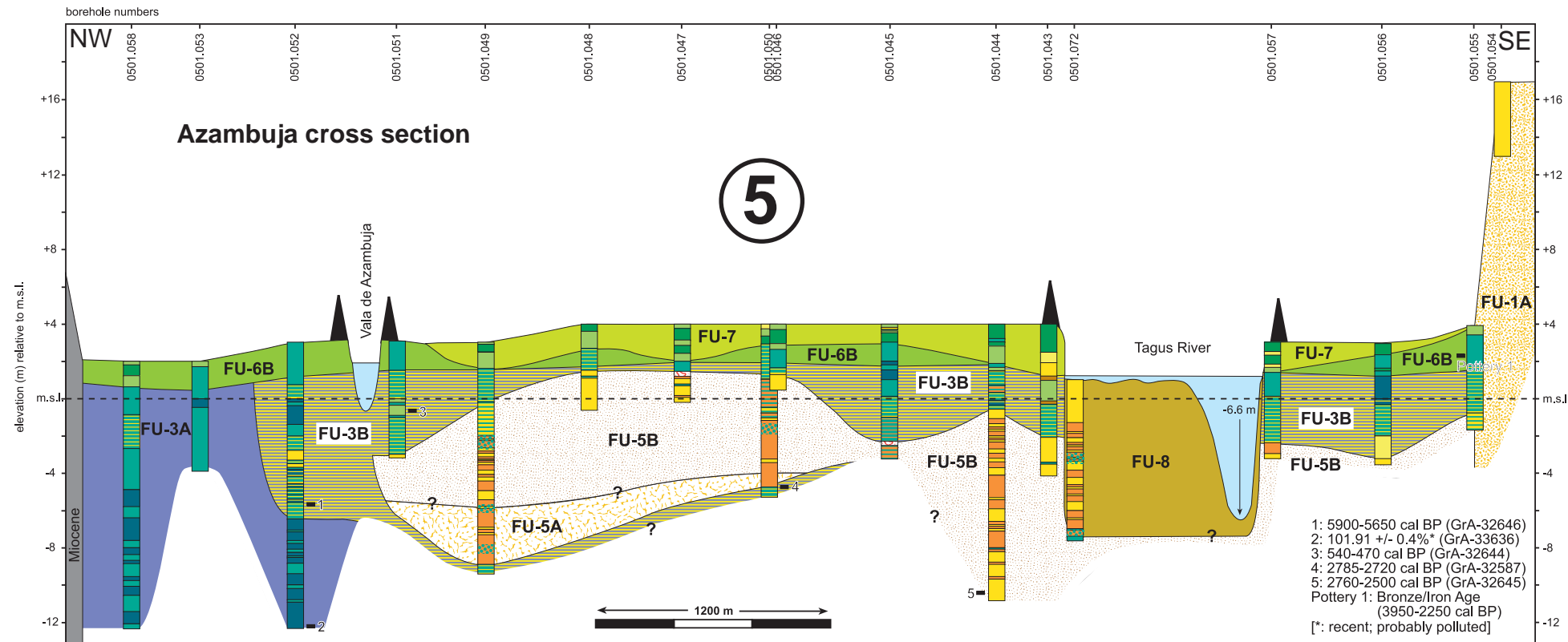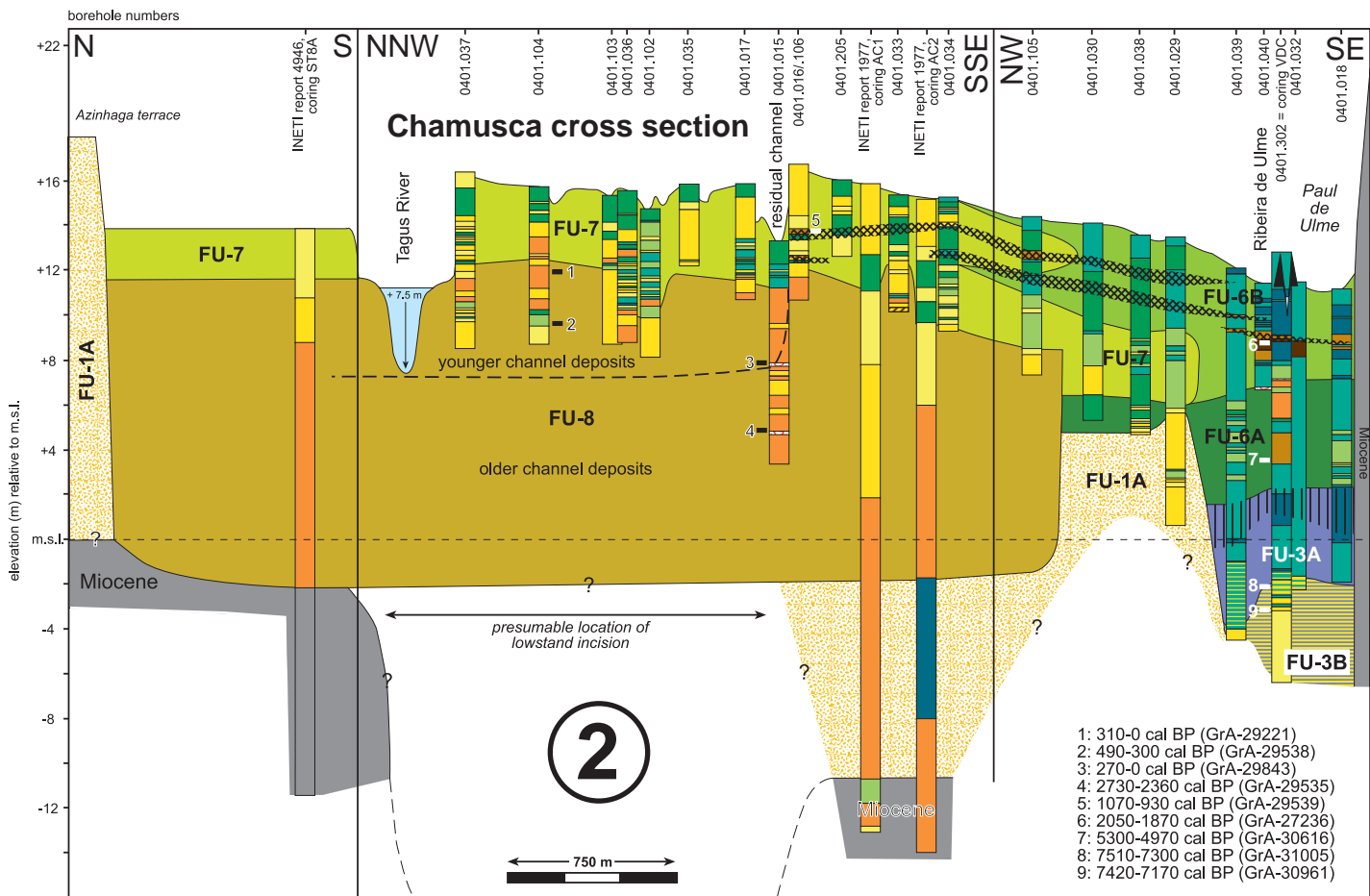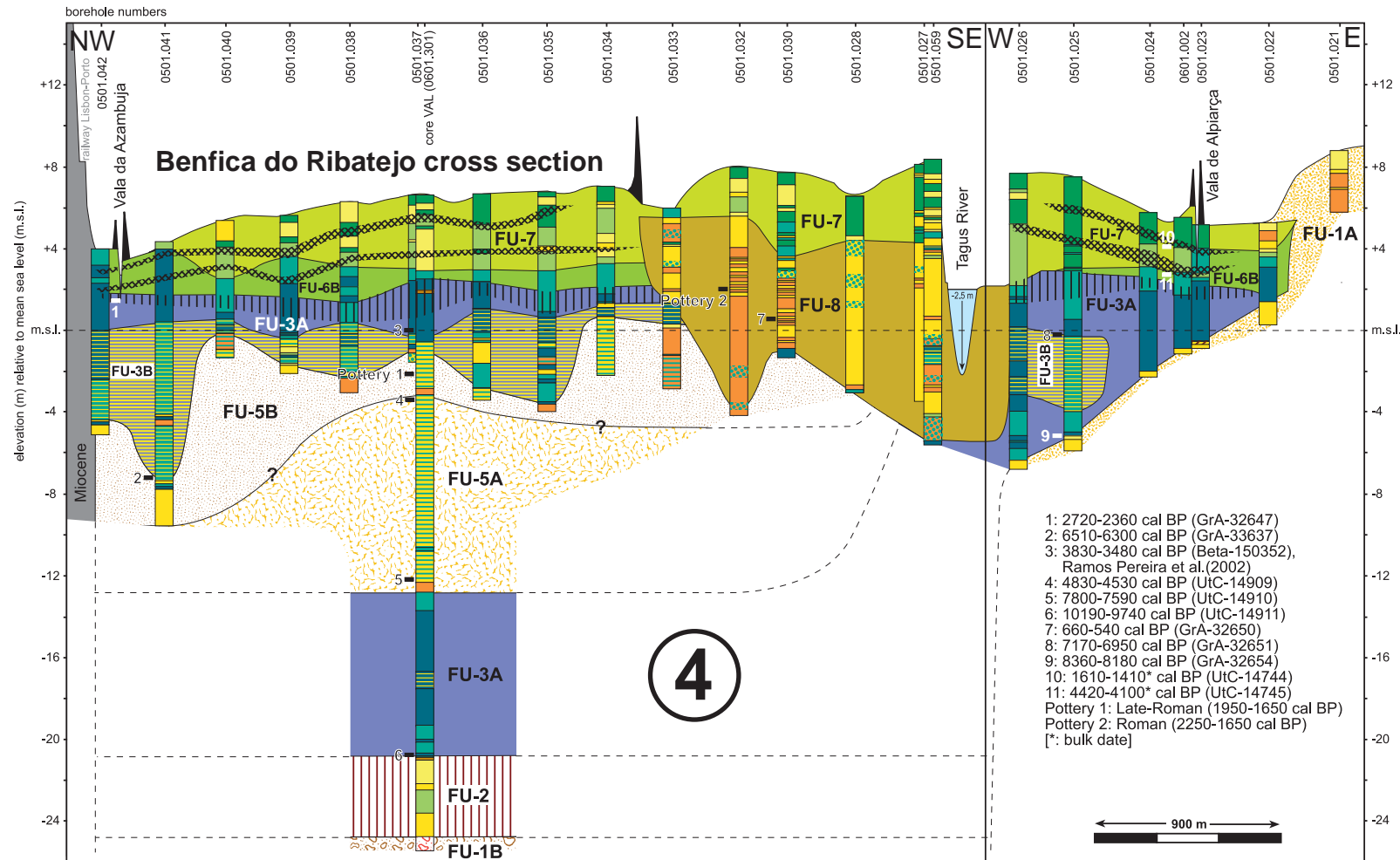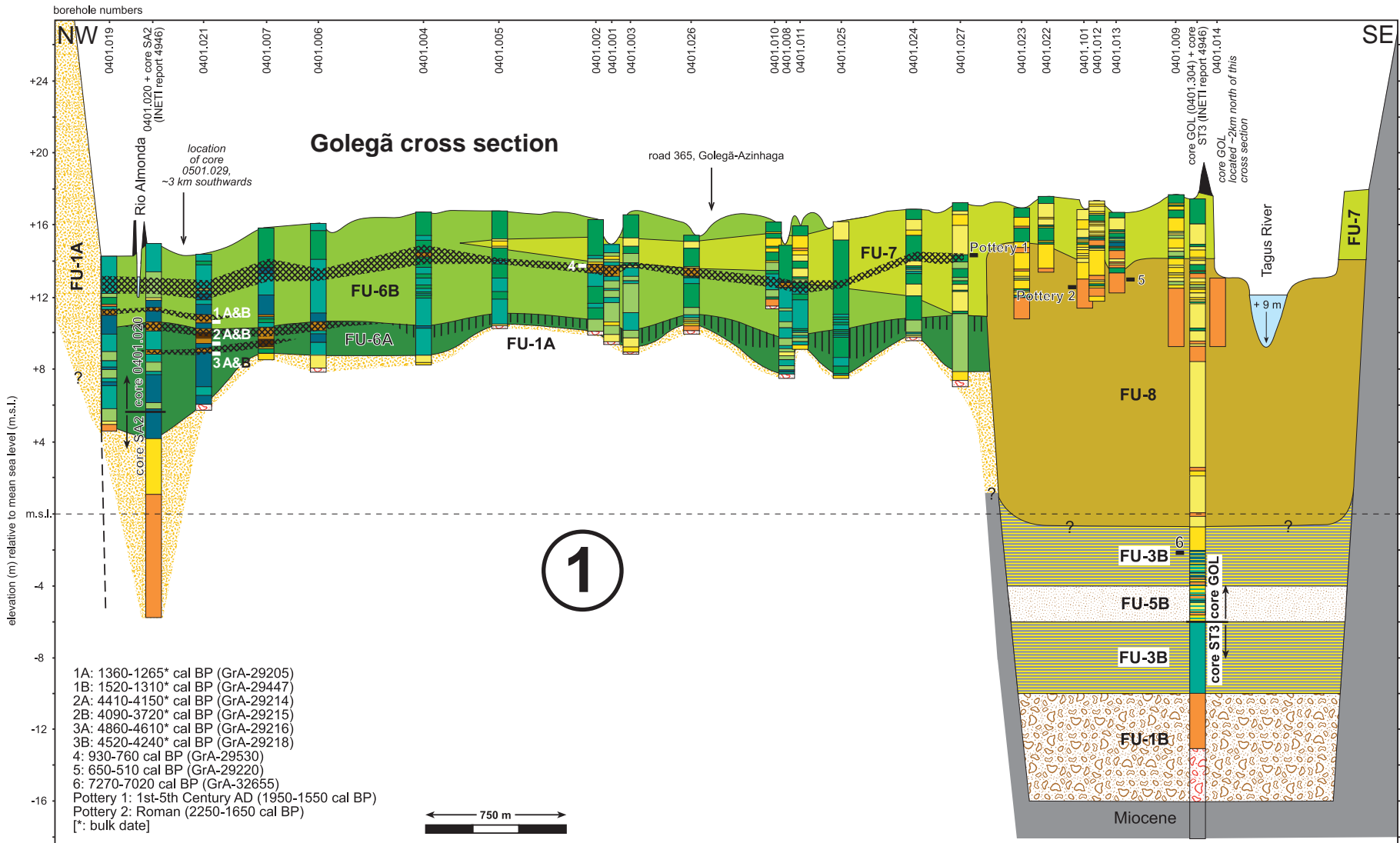
FU-8 FU-6B/7 FU-3B FU-5B GOL ST3 FU-1B FU-5B FU-5A FU-5B FU-5A FU-4 FU-3A FU-3A FU-1B FU-2

Miocene

C S VFF M C G

carbonate: >5% = black
recovery: grey = recovered

⑦

1: 650-510 cal BP (GrA-29220) (taken from 0401.013)
2: 7270-7020 cal BP (GrA-32655)
3: 3640-3460 cal BP (Beta-184659)
4: 7020-6800 cal BP (Beta-184660)
5: 9030-8750 cal BP (GrA-32584)
6: Late-Roman mortar fragment
7: 4830-4530 cal BP (UtC-14909)
8: 7800-7590 cal BP (UtC-14910)
9: 10190-9740 cal BP (UtC-14911)
10: 2760-2500 cal BP (GrA-32645)
11: 4090-3850 cal BP (UtC-14904)
12: 7270-7010 cal BP (UtC-14905)
13: 10200-9780 cal BP (UtC-14906)
14: 11800-11200 cal BP (UtC-14907)
15: 14260-13780 cal BP (UtC-14908)

Horizontal distance not to scale.

PALAEOGEOGRAPHY OF THE LOWER TAGUS VALLEY (Chapter 3)

~20,000 cal BP — possible waterfall — ATLANTIC OCEAN — LISBON — Vila Franca de Xira — Santarém — Golegã — Chamusca — Alpiarça — Almeirim — Benfica do Ribatejo — Muge — Azambuja — Porto Alto — Vale de Estoril

12,000 cal BP

~7000 cal BP — Central basin — SHALLOW MARINE PRODELTA

~4000 cal BP — VALE DOS TEJEIROS — VALE DE ATELA — central basin

~1000 cal BP — MARINE PRODELTA — Fluvial (FU-8) — Tidal (FU-5)

LEGEND
- Quaternary terraces (FU-1A)
- Lowstand fluvial system (FU-1B)
- Fluvial overbank environment (FU-2)
- Tidal flats and marshes (FU-3)
- Tidal bars and channels (FU-5)
- Fluvial channels (FU-8)
- Fluvial overbank environment (FU-6A)
- Fluvial overbank environment (FU-6B & 7)
- Buried submarine valley
- Surface elevation (in m relative to present-day m.s.l.)
- Present-day coastline
- Bathymetry (based on INETI/DGM)
- Cross section
- $ Cities & villages